# MECHANICS, DIVERSITY, AND ECOLOGY OF GECKO ADHESION

A Dissertation

Presented in Partial Fulfillment of the Requirements for the

Degree of Doctor of Philosophy

with a Major in Biology

in the

College of Graduate Studies

University of Idaho

by

Travis Jay Hagey

August 2013

Major Professor: Luke. J. Harmon, Ph.D.

AUTHORIZATION TO SUBMIT

DISSERTATION

This dissertation of Travis J. Hagey, submitted for the degree of Doctor of Philosophy with a major in Biology and titled "Mechanics, Diversity, and Ecology of Gecko Adhesion," has been reviewed in final form. Permission, as indicated by the signatures and dates given below, is now granted to submit final copies to the College of Graduate Studies for approval.

| | | |
|---|---|---|
| Major Professor | _____ Luke J. Harmon | Date _____ |
| Committee Members | _____ Craig P. McGowan | Date _____ |
| | _____ Jack M. Sullivan | Date _____ |
| | _____ Kellar Autumn | Date _____ |
| Department Administrator | _____ James J. Nagler | Date _____ |
| College of Science Dean | _____ Paul Joyce | Date _____ |

Final Approval and Acceptance by the College of Graduate Studies

_____ Date _____
Jie Chen

**Abstract**

The question of why animals are shaped the way they are has intrigued scientists for hundreds of years. Studies of ecological morphology (the relationship between an organism's form, function, and environment) often bridge multiple disciplines including biomechanics, ecology, phylogenetics, and comparative methods. In this dissertation, I gathered data and tested hypotheses that considered the link between morphology and performance and the relationship between performance and ecology. I focused my research on the adhesive abilities of geckos. Geckos are an understudied, diverse group of lizards, well known for their adhesive toe pads. I propose that geckos are an excellent group to consider ecological morphology due to the breadth of morphological, performance, and ecological variation across species, the presence of many recent phylogenetic hypotheses detailing evolutionary relationships among gecko species, and the fascinating characteristics inherent in the gecko adhesive system.

My first research chapter (Chapter 2) focused on the relationship between gecko setal morphology and performance. In this chapter I found that previously described mechanical models of setal performance can likely be applied to a broad range of gecko species, but these models may also be improved for better accuracy. My next chapter (Chapter 3) considered the diversity of adhesive performance across padded lizards. I found that anole lizards, Gekkonidae and Phyllodactylidae geckos, and Diplodactylidae geckos, representing three previously proposed independent origins of adhesive pads, likely exhibit different adhesive performance capabilities and different setal mechanics. In my last research chapter (Chapter 4), I evaluated correlations between gecko adhesive performance, limb morphology, and microhabitat use and found correlations that suggest unique ecomorphological

relationships may be present in geckos. Overall, my results suggest geckos represent an excellent ecological morphology study system and highlight the need for broader studies considering gecko locomotion kinematics, setal mechanics, and habitat use in the context of ecological adaptation.

**Acknowledgments**

I would like to first thank my current and previous advisors Luke Harmon and Roger Anderson. I cannot stress enough how instrumental they have been in my academic success thus far. Roger's field course was responsible for setting me on my current professional trajectory and introduced me to fieldwork and herpetology. I am also thankful for Luke's optimism and vision in giving a starry eyed undergrad such an amazing opportunity. More recently, Craig McGowan has been vital in helping me become a better biomechanist. The other members of my committee, past and present, also offered valuable constructive criticism along the way.

I would also like to thank everyone that has given me assistance, whether it be emotional support, a couch to crash on, or stimulating conversations over drinks. My family and friends, especially Shaunte, have helped me through the trials of graduate school. I would like to thank all my coauthors, multiple anonymous reviewers, and all the folks who helped me formulate my ideas and projects, specifically the past and present members of the Harmon, Autumn, McGowan, Rosenblum, Schwarzkopf, Bauer, Jackman, and Losos labs. Matt Big-Canada Pennell, Jon Eastman, Josef Uyeda, Brice DJ B-Plugg Sarver, Katie Shine, Alyssa Stark, Mitch Day, Tony Russell, Tony Gamble, Dan Beck, Matt Vucko, Aaron Bauer, and Todd Jackman all provided valuable conversations and constructive criticisms. Matt Wilkinson assisted immensely with laboratory and field equipment. Chloe Stenkamp-Strahm taught me about histology. Bobby Espinoza, Alissa Luken, JR Wood, Jesse Grismer, Lee Grismer, Mat Vickers, Andrew Schnell, Luke Mayfowleri Mahler, Bryan Falk, Yoel Stuart, Scott Harte, Dan Scantlebury, Rich Eliot Glor, Meghan Wagner, Andrew Gygli, Katie Pond, Christine Van Tubbe, Michael Cota, Miguel Landestoy, Missy Thompson, Alan Odenborg,

BJ Schenck, Russ Porter, Terry Soule, Eric Wolbrecht, Richard Duffy, Emily Kay, Rose Carlson, and Neely's Travel all helped me build equipment, plan trip logistics, collect data in the laboratory and field, or graciously lent me a couch to sleep on.

Many of my projects would not have been possible without the assistance of staff members and other personnel at the University of Idaho and other facilities, specifically the MCZ and AMNH museum staff, Jon Boone for access to his animals, and the James Cook University Biology staff and motor pool. The Australian Wildlife Conservancy and the Queensland landowners allowed me access to their properties. The University of Idaho, James Cook University, and Lewis and Clark animal care and ethics committees, and the Queensland Government provided vital project approvals and collection permits.

I received funding from multiple sources to attend meetings and conduct research, both of which have been invaluable to my growth as a scientist. Funding sources included the BEACON Center for the Study of Evolution in Action, National Geographic/Waitt Institute, Idaho Graduate and Professional Student Association, Society for the Study of Amphibians and Reptiles, American Society of Naturalists, the Idea Network of Biomedical Research Excellence (IDAHO INBRE), the National Science Foundation, University of Idaho Student Grant Program, and the Western Washington University Undergraduate Research Grant Program. I also received logistical support from the University of Idaho's Institute for Bioinformatics and Evolutionary Studies (IBEST).

**Table of Contents**

**List of Figures**

**List of Tables**

## Chapter 1. Introduction

The question of why animals are shaped the way they are has intrigued scientists for hundreds of years. The field of ecological morphology (or ecomorphology; coined by Klaauw, 1948) incorporates functional morphology and ecology to investigate the relationship between an organism's form and environment (Wainwright and Reilly, 1994). The study of ecological morphology requires many different kinds of data be gathered to considerer the relationships among an organism's morphology, performance, and habitat. As a result, ecomorphological studies bridge multiple disciplines, including biomechanics, ecology, phylogenetics and comparative methods.

There are four components to consider when investigating ecomorphological patterns. The first is the relationship between morphology and performance. An organism's morphology is directly linked to its performance capabilities and behavior (Figure 1.1; modified from Wainwright and Reilly, 1994). Studies of biomechanics seek to describe this causal relationship by quantifying morphology, proposing and evaluating biomechanical models, and conducting performance tests. The second component of ecological morphology is the relationship between performance and ecology. An organism presumably uses its abilities and behavior to perform ecologically relevant tasks such as finding food, avoiding predation, and attracting mates (top half of Figure 1.1). To investigate this relationship, ecological observations are often gathered to infer correlations between performance (or morphology if its relationship with performance is known or assumed) and a particular aspect of the organism's ecology. The third relationship to consider in an ecological morphology framework is the relationship between an organism's fitness and the ecological trait in

question (or associated performance or behavior). Selection may occur if the considered ecological tasks are heritable and affect the organism's fitness, and as a result, the organism's morphology may evolve as a product of adaptation. Studies investigating the relationship between traits and fitness can use a mark-recapture approach to infer differential survival of individuals. Lastly, the relationships among species must be considered to understand how morphological traits may have changed through time and to account for the fact that morphology is inherited from a species' ancestor and correlated morphology, performance, and ecological traits may be due to shared ancestry and not adaptation. Studies typically use phylogenetic hypotheses and statistical comparative methods such as independent contrasts or phylogenetic generalized least squares (Felsenstein, 1985; Pagel, 1999) to account for the non-independence of species.

In this dissertation I gathered data and tested hypotheses concerning three of the above ecological morphology components: the link between morphology and performance and the relationship between performance and ecology while also considering the relationships among species. I focused my research on the adhesive abilities of geckos. Geckos are an understudied, diverse group of lizards well known for their adhesive toe pads and an excellent group to consider ecological morphology due to the breadth of morphological, performance, and ecological variation across species (Gamble et al., 2012; Irschick et al., 1996; Peattie, 2007; Pianka and Huey, 1978; Pianka and Pianka, 1976; Ruibal and Ernst, 1965; Russell, 1972; Russell, 1979; Russell and Johnson, 2007), the presence of many recent phylogenetic hypotheses detailing evolutionary relationships among geckos (Gamble et al., 2012; Pyron et al., 2013), and the fascinating characteristics inherent in the gecko adhesive system. Further, this system likely evolved multiple times across lizards and

within geckos (Autumn et al., 2006a; Autumn et al., 2006b; Autumn et al., 2002; Gamble et al., 2012; Gravish et al., 2008; Hansen and Autumn, 2005; Stark et al., 2012). There is also much interest in the use of gecko-like synthetic adhesives in industrial and commercial applications. This creates a unique opportunity in which studies of biomimicry and ecological morphology of geckos can benefit one another (Menon et al., 2004; Russell et al., 2007).

The three research chapters of my dissertation focused on the relationship between gecko setal morphology and three measures of performance (Chapter 2), the diversity of adhesive performance across padded lizards (Chapter 3), and correlations between gecko adhesive performance, limb morphology, and microhabitat use (Chapter 4).

In my first research chapter (Chapter 2), *Variation in Setal Micromechanics and Performance of Two Gecko Species*, I compared predictions from three gecko adhesion biomechanical models (the frictional adhesion model, work of detachment model, and the effective modulus model) to experimental observations to examine if my focal models can be expanded beyond the single species in which they were originally described. I also quantified differences in setal micromechanics between two focal species, *Gekko gecko* and *Phelsuma grandis*. The mathematical models I considered successfully estimated most of my experimentally measured performance values, validating my focal mathematical models and suggesting common setal mechanics for my focal species and possibly for all fibular adhesives.

My results also suggest the coupling of frictional and adhesive forces in isolated setal arrays first observed in *G. gecko* is also present in *P. grandis*, although *P. grandis* displayed a higher performance limit (angle of toe detachment, Figure 2.2, Table 2.3). This suggests *P.*

*grandis* produces relatively more adhesion compared to *G. gecko*. When I considered the energy stored during setal attachment, I observed less work to remove *P. grandis* arrays when compared to *G. gecko*, suggesting *P. grandis* arrays may store less energy during attachment; a conclusion supported by my model estimates of stored elastic energy (Figure 2.8, Table 2.4). My predictions of the effective elastic modulus model suggested *P. grandis* arrays are softer with a lower effective modulus, yet my experimental assays did not show differences between the species (Table 2.4).

My next chapter, *Modeling the Evolution of Adhesive Performance across Padded Lizards*, considered adhesive performance (angle of toe detachment) across 55 species of geckos and anoles to examine how performance may very across independent origins of adhesive pads (Gamble et al., 2012; Irschick et al., 1996). I found extensive variation in performance across species (Figure 3.2, 3.3, Table 3.1). I then fit single and multiple-rate Brownian motion and Ornstein-Uhlenbeck models (Orme et al., 2011) to my data and found that anoles, Diplodacylidae geckos and Gekkonoidea geckos, representing three hypothesized evolutionary origins of adhesive pads, may have unique performance means (Table 3.2). Lastly, I investigated correlations between adhesive performance, setal morphology and pad type and found setal length to be negatively correlated with performance in Gekkonidae and Phyllodactylidae geckos (Figure 3.4, Table 3.3). Pad type was also significantly associated with performance across padded lizards, but only prior to accounting for phylogenetic relationships among species (Table 3.3).

My last research chapter, *How Geckos Stick in Nature: Ecology and Biomechanics of Gecko Feet*, is one of the first studies to consider gecko adhesive performance and specific microhabitat parameters of geckos in their natural environments. I quantified morphology,

adhesive performance, and habitat use of 13 gecko species from Australia including tropical, arid, arboreal, and rock-dwelling species (Figure 4.2, Table 4.1). I found toe detachment angle to be correlated with residual limb length (Figure 4.7). I also found residual limb length to be correlated with the use of arboreal and rock microhabitats as well as negatively correlated with perch diameter (Figure 4.4, 4.6).

Through the course of my research, I identified form and function relationships within geckos that had not previously been identified in other lizard groups, suggesting novel ecomorphological relationships may be present. Broader assessments of ecomorphology comparing geckos to other arboreal and rock dwelling lizards may illustrate convergent suites of traits and microhabitats. In addition, studies of gecko locomotion kinematics and setal mechanics would also be very informative regarding how macro and microscale adhesive and limb morphology may lead to divergent performance and behavior as well as patterns of ecological adaptation.

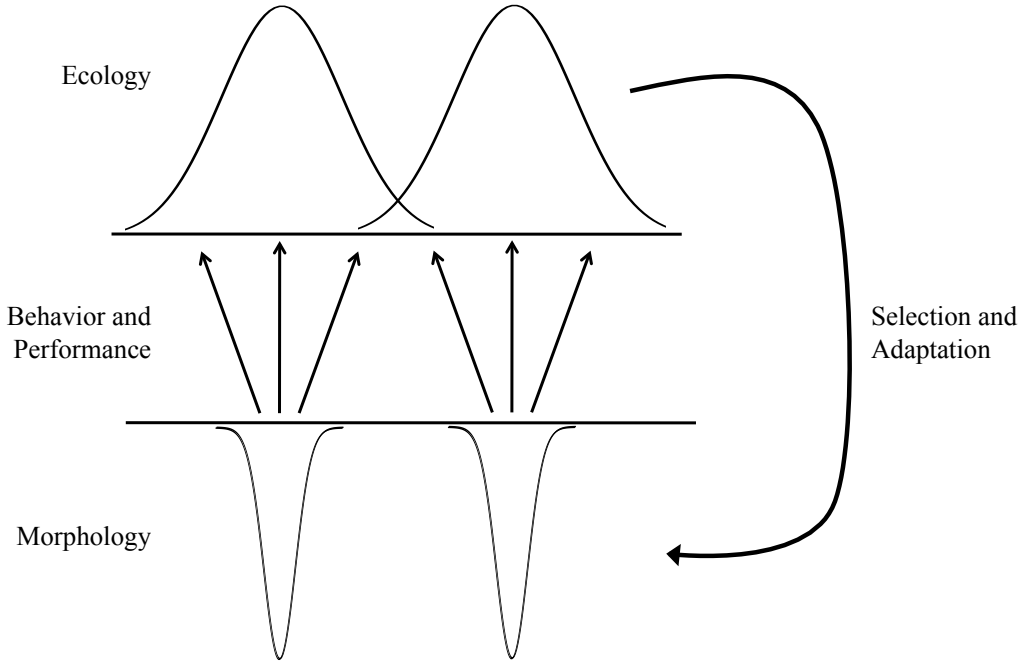


Figure 1.1. Linkage Between an Organism's Morphology, Performance, and Ecology

An organism's morphology is mechanically linked to its performance and behavior. In addition, the organism may use these abilities and behaviors to perform ecologically relevant tasks. If these tasks have fitness consequences for the organism, selection may shape the organism's morphology over many generations (modified from Wainwright and Reilly, 1994).

**Chapter 1. Bibliography**

Autumn, K., Dittmore, A., Santos, D., Spenko, M. and Cutkosky, M. (2006a). Frictional adhesion: a new angle on gecko attachment. J. Exp. Biol. 209, 3569-3579.

Autumn, K., Majidi, C., Groff, R. E., Dittmore, A. and Fearing, R. (2006b). Effective elastic modulus of isolated gecko setal arrays. J. Exp. Biol. 209, 3558-3568.

Autumn, K., Sitti, M., Liang, Y. A., Peattie, A. M., Hansen, W. R., Sponberg, S., Kenny, T. W., Fearing, R., Isrealachvili, J. N. and Full, R. J. (2002). Evidence for van der Waals adhesion in gecko setae. Proc. Natl. Acad. Sci. USA 99, 12252-12256.

Felsenstein, J. (1985). Phylogenies and the comparative method. American Naturalist, 1-15.

Gamble, T., Greenbaum, E., Jackman, T. R., Russell, A. P. and Bauer, A. M. (2012). Repeated Origin and Loss of Adhesive Toepads in Geckos. PLoS ONE 7.

Gravish, N., Wilikinson, M. and Autumn, K. (2008). Frictional and elastic energy in gecko adhesive detachment. J. R. Soc. Interface 5, 339-348.

Hansen, W. R. and Autumn, K. (2005). Evidence for self-cleaning in gecko setae. Proc. Natl. Acad. Sci. USA 102, 385-389.

Irschick, D. J., Austin, C. C., Petren, K., Fisher, R. N., Losos, J. B. and Ellers, O. (1996). A comparative analysis of clinging ability among pad-bearing lizards. Biol. J. Linn. Soc. 59, 21-35.

Klaauw, C. J. V. d. (1948). Ecological Studies and Reviews. IV. Ecological Morphology. Leiden: Brill.

Menon, C., Murphy, M. and Sitti, M. (2004). Gecko Inspired Surface Climbing Robots. In Proceedings of the 2004 IEEE International Conference on Robotics and Biomimetics, pp. 431-436. Los Alamitos, CA, USA: Institute of Electrical and Electronics Engineers.

Orme, C. D. L., Freckleton, R. P., Thomas, G. H., Petzoldt, T. and Fritz, S. A. (2011). caper: Comparative Analyses of Phylogenetics and Evolution in R. (http://R-Forge.R-project.org/projects/caper/).

Pagel, M. (1999). Inferring the historical patterns of biological evolution. Nature 401, 877-884.

Peattie, A. M. (2007). The Function and Evolution of Gekkotan Adhesive Feet, vol. Doctor of Philosophy, pp. 61. Berkeley: University of California, Berkeley.

Pianka, E. R. and Huey, R. B. (1978). Comparative Ecology, Resource Utilization and Niche Segregation among Gekkonid Lizards in the Southern Kalahari. Copeia, 691-701.

Pianka, E. R. and Pianka, H. D. (1976). Comparative Ecology of 12 Species of Nocturnal Lizards (Gekkonidae) in Western Australian Desert. Copeia, 125-142.

Pyron, R. A., Burbrink, F. T. and Wiens, J. J. (2013). A phylogeny and revised classification of Squamata, including 4161 species of lizards and snakes. Bmc Evolutionary Biology 13, 93.

Ruibal, R. and Ernst, V. (1965). The structure of the digital setae of lizards. J. Morphol. 117, 271-293.

Russell, A. P. (1972). The foot of gekkonid lizards: a study in comparative and functional anatomy, vol. PhD. University of London.

Russell, A. P. (1979). Parallelism and Integrated Design in the Foot Structure of Gekkonine and Diplodactyline Geckos. Copeia 1979, 1-21.

Russell, A. P. and Johnson, M. K. (2007). Real-world challenges to, and capabilities of, the gekkotan adhesive system: contrasting the rough and the smooth. Can. J. Zoolog. 85, 1228-1238.

Russell, A. P., Johnson, M. K. and Delannoy, S. M. (2007). Insights from studies of gecko-inspired adhesion and their impact on our understanding of the evolution of the gekkotan adhesive system. J. Adhesion Sci. Technol. 21, 1119-1143.

Stark, A. Y., Sullivan, T. W. and Niewiarowski, P. H. (2012). The effect of surface water and wetting on gecko adhesion. Journal of Experimental Biology 215, 3080-3086.

Wainwright, P. C. and Reilly, S. M. (1994). Ecological Morphology. Chicago IL: University of Chicago Press.

**Chapter 2. Variation in Setal Micromechanics and Performance of Two Gecko Species**

Travis J. Hagey, Jonathan B. Puthoff, Madisen Holbrook, Luke J. Harmon, and Kellar Autumn

Abstract

Biomechanical models of the gecko adhesive system typically focus on setal mechanics from a single gecko species, *Gekko gecko*. In this study, we compared the predictions from three mathematical models to experimental observations considering two gecko species, *G. gecko* and *Phelsuma grandis*, to quantify variation between species setal micromechanics. We also considered the accuracy of our three focal models: the frictional adhesion model, work of detachment model, and the effective modulus model. In addition, we report a novel approach to quantity the angle of toe detachment using the Weibull distribution.

Our results suggest the coupling of frictional and adhesive forces in isolated setal arrays first observed in *G. gecko* is also present in *P. grandis* although *P. grandis* displayed a higher toe detachment angle, suggesting they produce more adhesion relative to friction than *G. gecko*. We also found the angle of toe detachment accurately predicts a species' maximum performance limit when fit to a Weibull distribution. When considering the energy stored during setal attachment, we observed less work to remove *P. grandis* arrays when compared to *G. gecko*, suggesting *P. grandis* arrays may store less energy during attachment, a conclusion supported by our model estimates of stored elastic energy. Our predictions of the effective elastic modulus model suggested *P. grandis* arrays to have a lower modulus, $E_{\text{eff}}$, but our experimental assays did not show differences in moduli between the species.

The considered mathematical models successfully estimated most of our experimentally measured performance values, validating our three focal models as template models of gecko adhesion (see Full and Koditschek, 1999), and suggesting common setal mechanics for our focal species and possibly for all fibular adhesives. Future anchored models, built upon the above templates, may more accurately predict performance by incorporating additional parameters, such as variation in setal length and diameter. Variation in adhesive performance may be important for how geckos move through their environment. Ecological observations will help determine how species with different performance capabilities use their habitat.

## Introduction

Geckos are well known for their climbing abilities. The gecko adhesive system uses arrays of setae, which are hair-like keratinized epidermal derivatives on the underside of each toe (Alibardi et al., 2007; Federle, 2006; Maderson, 1964; Peattie, 2009; Ruibal and Ernst, 1965; Russell, 2002). Geckos' specialized toe pads are capable of generating large frictional and adhesive forces (Autumn et al., 2000; Irschick et al., 1996). Each seta is branched into hundreds of terminal ends called spatulae that interact with a substrate via van der Waals interactions (Autumn et al., 2000; Autumn et al., 2002; Puthoff et al., 2010). Though these substrate/seta interactions are individually minute, the net attraction can be considerable given the multiplicity of these structures (Autumn et al., 2000).

The performance of the gecko adhesive system is influenced strongly by the morphology of setae, the toe, and foot (Peattie, 2007; Russell, 2002), which together create the sum of the hierarchical gecko adhesive system. Despite the biomechanical complexity of

the system, relatively simple models have been developed describing particular performance aspects of isolated setal arrays (Autumn et al., 2006a; Autumn et al., 2006b; Gravish et al., 2008; Hansen and Autumn, 2005; Pesika et al., 2009; Pugno and Lepore, 2008b; Tian et al., 2006). In this study, we focused on predicted and observed performance at the setal array level. Most setal biomechanical models were derived using data from only a single species, *Gekko gecko.* Among gecko species, there is considerable diversity in setal morphological characteristics such as length, width, packing density, and branching pattern (Bauer, 1998; Peattie, 2007; Ruibal and Ernst, 1965; Williams and Peterson, 1982). We propose that small differences in setal morphology will directly influence the performance of setal arrays. We investigated similarities and differences in setal morphology and performance between the gecko species *G. gecko* and the distantly related gecko species *Phelsuma grandis* (Gamble et al., 2012). We chose these two species for our study because, though they are distantly related, they have similar setal shape and organization. Both species exhibit setal curvature and have setae that are angled at rest, suggesting common setal mechanics.

We compared observed and expected setal performance values using three previously described models with the goal of highlighting strengths and weakness of these models when applied to multiple gecko species (Autumn et al., 2006a; Autumn et al., 2006b; Gravish et al., 2008). Our model estimations and experimental measurements predominately considered two types of forces: negative forces normal to the plane of contact, called adhesive forces, and frictional forces, which are parallel to the contact surface. The frictional adhesion (FA) model describes the interplay between frictional and adhesive forces generated by a setal array (Autumn et al., 2006a; Figure 2.1a). The work of detachment (WoD) model describes changes in stored elastic energy and frictional losses during setal removal from a substrate

(Gravish et al., 2008; Figure 2.1b). Lastly, the effective modulus model (EM) considers the homogenized compressive deformation properties of a setal array (Autumn et al., 2006b; Figure 2.1c). These three models provide a quantitative basis for comparing the performance of our focal species by direct experiment and theoretical estimation, with the two latter models using setal morphology as input values. These approaches allowed us to investigate what affect morphological differences will have on adhesive performance as well as investigate the generality of our focal models beyond *G. gecko*. Our proposed hypotheses also have broader ramifications for connections between setal morphology, array performance, and whole-animal locomotion and ecology. We describe the three models of interest in more detail below.

*Frictional adhesion (FA) model*

"Frictional adhesion" refers to the coupling of frictional and adhesive forces generated by a setal array in contact with a substrate (Autumn et al., 2006a). Figure 2.1a inset (i) illustrates typically observed adhesion forces (blue) and frictional forces (green) during a steady drag across a substrate. Under the FA model, the adhesion of a gecko toe is related to the strength of the frictional force. If a setal array generates a friction force of $F_{\parallel}$, then the adhesion force ( $F_{\perp}$) produced cannot exceed $F_{\parallel}$ tan(α*) as summarized by:

$$F_{\parallel} \geq -\frac{F_{\perp}}{\tan \alpha^*}, \qquad \text{Eq. 2.1}$$

where α* is the critical force angle at which setae detach spontaneously from the substrate (Autumn et al., 2006a). Higher α* values allow more adhesion to be generated considering a given amount of friction (Autumn et al., 2006a). The physical basis of the frictional adhesion

effect in setal arrays is currently a very active area of research (see Chen et al., 2008a; Chen et al., 2008b; Tian et al., 2006; Yamaguchi et al., 2009).

Since α* is a property of individual setae and requires laboratory instruments to measure, Autumn et al. (2006a) proposed a whole animal performance assay as a proxy to measure a species' maximum critical angle. This assay, called TAD (toe angle of detachment, $\bar{\alpha}^*$), quantifies the maximum angle of a surface in which a suspended gecko's toe can adhere to using the Weibull distribution (see Methods; Figure 2.1a, inset iii; Figure 2.2). This assay is easier to conduct than assays using isolated setal arrays, and can even be employed in the field. In addition, this assay is weight independent and likely related to setal morphology (Figure 2.2; Autumn et al., 2006a). Using TAD observations, we can quantify the maximum ratio of adhesion and friction a species can generate, as dictated by the FA model.

We can use $\bar{\alpha}^*$ to represent the maximum α* value achievable by isolated setal arrays. Both $\bar{\alpha}^*$ and α* can be described as force angles or as force ratios where the tangent of α* or $\bar{\alpha}^*$ is greater than or equal to $\frac{-F_{\perp}}{F_{\parallel}}$. Figure 2.1a inset (ii) illustrates frictional and adhesive force measurements from isolated setal arrays during a steady drag across a substrate. The adhesion/friction ratio upper limit for *G. gecko* (red line) can be observed in quadrant IV. This line has a slope of $\tan(\bar{\alpha}^*)$ from Autumn et al. (2006a).

We quantified and compared α*, the observed critical angle of setal detachment from setal shear and normal force measurements, and $\bar{\alpha}^*$, a species' toe detachment angle inferred from a collection of toe detachment observations, of our two focal species. We tested whether toe detachment angle $\bar{\alpha}^*$ predicts the maximum force angle α*, as predicted by the

FA model. We anticipated that the FA model accurately describes forces generated by *P. grandis* and *G. gecko* setal arrays, although each species may exhibit different performance due to their respective setal morphology.

*Work of detachment (WoD) model*

When a gecko deploys its adhesive system, the individual adhered setae are placed under tension, changing from a relaxed, curved shape to a straight configuration (Gravish et al., 2008). As a result, energy is stored in the setal array. We can examine how much energy is stored by quantifying the work required to remove the setae from the substrate, shown in Figure 1b. During detachment, the work required depends on the angle at which the isolated setal array is removed from the substrate, i.e. the pull-off angle (θ). During WoD performance assays, θ is an independent variable that is controlled over a range of values, including a proximal removal of the array (θ < 90º), a vertical removal (θ = 90º), or a distal removal (θ > 90º). With measurements of WoD over a range of pull-off angles, we can generate a WoD vs. pull-off angle data series.

Gravish et al. (2008) suggested that frictional sliding of the setal spatulae during detachment at proximal pull-off angles (θ < 90º) contributes the majority of the energy required to detach the array. At pull-off angles near 120º, spatulae sliding is minimal and the release of stored elastic energy dominates the detachment process. The frictional energy loss during detachment due to spatulae slippage ($W_{\|\text{-slip}}$) across detachment angles (θ) and the energy released during detachment at 120º (both normal and lateral components i.e. $W_{\|\text{-elastic}}$ and $W_{\perp\text{-}elastic}$) can all be addressed independently. Energy lost due to spatulae slippage ($W_{\|\text{-slip}}$) is given by

$$W_{\parallel-slip}(\theta) = \frac{F_{\parallel}}{A} s_{slip} = \frac{F_{\parallel}}{A}\left[L\left(\cos(\alpha_0) - \cos(\bar{\alpha}^*) + \frac{\sin(\bar{\alpha}^*) - \sin(\alpha_0)}{\tan\theta}\right)\right], \qquad \text{Eq. 2.2}$$

where $F_{\parallel}/A$ is frictional stress, $s_{\text{slip}}$ is the distance the setal tip slides along the substrate, $L$ is the setal length, $\bar{\alpha}^*$ is the maximum critical force angle (the same parameter estimated in the FA model), and $\alpha_0$ is the angle the seta makes with the substrate when under drag tension. $\alpha_0$ can be estimated as $\alpha_0 = \sin^{-1}\left(\frac{H-d}{L}\right)$, where $H$ is the undisturbed array height and $d$ is the working depth (Gravish et al., 2008; see methods). Note that the variables $L$, $H$, and $d$ can be directly inferred from measurements of setal observations where as $\theta$ is controlled experimentally.

Pull-off angles of $\theta \approx 120^{\circ}$ allow very little spatulae slippage (Gravish et al., 2008). Near this pull-angle, elastic energy is returned from the relaxing setae ($W_{\parallel\text{-elastic}}$ plus $W_{\perp-elastic}$). The spring constant ($k$) for this configuration change can be estimated as (Gravish et al., 2008; Persson, 2003)

$$k = C\frac{ER^4}{L^3}, \qquad \text{Eq. 2.3}$$

where $C$ is a geometrical factor of 10 according to Persson (2003), $E$ is the Young's modulus of β-keratin and $R$ is setal radius. It is notable that elastic return is highly dependent on setal curvature; only curved setae can readily store and release elastic energy. Using Eq. 2.3, we can estimate the lateral elastic energy return during detachment as (Gravish et al., 2008)

$$W_{\parallel-elastic} = \frac{1}{2}\rho k x^2, \qquad \text{Eq. 2.4}$$

where $\rho$ is setal density, $k$ is the setal spring constant and $x$ is the lateral setal displacement during energy storage.

Energy storage in the normal direction ($W_{\perp-elastic}$) can be estimated as (Gravish et al., 2008)

$$W_{\perp-elastic} = \frac{E_{eff}(\Delta H)^2}{2H}, \quad \text{Eq. 2.5}$$

where $E_{\text{eff}}$ is the effective elastic modulus of a setal array (described below), $\Delta H$ is the change in array height, and $H$ is the undisturbed array height. The work required to detach arrays and the energy stored during attachment can be modeled with the above equations, using array morphology as well as other values as inputs. In this study, we use the above equations and experimental observations to compare the energy stored during setal attachment of our two focal species.

*Effective modulus (EM) model*

A gecko's climbing ability depends on how closely its toe pads and setae can conform to the topography of a terrain (Peattie, 2009; Russell and Johnson, 2007). The ability to establish intimate contact is typically a characteristic only of soft easily deformed materials. Gecko setae are made of β-keratin, a material that is quite stiff in bulk and theoretically unsuitable for adhesion (Autumn et al., 2006b). Nevertheless, setal arrays exhibit considerable sticking force on a wide variety of terrain. This is because, though the individual elements of the array are stiff, the array is, overall, considerably compliant. An intrinsic property of a gecko setal array, called the homogenized or "effective" modulus ($E_{\text{eff}}$), describes the overall stiffness of a setal array. This value can be determined experimentally, similar to a tensile compression test performed on a bulk material specimen. It is important to note that there are secondary effects related to setal crowding during

compression (Figure 2.1c; Pesika et al., 2009), so care must be taken to isolate the correct deformation regime during analyses. The effective modulus can also be estimated from measurements of setal morphology. The compression properties of the array depend on the bending behavior of the individual seta, which can be described by traditional materials mechanics. Autumn et al. (2006b) determined that

$$E_{eff} = \frac{3EI\rho \sin\phi}{L^2 \cos^2 \phi}, \qquad \text{Eq. 2.6}$$

where $E$ is the Young's modulus of β-keratin, $L$ is setal length, $I$ is the second moment of area for the setae (for a cylinder $I = \pi R^4/4$ with $R$ as the radius), ρ is the setal density, and ϕ is the setal resting angle. In this study, we considered $E_{\text{eff}}$ experimentally by compressing setal arrays of both focal species and simultaneously recording the force required to do so (see Methods). We also used setal measurements to estimate the expected $E_{\text{eff}}$.

Hypotheses

Our three models make predictions about setal performance. The WoD and EM models describe mechanical relationships between setal morphology and expected performance. The FA model connects setal critical angle, α*, to the ratio of friction and adhesion generated, without a direct relation to setal morphology (but see Chen et al., 2008a; Chen et al., 2008b; Tian et al., 2006; Yamaguchi et al., 2009). These models were developed considering a single species, *Gekko gecko*, and in this study we hypothesize that they will also accurately predict *Phelsuma grandis* performance.

*Hypothesis 1 (Frictional Adhesion)*: The relative ratio of friction to adhesion generated by isolated setal arrays will be limited by a constant force angle (α*, Eq. 2.1) that we can estimate from the angle of toe detachment ($\bar{\alpha}$*) for both *G. gecko* and *P. grandis*.

*Hypothesis 2 (Work of Detachment)*: Using setal morphology as inputs, the WoD model will predict observed work of detachment as a function of pull-off angle ($W_{\|\text{-slip}}$, Eq. 2.2) and stored energy when spatulae slippage is not present ($W_{\perp\text{-}elastic}$ Eq. 2.3, 2.4; and $W_{\|\text{-elastic}}$ Eq. 2.5) for both *G. gecko* and *P. grandis*.

*Hypothesis 3 (Effective Modulus)*: Using setal geometry as inputs, the EM model (Eq. 2.6) will predict the observed effective modulus of ($E_{\text{eff}}$) isolated setal arrays for both *G. gecko* and *P. grandis*.

## Materials and Methods

### *Setal array collection and substrate preparation*

Glass and Teflon coated microscope slides (Erie Scientific, Portsmouth, NH, USA) were used to remove arrays and as test substrates. Slides were cleaned prior to use with a 15 minute 2M NaOH bath, followed by a triple deionized water rinse, dried with Kim Wipes (Kimberly-Clark, Neenah, WI, USA) after every rinse, and set aside for up to 24 hours.

We harvested intact setal arrays from our two focal species (*G. gecko* and *P. grandis*) by pulling each animal's toe proximally across a clean glass microscope slide, causing a small area of the outer skin layer containing setae to separate from the inner layers (Autumn et al., 2006a). This operation can be performed on non-anesthetized animals with no lasting effects, with setae regrown and adhesive function recovered after the next molt (Autumn et al., 2006a). We mounted our collected setal arrays on aluminum scanning electron

microscope (SEM) stubs using cyanoacrylate glue (Loctite 410). Handled delicately, these specimens can perform at full capability through many tests (Autumn et al., 2006b). Arrays were collected using the above technique for both setal morphological measurements and performance assays.

*Setal morphology measurements*

We used seven and nine setal arrays from one *P. grandis* and two *G. gecko* live specimens, respectively. Scanning electron microscope images were collected using an FEI Phenom microscope (Hillsboro, OR, USA). A variable tilt mount provided a wide range of viewpoint options during imaging. Best results were obtained when the array was viewed from the side, with the line of sight perpendicular to the shaft of the setae.

Image analysis was performed with ImageJ analysis software (Version 1.44, National Institutes of Health). Using the scale bar imbedded within microscope images, we measured setal length (*L*; using a four segment line along the setal shaft), setal radius (*R*; at locations mid-shaft, prior to branching and the setae's distal curvature), resting angle ($\phi$), and array height (*H*). An illustration of these measurements can be seen in Figure 2.3.

*Frictional adhesion measurements*

To determine $\alpha^*$, we measured frictional and adhesive forces of isolated setal arrays during a steady drag across a glass substrate using a custom mechanical testing platform called "RoboToe," and employed analysis techniques described in Autumn et al. (2006a). The RoboToe testing platform consisted of a three-axis piezoelectric force sensor (Kistler, Winterthur, Switzerland) attached to a specialized chuck for SEM specimen stubs. NaOH-

cleaned glass slides were rigidly affixed to a frame mounted on two linear actuators (Aerotech, Pittsburgh, PA, USA; see Figure 2.4). Hardware motion was directed and sensor outputs were monitored with a custom LabVIEW program (National Instruments, Austin, TX, USA; see Gravish et al., 2008). By using the two axes of motion provided by the twin actuation stages, we can simulate a lizard pulling its toe proximally across a substrate using displacement-controlled motion. We used a camera attached to a long-working-distance microscope (Optem Zoom 100C microscope, Qioptiq, Rochester, NY; DFK 31AF03 CCD camera, Imaging Source, Charlotte, NC) mounted within RoboToe to visualize arrays during testing and measure setal array area ($A$).

RoboToe can perform multiple automated tests using variable test parameters, such as drag speed and approach distance. An environmental enclosure allowed us to monitor and control temperature and atmospheric humidity. All tests were performed at 30% relative humidity and 25°C. We recorded frictional and adhesive forces generated by an array during the steady-state "drag" portion of a test at a speed of 0.5 mm/s. By varying the distance between the glass substrate and the base of the array, where it is bonded to a mounting stub, we can identify the optimum working depth of each individual array. A smaller working depth brings the array base closer to the substrate. Optimum depth was defined as the distance in which the highest amount of adhesion was observed. Following the identification of each array's optimum depth, we perform five load-drag-pull (LDP) assays at this depth for each array. A LDP assay allowed an isolated setal array to make contact with a clean glass substrate (load), then move across the substrate while in contact (drag), and then be removed vertically from contact (pull). From the recorded frictional and adhesive force values, we can calculate the critical force angle $\alpha^*$ using Eq. 2.1 for each trial of each array. We used ten

isolated setal arrays from four individual live *G. gecko* specimens, and seven arrays isolated from two *P. grandis* individuals for our frictional adhesion measurements.

To measure $\bar{\alpha}^*$, we used 14 live, non-sedated *G. gecko* and five *P. grandis* specimens and an instrumented TAD device similar to that employed by Autumn et al. (2006a). The apparatus consists of a rotational stage suspended from a force sensor that is controlled and monitored using a custom LabVIEW program. Lizards were suspended from a cleaned glass microscope slide by a single rear center toe. The glass slide was mounted rigidly to the rotational stage and rotated at 1º per second from vertical towards inverted, until the animal spontaneously detached and dropped onto a cushion, an event that was detected by the force sensor. The angle of the glass slide at detachment, relative to vertical, was recorded as an individual toe detachment trial ($\bar{\alpha}$). Multiple TAD trials were conducted with each individual, with a minimum of five trials per individual.

To analyze a dataset of toe detachment measurements, we used the Weibull distribution (Figure 2.1a inset iii). The Weibull distribution is a continuous probability distribution commonly used to conduct failure analyses (McCool, 2012; Pugno and Lepore, 2008a, Yang and Xie, 2003). The two-parameter Weibull distribution $p(\bar{\alpha}; m, \lambda)$ provides a failure rate that is proportional to the angle of detachment raised to a power. This is in contrast to the exponential distribution, the expected distribution of waiting times when the failure rate is equal at all times. Using the Weibull probability distribution function, the probability of failure is described as

$$P(\bar{\alpha};m,\lambda) = \frac{m(\bar{\alpha})^{m-1}}{\lambda} e^{-\left(\frac{\bar{\alpha}}{\lambda}\right)^m}, \quad \text{Eq. 2.7}$$

where λ is the scale parameter relating to the mean value, and *m* is a power-law exponent for the distribution (called the "shape parameter," also known as the Weibull modulus). The mean of the distribution equals

$$\bar{\alpha}^* = \lambda\Gamma\left(1+\frac{1}{m}\right), \quad \text{Eq. 2.8}$$

where Γ is the gamma function. We fit each individual lizard's set of observed detachment angles ($\bar{\alpha}$) to a Weibull distribution using maximum likelihood to estimate the mean distribution value for each individual lizard. To estimate a species' mean detachment angle ($\bar{\alpha}^*$) with standard deviations, we calculated the mean and standard deviation of all the species' individual distribution means. We also constructed Quantile-Quantile (Q-Q) plots to investigate the fit of our data to the Weibull distribution.

*Work of detachment measurements*

To directly measure WoD vs. pull-off angle, we used the RoboToe testing platform and the same isolated setal arrays as our FA assay. We used a similar testing procedure as the FA assay (LDP), but with different pull-off angles θ: 30º, 60º, 90º, 120º, and 150º (during our FA assays, arrays were removed vertically, i.e. 90º from the substrate). Angles under 90º detach in the same direction as the drag phase of testing (proximal with respect to the original orientation of the arrays on the animal before removal). An angle of 90º indicates removal of the array perpendicular to the substrate. Tests with pull-off angles greater than 90º produce retrograde displacement relative to the drag direction, simulating a gecko moving its toe distally while removing it from a substrate. Using the RoboToe testing platform, we are able

to produce force-position curves in both the normal and lateral directions. To calculate the work, i.e. energy lost (positive work) or energy recovered (negative work) by the system during each trial in both the normal and lateral directions, we numerically integrated under these curves. We conducted three trials at each angle for each of our 17 isolated setal arrays for a total of 225 trials.

To calculate the expected amount of lateral work ($W_{\|\text{-slip}}$) required to detach setal arrays from a substrate across a set of pull-off angles (θ) we used Eq. 2.2, our observed mean frictional stress values ($F_{\|}$/area) and toe detachment angles ($\bar{\alpha}^*$; see Introduction and Table 2.4). To calculate $W_{\|\text{-elastic}}$, we followed Gravish et al. (2008) and Persson (2003) using the value 10 in Eq. 2.3 for the geometrical factor $C$. We also used a setal lateral displacement distance ($x$) of 10 and 8 μm for *G. gecko* and *P. grandis* respectively, which is approximately 10% of setal length (Gravish et al., 2008), and our observed $E_{\text{eff}}$ setal measurements.

*Effective modulus measurements*

We gathered effective modulus measurements on the same 17 isolated arrays that were used for our FA and WoD tests. Our effective modulus experiments require a different testing routine than our other assays. Since we are only interested in the properties of the array under normal compression, the arrays were brought into contact with cleaned Teflon coated glass slides, compressed to their optimum working depth, and then retracted, all along the normal axis. We recorded the normal force generated by each array through a cycle of five vertical compressions (see Figure 2.1c for typical results).

Within each resulting force-displacement curve, we identified the beginning and end of the initial elastic loading zone. Elastic loading started when the array came into contact

with the substrate, indicated by a significant deviation from zero in observed force, taking into account sensor noise. Without a lateral drag, setal crowding can occur before the array's optimum depth is reached during vertical compression. As a result, we assumed the elastic zone ended at a depth of 60% of an arrays working depth (Pesika et al., 2009; Figure 2.1c). We fit a straight line to the elastic loading zone of the force-displacement curve. The slope of this line is the spring coefficient for the array. We performed additional analyses on our force curves, fitting a two-segmented line (as would be expected if distinct phases of compression were present) as well as an exponential curve to investigate the shape of the force curves.

We calculated the array effective modulus by multiplying our estimated spring coefficient by the observed array height (see Autumn et al., 2006b for a more detailed description). These constants are then employed in the calculation of $E_{\text{eff}}$. It is important to note that in these calculations, the final values are normalized for array area, by dividing each array's performance by it's area, so $E_{\text{eff}}$ is an intrinsic property of the setal array.

*Analyses*

To estimate species means and standard errors from our observed performance assays (FA, WoD, and EM), we calculated individual mean performance values, and averaged these values together. To determine mean species setal morphological measurements, we pooled our observed setal measurements within each species. To compare performance observations between species, we used nested linear mixed-effects models, taking into account within-individual and within-array variation. Using our observed setal morphology means, we used the above biomechanical models to calculate expected performance values. We used setal

density values of 14400 setae/mm$^2$ and 28000 setae/mm$^2$ for *G. gecko* and *P. grandis* (Peattie, 2007). In previous articles, different values of Young's modulus for β-keratin have been used, with 1.4 GPa in Gravish et al. (2008) and 3.0 GPa in Autumn et al. (2006b). We estimated our expected performance values using both values when appropriate to get a range of expected values. Statistical analyses were conduced in both R statistical software version 2.12.2 (R Core Development Team 2010) and Mathematica version 8.0 (Wolfram Research, Champaign, IL, USA).

## Results

### *Morphological comparisons*

Both *G. gecko* and *P. grandis* have branched setae of similar length and diameter with undivided sub-digital scansors, but setal organization differs between the species. *G. gecko* setae are arranged into sets of four, where as *P. grandis* have unorganized setae (see Peattie, 2007). The setae of *G. gecko* and *P. grandis* are qualitatively very similar, yet we found significant differences in all observed setal measurements (see Table 2.2; setal length $F_{1,105} = 88.4$, $p < 0.001$; base to tip $F_{1,107} = 78.0$, $p < 0.001$; radius $F_{1,132} = 170.0$, $p < 0.001$; resting angle $F_{1,55} = 63.4$, $p < 0.001$; array height $F_{1,42} = 53.3$, $p < 0.001$). We suspect these morphological differences, specifically setal length and array height, are responsible for the observed difference in optimum array testing depth (*d*) between species (see Table 2.2).

### *Frictional adhesion measurements*

Our experimental results, displayed in Table 2.3, suggest that the frictional adhesion model effectively describes the performance we observed for both *G. gecko* and *P. grandis*

arrays, with friction and adhesion exhibiting a coupled relationship. Figure 2.5 displays mean array force measurements as stress after being normalized for array area for G. gecko (a) and P. grandis (b). We calculated adhesion to friction force ratios ($F_{\perp}/F_{\parallel}$) using the middle steady-state portion of the observed force-time data. Isolated setal arrays from *P. grandis* exhibited significantly lower mean force ratios than those from *G. gecko* (see Table 2.3; $t_4 = 3.53$, $p = 0.02$). Using the FA model, we translated these observed setal array force ratios into α* (see Introduction and Table 2.3) to make comparisons to our observed toe detachment and setal shaft angles.

To assess the fit of our toe detachment data to the Weibull distribution, we generated Q-Q plots, and found that our toe detachment observations do match values expected from the Weibull distribution (Figure 2.6). After fitting each species toe detachment observations to a Weibull distribution and calculating the distribution mean ($\bar{\alpha}^*$), we found *P. grandis* to have a significantly higher mean toe detachment angle than *G. gecko* ($t_{9.5} = -10.1$, $p < 0.001$). We also compared our observed α* values (calculated from $-\arctan[F_{\perp}/F_{\parallel}]$) to our observed toe detachment ($\bar{\alpha}^*$) species means. We found our α* values to all be less than our $\bar{\alpha}^*$ values (see Figure 2.7), demonstrating that the toe detachment assay is a good predictor of a species' maximum force ratio, as required by the FA model by the use of the inequality in the equation. When we consider our largest observed α* values (see Table 2.3 and Figure 2.7), they are only slightly less then our $\bar{\alpha}^*$ values, suggesting some of our isolated setal arrays were functioning near the upper limit of their performance capabilities.

*Work of detachment measurements*

Our observed lateral work of detachment measurements (colored dotted lines) are shown alongside our predicted values ($W_{||\text{-slip}}$, black solid lines) in Figure 2.8, Table 2.3, and Table 2.4. We experimentally observed similar patterns of detachment work across pull-off angles for *G. gecko* (a) and *P. grandis* (b). For both species, normalized work decreased to zero or below over pull-off angles from $\theta = 30^{\circ}$ to $\theta = 120^{\circ}$, then increased, suggesting similar overall micromechanics during detachment. To statistically compare our experimentally observed results between species, we used a linear model, testing for the effect of pull-off angle, species, and the interaction term between species and pull-off angle (excluding the measurements at $\theta = 150°$ because the amount of work required for detachment rises with pull-off angles above 120°). When we considered the total work required, with the total work combining shear and normal components, we found the pull-off angle ($p < 0.001$) and species by pull-off angle interaction ($p = 0.04$) terms were significant; suggesting that the slope of the total work curve across pull-off angles differs between species. When the same linear model was used considering only the lateral work component, pull-off angle was still significant ($p < 0.001$) while the interaction term was not ($p = 0.06$). We also used a linear model to compare our expected lateral work between species using the terms species, pull-off angle and the interaction term between species and pull-off angle (excluding $\theta = 150°$). In this comparison, the interaction term was significant ($p = 0.009$), similar to analyses from our observed work (see above).

When we consider the similarity between our predicted and observed lateral work values, (Figure 2.8), we found our models accurately predicted the shape of the curve, with work decreasing towards pull-off angles of 120º. We predicted less lateral work at higher

pull-off angles for *G. gecko* (Figure 2.8a), although our predicted work values are all within two standard deviations of our observed values except for when θ was 90º. Our observed and predicted lateral work for *P. grandis* also appear similar (Figure 2.8b), but our predicted values were over two standard deviations above from our observed values for θ = 90, 120, and 150º.

We also estimated the returned elastic energy per area stored in the setae during detachment paths with little to no spatulae slippage ($W_{\|\text{-elastic}}$ and $W_{\perp-elastic}$) and compared these values to our lateral and normal observed work measurements at θ = 120° (see Eq. 2.3, 2.4 and 2.5, Table 2.3 and Table 2.4). Due to the returned energy stored in the setae and very little spatulae slippage, we expect the work of detachment at a pull-off angle of 120° to be negative. We found our expected lateral energy return values, which considered multiple values for Young's modulus of β-keratin, to be within two standard deviations of our observed values for both focal species. However, our expected normal energy return values were over two standard deviations less than our observed measurements for both species.

*Effective modulus measurements*

The isolated setal arrays of both focal species behaved as linear springs (initially) when compressed in the normal direction, producing similar effective modulus values for both species. Different regimes of stiffness, corresponding to different degrees of crowding among the setae could be seen in our results. To evaluate the presence of discrete phases of contact, we fitted a two-segmented line to our force-displacement curves. If distinct phases of compression were present, i.e. elastic compression switching to setal crowding, where the setae being to contact each other, we should find a two-segmented line to fit our data well.

We also fit an exponential curve to our force-displacement measurements. We found some trials did fit the expected pattern with distinct zones of contact, while other trials were very curve-like. There was also a species effect, with *G. gecko* trials more often curve-like then *P. grandis*, suggesting complex interactions between setae during compression. When comparing our expected isolated setal array effective modulus, calculated using a range of values for the Young's modulus of β-keratin, to our observed values, we found the entire range of our modulus estimates (Table 2.4) to be within two standard deviations of our observations for both focal species.

## Discussion

### *Model Accuracy*

We tested the validity of established gecko performance models against the empirical performance of isolated setal arrays from two species of geckos. We found that these models did succeed in predicting many aspects of array performance, but also indicated some interesting differences from our observed values. We found the FA model to accurately described the relationship between setal critical angle, friction, and adhesion generated for both focal species. Our WoD model calculations reproduced the form of the $W_{\|\text{-slip}}(\theta)$ curves (Eq. 2.2, Figure 2.8), but there were significant quantitative differences. In our calculations of $W_{\|\text{-slip}}$, we used our toe detachment estimates, $\bar{\alpha}^*$, as the critical detachment values. Autumn et al. (2006a) cited setal detachment angle ($\alpha^*$) as 30º for *G. gecko*, approximately 120% of toe detachment angle. Using this factor, we estimated *P. grandis* setal detachment angle and reevaluated Eq. 2.2 using setal detachment angle ($\alpha^*$) in place of $\bar{\alpha}^*$. These alternative $W_{\|\text{-slip}}$ values still displayed idiosyncratic inaccuracies, with estimates at low

angles more accurate for *G. gecko*, but less accurate at higher pull-off angles. Estimates for *P. grandis* were less accurate and higher then previous predictions across all pull-off angles.

When considering the EM model, we were able to accurately predict the observed effective modulus of isolated setal arrays for both *G. gecko* and *P. grandis* (Eq. 2.6), but our results also suggest that setal arrays may not always exhibit clearly delineated phases of compression, occasionally displaying non-linear force-displacement curves. This result suggests setal crowding may be a complex process (Pesika et al., 2009), possibly influenced by setal organization, morphology and the condition of the specimen. Using a model incorporating non-linear stiffness, with the effective modulus also dependent on compression depth, may more accurately predict array performance.

The existing model approaches (Autumn et al., 2006a; Autumn et al., 2006b; Gravish et al., 2008) were validated by this study and are useful as general principles of how geckos' complex adhesive system functions. These models are templates – the simplest model that explains general system function (Full and Koditschek, 1999). Our results suggest that models more fully anchored in the morphology of the animal will be required to study the variation among and within species (Full and Koditschek, 1999). Previous work has illustrated substantial setal variation within an individual gecko's toe pad, as well as between species. Setal length in *G. gecko* ranges from under 5 μm to over 100 μm (Johnson and Russell, 2009; Russell, 1979). Additional model complexity, such as drawing from distributions of setal lengths in place of point estimates to predict a distribution of possible performance values or incorporating scansor shape, will help to elucidate the effect macro- and micro- morphological variation across the toe pad may have on performance. With this

approach, we can move toward a better understanding of the evolutionary processes that led to the origination and refinement of this novel biological adhesive system.

*Species Comparisons and Ecology*

Our study found many interesting similarities and differences between our focal species. Overall our results suggest similar setal mechanics for both species regarding the production of adhesion, energy storage during setal attachment, and the effective stiffness of setal arrays. While we found support for similar processes that may represent a common theme for how all gecko setae operate, we did find performance differences between our species that suggest small morphological differences likely have large effects on performance. Our observed differences in adhesive performance cannot be explained simply by a difference in setal shaft angle under tension, $\alpha_0$, as might have been expected. Other setal morphological characters likely contribute to variation in $\bar{\alpha}^*$ between species, such as the miter angle, which measures how the spatulae are aligned in space at the tip of the setae (Figure 2.2).

Our results also pose the question of how the gecko adhesive system may be adapted to particular microhabitats. Hecht (1952) found selection for more lamellae in large *Aristelliger praesignis* geckos. Generating larger amounts of adhesion may be beneficial on highly inverted perches, where a large part of the animal's body weight needs to be supported by the adhesive system, or on rough perches where only a small amount of surface area is available for contact (Huber et al., 2007; Pugno and Lepore, 2008b; Russell and Johnson, 2007). Another consideration is that large adhesives forces may not always be beneficial. There is a potential trade-off regarding the production of adhesion and friction. Species with

high detachment angles may have setae and spatuale that perform best with large setal shaft angles, producing both friction and adhesion, but less absolute friction than if the seta shaft angle were smaller. In this scenario, a species with a high detachment angle may sacrifice the amount of absolute friction generated for a combination of adhesion and friction.

Studies of *Anolis* lizards, a well-studied group of non-gecko lizards with convergent adhesive toe pads (Losos, 2009), have found that species with more lamellae or larger pads use perches higher in the canopy (Elstrott and Irschick, 2004; Glossip and Losos, 1997; Irschick et al., 2006). *Anolis* lizards have short setae, ranging from 15 to 30 μm, and generate low levels of adhesion with detachment angles from 15º to 20º (T. Hagey, unpublished; Ruibal and Ernst, 1965). They are also very rarely, if ever, observed on fully inverted perches (J. Losos and R. Glor, personal communication). We can use this insight to make habitat use predictions for gecko species with similar morphology and performance. For example, *Rhacodactylus ciliatus*, an arboreal gecko species found in New Caledonia, have short setae (47 μm long; Peattie, 2007) and exhibit a low detachment angle of 19º (T. Hagey, unpublished). Based on this information, we may predict *R. ciliatus* typically occupy vertical perches similar to *Anolis* lizards, a prediction supported by observations of *R. ciliatus* in captivity (TH, pers. obs.).

When we consider our WoD results, we again find evidence of a common mechanism of energy storage for gecko species with similar setae, but with species-specific differences. *P. grandis* was found to store less energy during attachment. This difference may affect how our focal species move and detach their feet and toes during locomotion in the wild. Perch angle is known to effect foot orientation (Russell and Higham, 2009), and hence perches with different orientations may require different strategies while also maintaining stability, such as

the use of digit hyperextension or distal movement of the toe. Work of detachment may have a complex interaction with gecko walking and running kinematics on horizontal, vertical, and fully inverted surfaces (Spezzano and Jayne, 2004).

Lastly, the effective moduli of our focal species were similar, but this may not be true for all geckos. For example, *Rhacadactylus ciliatus* have a relatively low setal aspect ratio of 0.032, with a setal diameter of 1.5 μm and length of 47 μm, as compared to *Thecadactylus rapicauda*, an arboreal species from South America, with an aspect ratio of 0.064 due to setae 6.0 μm in diameter and 94 μm in length (Peattie, 2007). Considering only aspect ratio, we may predict *R. ciliatus* to have a lower effective modulus as compared to *T. rapicauda*.

Natural surfaces are rarely perfectly flat, such as tree bark or rocks. Intimate contact between a gecko's adhesive system and their substrate is required for such attachment and the effective modulus of setae may dictate this interaction. Softer arrays may contact more surface area on rough surfaces with highly variable topology, while stiffer arrays may store more energy under tension, allowing for more friction and stronger attachment on smoother surfaces. If an environment requires setae to be highly compliant, i.e., favoring a low effective modulus such as is found in species with low setal density or aspect ratio, there may exist a trade-off between compliance and attachment strength, suggesting different morphologies and capabilities will be beneficial in different environments.

The ability to move through an environment quickly and consistently is immensely valuable for geckos in the wild, requiring a finely tuned adhesive system that balances adhesion and friction generation, detachment and compliance requirements on a wide variety of surface topologies. Few studies have considered habitat use of geckos in the wild (see Russell and Johnson, 2007), yet there are over 1400 described gecko species from over 100

genera (Gamble et al., 2012). Across these species, there is a wide variety of gross and microscopic morphological variation in the adhesive system (Gamble et al., 2012; Johnson and Russell, 2009; Russell, 1979) suggesting variation in performance capabilities may be important for how different species of geckos navigate their environments. Ecological observations of geckos with various setal morphologies in natural settings will allow a stronger understanding of the evolutionary and ecological pressures present on the gecko adhesive system, specifically describing how particular morphologies and capabilities are linked to different microhabitats. Evaluating how different toe-pad and setal morphologies influence adhesive performance can help us understand how geckos have adapted to different habitats.

Acknowledgements

We thank three previous anonymous reviewers, Craig McGowan, Mitch Day, Chloe Stenkamp-Strahm, the Harmon, Rosenblum, and Autumn labs for helpful advice and comments, Matt Wilkinson for assistance with laboratory equipment, Katie Pond and Christine Van Tubbe for help with animal care, Meghan Wagner and Andrew Schnell for assistance in the lab, and the University of Idaho IACUC for approval of the project (Protocol #2010-40). Aaron Bauer and Todd Jackman also provided assistance and support. We thank the University of Idaho and the National Science Foundation (DEB-0844523, IOS-0847953 and NBM-0900723) for funding.

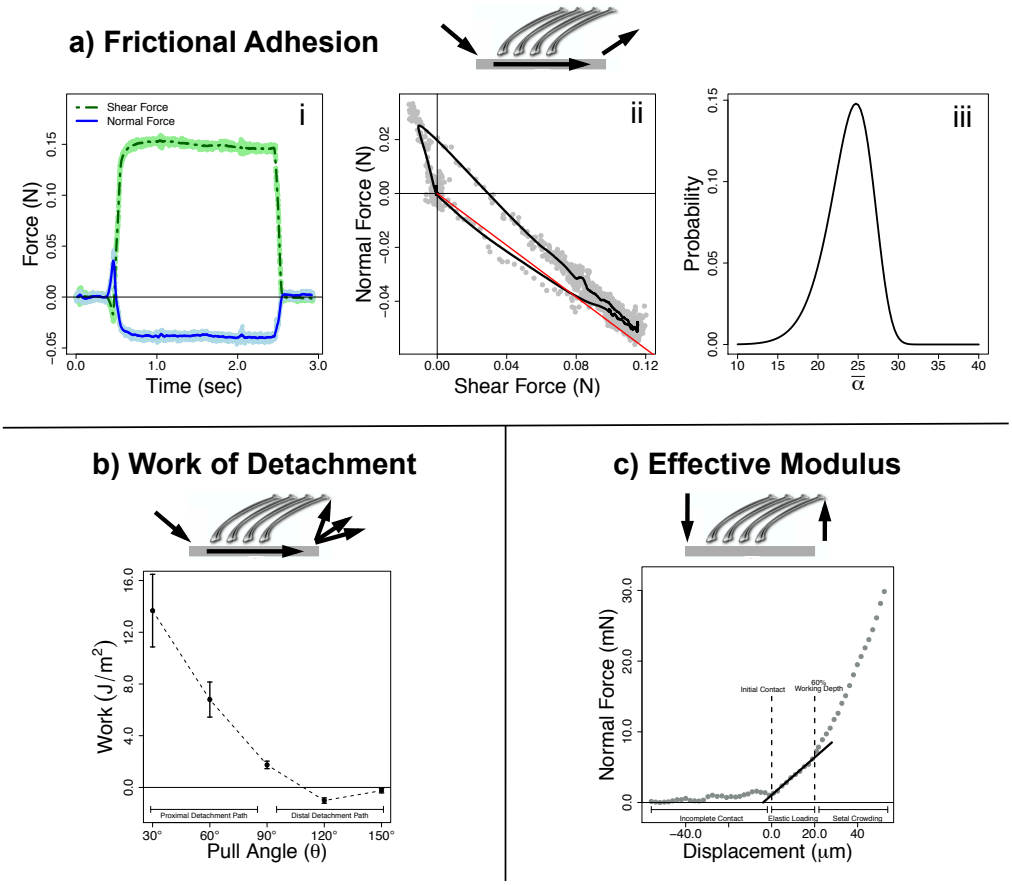


Figure 2.1. Biomechanical Models of Interest

Our three biomechanical models of interest are the frictional adhesion (FA) model (section a, shown at top), work of detachment (WoD, section b, lower left), and effective modulus (EM, section c, lower right). At the top of each compartment, we illustrate the kinematics of the testing procedure. Generalized graphs, highlighting typical measurements from our assays are also illustrated. In assays regarding the FA model (a), we use a load-drag-pull protocol (see methods). Plot i illustrates typical frictional and adhesive forces (green and blue respectively) produced by an isolated setal array through the course of a singe performance trial measured through time. Plot ii displays typically observed frictional and adhesive forces plotted against one another. From these data we can determine α* (see methods section and Autumn et al. 2006a and for details). The red line represents the maximum force angle typically determined from toe detachment trials with a slope of tan ($\bar{\alpha}$*). In the third plot, iii, we illustrate a Weibull probability distribution (p[$\bar{\alpha}$]; λ = 26, m = 10). Note the distribution's tails, illustrating how the Weibull distribution is different from the normal distribution. The left tail accounts for early failures as expected by a time-dependent failure process.

In section b, kinematics of a modified LDP used for our WoD assays can be seen, illustrating multiple pull-off angles. We used pull-off angles (θ) of 30°, 60°, 90°, 120°, and 150°. Pull-off angles under 90° result in proximal movement of array relative to the original orientation on the animal. Angles over 90° represent movement opposite the testing drag

direction, and distal relative to the array's location on the animal before removal. Observed work typically decreases as pull-off angle approaches 120°.

During our EM testing (c), we removed the drag section of the LDP procedure, allowing the array to make contact and be removed vertically from the substrate without any lateral movement. Using the observed normal force and vertical displacement values, we can determine the three phases of compression; incomplete contact, elastic compression and setal crowding and estimate effective modulus as the slope of a line through the elastic compression stage of loading.

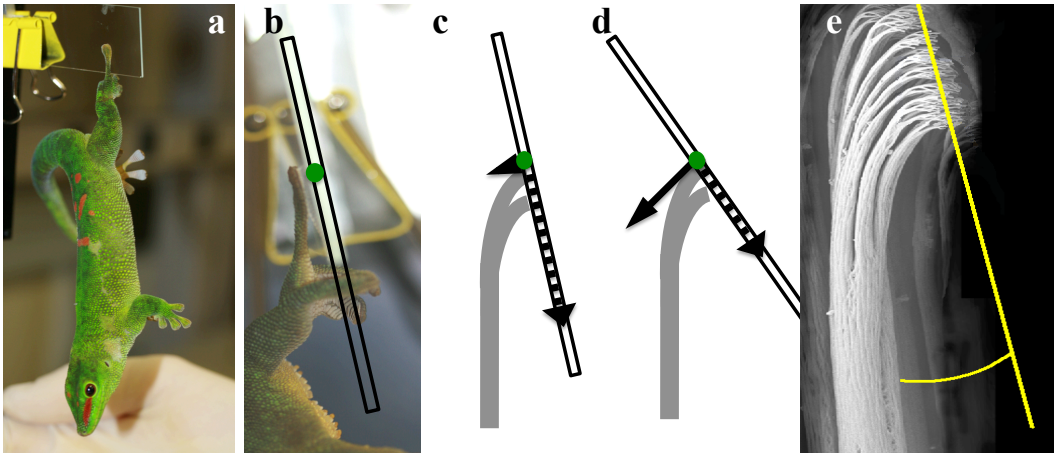


Figure 2.2. Measuring Toe Detachment Angle

To measure toe detachment angle (TAD), we suspended a live, non-sedated gecko from a single rear, middle toe from a clean glass microscope slide using the animal's natural clinging ability (a and b). Force diagrams (c and d) illustrate an idealized seta interacting with the substrate as it moves from vertical to an inverted orientation. During the assay, the setal shaft angle increases relative to the substrate and the generated forces transition from friction to a combination of friction and adhesion until the toe pad spontaneously detaches. At the angle of toe detachment, the seta is at the force angle limit described by the FA model. Autumn et al. (2006a) hypothesized the angle of spontaneous detachment is related to the setal miter angle (e).

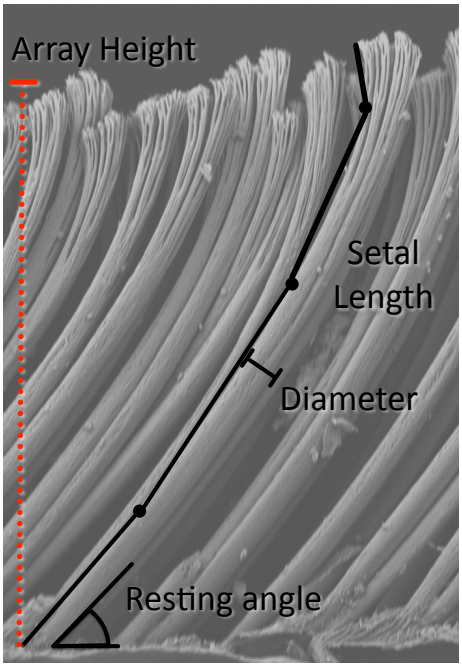


Figure 2.3. Quantifying Setal Morphology

Our setal morphological measurements were gathered from scanning electron images. We measured four metrics using the integrated image scale bars. Setal resting angle was the angle between the base of the setal shaft and the basal skin layer (lower left). Setal shaft diameter was measured mid-shaft below the onset of setal branching, setal shaft length was calculated as the summed length of a four segment line, and array height was measured as the overall mean height of the setal array (red dotted line).

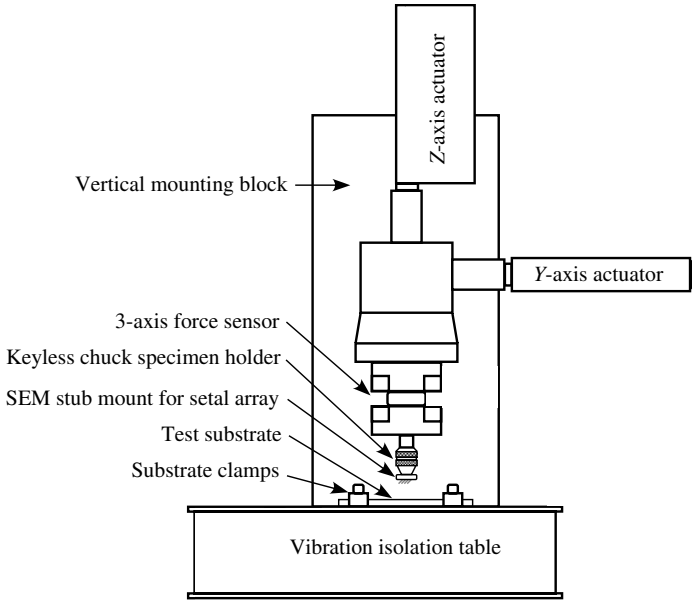


Figure 2.4. The Robotoe Equipment

The Robotoe setup includes a three-axis force sensor suspended by two linear actuators. Our isolated setal arrays were mounted on SEM stubs and securely attached to the force sensor. The motion of the array was controlled in two dimensions by the actuators. With this setup, we can control the arrays distance from the glass substrate as well as its location on the glass (see methods section and Gravish et al., 2008 for detailed description; Figure modified from Autum et al., 2006b).

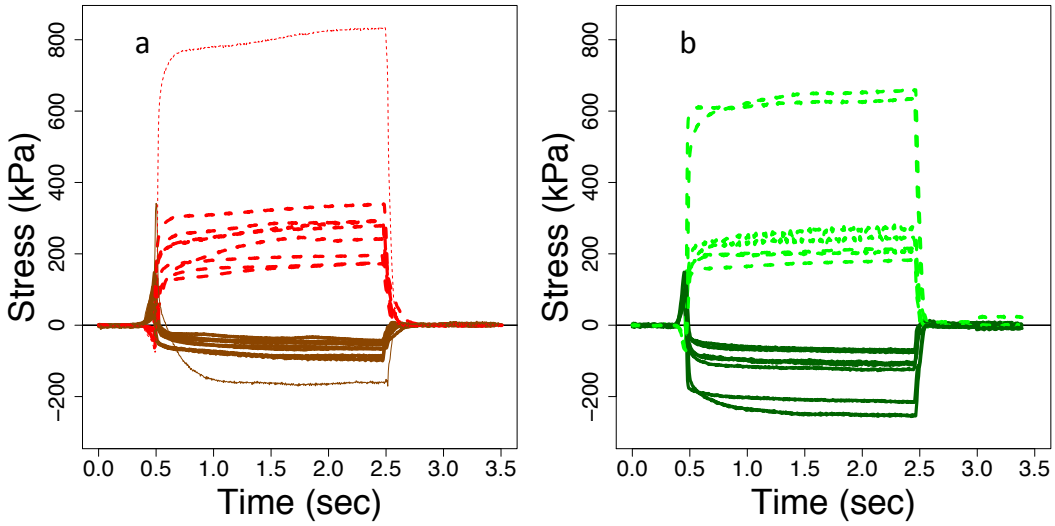


Figure 2.5. Observed Frictional and Adhesive Stress Through Time

We directly observed frictional and adhesive stress generated over time of each isolated setal array for *Gekko gecko* (plot a, red dashed lines are frictional stress, brown solid lines are adhesive stress) and *Phelsuma grandis* (plot b, green dashed lines are frictional stress, dark green solid lines are adhesive stress). The five LDP trials of each array were averaged for each time point. Stresses were calculated by dividing the mean observed forces by array area allowing for within and between species comparisons. Note that stress on the y-axis ranges from -200 to 800 kPa for both plots to allow the performance variation between arrays to be seen. There is one *G. gecko* and two *P. grandis* arrays that generated substantially more stress then the others. This is due to their smaller size, roughly half as large as the others. When using smaller arrays, a larger proportion of setae are able to make appropriate contact with the substrate, with fewer setae over-compressed into the substrate. As a result, when adjusted for area, smaller arrays generate higher stress.

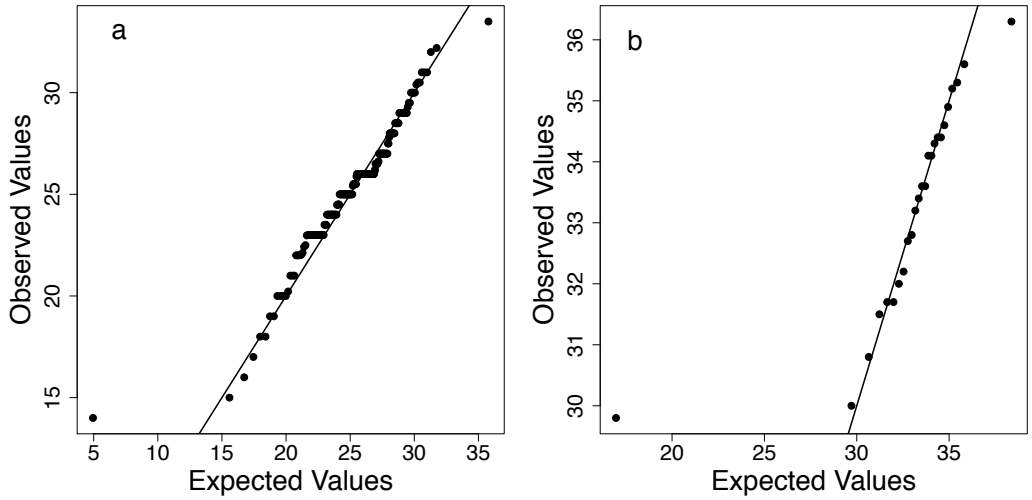


Figure 2.6. Fit of Toe Detachment Data to the Weibull Distribution

To evaluate the fit of our toe detachment observations ($\bar{\alpha}^*$) to the Weibull distribution, we constructed Q-Q plots. In these plots, expected values from the Weibull distribution ($m = 10$ and $\lambda = 26$ and 33 for *G. gecko* and *P. grandis* plots respectively) are plotted against observed values. If the Weibull distribution is a good fit to our data, the resulting points should lie on a line through the origin with slope of 1. Based on our plots, we can conclude that our data fits the Weibull distribution well. The datasets from both our focal species display extreme points that do not lie on this line. These points suggest that, rarely, the Weibull distribution would contain additional values that are larger and smaller then our observed values (We simulated 10,000,000 using the Weibull distribution to construct these plots).

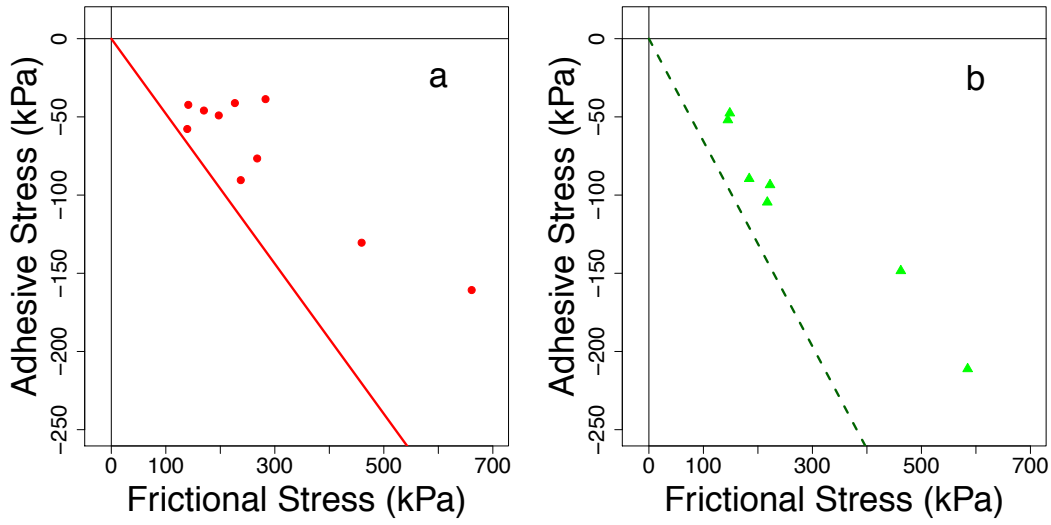


Figure 2.7. Observed Frictional Stress vs. Adhesive Stress

We directly observed the mean frictional and adhesive stresses generated by each isolated setal array for *G. gecko* (plot a, red dots) and *P. grandis* (plot b, green triangles). Stresses were calculated by averaging the observed forces divided by array area from each array's set of five LDP trials. Note that the y and x-axes are equivalent in both plots to allow the performance variation between arrays to be seen. Our observed toe detachment species means ($\bar{\alpha}^*$), are plotted as the limiting force angle indicated as a line with slope equal to $\tan(\bar{\alpha}^*)$, illustrated as a red, solid line in the *G. gecko* plot and a dark green dashed line in the *P. grandis* plot. All of our observed setal force ratios fall to the right of the limiting values established by the TAD measurements, suggesting toe detachment is a good predictor of a species maximum force ratio.

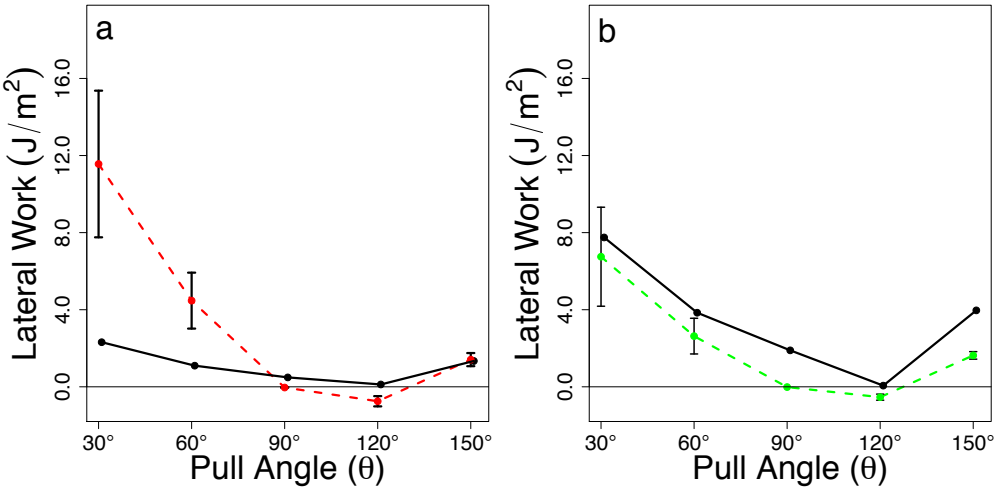


Figure 2.8. Observed Setal Lateral Work

We directly observed the lateral work per area associated with setal array detachment across a set of detachment angles for *G. gecko* (red dashed line, plot a) and *P. grandis* (green dashed line, plot b). It can be seen that work per area decreases as pull-off angle approaches 120°. Additionally, we estimated lateral work per area using setal morphology ($W_{\|\text{-slip}}$, solid black lines). Notice in both graphs, the y-axis (normalized lateral work) ranges from 0 to 16 J/m$^2$. Our predictions of lateral work per area do exhibit a similar pattern across pull-off angles, with decreasing work from pull-off angles of 30° to 120°, but with species-specific inaccuracies (see Results and Discussion).

*Phenotypic variables*

| | |
|---|---|
| $L$ | setal length |
| $R$ | setal radius |
| $\phi$ | setal resting angle |
| $H$ | array height |
| $A$ | setal array area |
| $\rho$ | setal density (Peattie 2007) |
| $d$ | array working depth |
| $E$ | Young's modulus of β-keratin (Autumn et al. 2006b; Gravish et al. 2008) |

*Frictional Adhesion model* (Autumn et al. 2006a)

| | |
|---|---|
| $F_{\parallel}$ | frictional force generated by isolated setal arrays in the shear direction |
| $F_{\perp}$ | adhesive or negative normal force generated by isolated setal arrays |
| $\alpha^*$ | critical force angle in which setae spontaneously detach with $\alpha^* \geq \tan^{-1}\left(F_{\perp}/F_{\parallel}\right)$ |
| $\bar{\alpha}^*$ | species-specific toe detachment angle |
| $\bar{\alpha}$ | a single toe detachment angle observation |
| $\lambda$ | Weibull scale parameter |
| $m$ | Weibull shape parameter or modulus |
| $\Gamma$ | Gamma function |

*Work of Detachment model* (Gravish et al. 2008)

| | |
|---|---|
| $\theta$ | array pull-off angle |
| $W_{\parallel\text{-slip}}$ | work of detachment in shear direction due to spatulae slippage |
| $\alpha_0$ | angle of setal shaft when under drag tension |
| $s_{\text{slip}(\theta)}$ | lateral spatulae slip distance for a given pull-off angle of $\theta$ |
| $W_{\parallel\text{-elastic}}$ | elastic energy recovered in the shear direction |
| $k$ | estimated setal array lateral spring constant |
| $C$ | curvature constant (Persson 2003) |
| $W_{\perp\text{-}elastic}$ | elastic energy recovered in the normal direction |
| $x$ | recoverable lateral array extension |

*Effective modulus model* (Autumn et al. 2006b)

| | |
|---|---|
| $E_{\text{eff}}$ | setal array effective elastic modulus |
| $I$ | second moment of area for setal fibers treated as cylinders |

Table 2.1. Symbols and Constants

These variables and constants were used throughout our analyses in Chapter 2

| **Morphological Results** | *Gekko gecko* | *Phelsuma grandis* |
|---|---|---|
| Mean Setal Length ($L$) | 108 ± 8 μm | 95 ± 6 μm |
| Mean Setal Radius ($R$) | 2.1 ± 0.3 μm | 1.6 ± 0.1μm |
| Mean Resting Setal Shaft Angle ($\phi$) | 48 ± 2º | 42 ± 3º |
| Mean Array Height ($H$) | 79 ± 7 μm | 65 ± 4 μm |
| Mean Array Area ($A$) | 0.6 ± 0.3 $mm^2$ | 0.4 ± 0.1 $mm^2$ |
| Mean Array Working Depth ($d$) | 39 ± 6 μm | 26 ± 3 μm |

Table 2.2. Morphological Results

All errors are reported as standard deviations. Morphological measurements were collected from SEM images and RoboToe observations.

| **Performance Results** | *Gekko gecko* | *Phelsuma grandis* |
|---|---|---|
| *Frictional Adhesion* | | |
| Mean Observed Adhesive Stress ($F_{\perp}/A$) | -90 ± 50 kPa | -110 ± 60 kPa |
| Extreme Observed Adhesive Stress ($F_{\perp}/A$) | -266.8 kPa | -295.2 kPa |
| Mean Observed Fricitonal Stress ($F_{\parallel}/A$) | 400 ± 300 kPa | 300 ± 100 kPa |
| Mean Observed Force Ratio ($F_{\perp}/F_{\parallel}$) | -0.22 ± 0.05 | -0.38 ± 0.04 |
| Extreme Observed Force Angles ($\alpha^*$) | 24.9º | 32.6º |
| Toe Detachment Estimate ($\bar{\alpha}^*$) | 26 ± 2º | 33 ± 1º |
| Weibull scale parameter ($\lambda$) | 27 ± 2 | 34 ± 1 |
| Weibull modulus ($m$) | 14 ± 6 | 39 ± 27 |
| *Work of Detachment* | | |
| Observed Lateral Work per Area | | |
| Pull Angle ($\theta$) of 30º | 12 ± 8 J/m$^2$ | 7 ± 4 J/m$^2$ |
| Pull Angle ($\theta$) of 60º | 5 ± 3 J/m$^2$ | 3 ± 1 J/m$^2$ |
| Pull Angle ($\theta$) of 90º | -0.04 ± 0.02 J/m$^2$ | -0.014 ± 0.002 J/m$^2$ |
| Pull Angle ($\theta$) of 120º | -0.7 ± 0.5 J/m$^2$ | -0.5 ± 0.2 J/m$^2$ |
| Pull Angle ($\theta$) of 150º | 1.4 ± 0.7 J/m$^2$ | 1.6 ± 0.3 J/m$^2$ |
| Observed Normal Work per Area ($\theta$ = 120º) | -0.3 ± 0.4 J/m2 | 0.0 ± 0.1 J/m$^2$ |
| *Effective Modulus* | | |
| Observed Setal Array Elastic Modulus ($E_{\text{eff}}$) | 200 ± 90 kPa | 200 ± 80 kPa |

Table 2.3. Performance Results

All errors are reported as standard deviations. These measurements were gathered from RoboToe and toe detachment assays.

| **Model Results** | Predicted *G. gecko* | Observed *G. gecko* | Predicted *P. grandis* | Observed *P. grandis* |
|---|---|---|---|---|
| *Work of Detachment* | | | | |
| Setal Shaft Angle Under Tension ($\alpha_0$) | 24.0º | -- | 25.2º | -- |
| Shear Work per Area ($W_{\|\|\text{-}slip}$) | | | | |
| Pull Angle (θ) of 30º | 2.3 J/m$^2$ | 12 ± 8 J/m$^2$ | 7.8 J/m$^2$ | 7 ± 4 J/m$^2$ |
| Pull Angle (θ) of 60º | 1.1 J/m$^2$ | 5 ± 3 J/m$^2$ | 3.8 J/m$^2$ | 3 ± 1 J/m$^2$ |
| Pull Angle (θ) of 90º | 0.49 J/m$^2$ | -0.04 ± 0.02 J/m$^2$ | 1.9 J/m$^2$ | -0.014 ± 0.002 J/m$^2$ |
| Pull Angle (θ) of 120º | 0.12 J/m$^2$ | -0.7 ± 0.5 J/m$^2$ | 0.061 J/m$^2$ | -0.5 ± 0.2 J/m$^2$ |
| Pull Angle (θ) of 150º | 1.3 J/m$^2$ | 1.4 ± 0.7 J/m$^2$ | 4.0 J/m$^2$ | 1.6 ± 0.3 J/m$^2$ |
| Setal Array Lateral Spring Constant ($k$) | 0.21 – 0.45 N/m | -- | 0.11 – 0.24 N/m | -- |
| Shear Elastic Return ($W_{\|\|\text{-}elastic}$) | -0.15 – -0.32 J/m$^2$ | -0.7 ± 0.5 J/m$^2$ | -0.10 – -0.21 J/m$^2$ | -0.5 ± 0.2 J/m$^2$ |
| Normal Elastic Return ($W_{\perp\text{-}elastic}$) | -2.4 J/m$^2$ | -0.3 ± 0.4 J/m2 | -2.1 J/m$^2$ | 0.0 ± 0.1 J/m$^2$ |
| *Effective Modulus* | | | | |
| Setal Array Elastic Modulus ($E_{\text{eff}}$) | 130 – 270 kPa | 200 ± 90 kPa | 82 – 180 kPa | 200 ± 80 kPa |

Table 2.4. Model Results

We predicted setal performance and compared these values to observed performance using our morphological measurements as input values into our WoD and EM mathematical models. When values of Young's the Young's modulus of β-keratin ($E$) were needed, we evaluated the models using both 1.4 GPa and 3.0 GPa to get a range of possible performance values.

**Chapter 2. Bibliography**

Alibardi, L., Toni, M., Valle L. D. (2007). Expression of beta-keratin mRNAs and proline uptake in epidermal cells of growing scales and pad lamellae of gecko lizards. J. Anat. 211, 104–116.

Autumn, K., Dittmore, A., Santos, D., Spenko, M. and Cutkosky, M. (2006a). Frictional adhesion: a new angle on gecko attachment. J. Exp. Biol. 209, 3569-3579.

Autumn, K., Liang, Y. A., Hsieh, S. T., Zesch, W., Chan, W. P., Kenny, T. W., Fearing, R. and Full, R. J. (2000). Adhesive force of a single gecko foot-hair. Nature 405, 681-685.

Autumn, K., Majidi, C., Groff, R. E., Dittmore, A. and Fearing, R. (2006b). Effective elastic modulus of isolated gecko setal arrays. J. Exp. Biol. 209, 3558-3568.

Autumn, K., Sitti, M., Liang, Y. A., Peattie, A. M., Hansen, W. R., Sponberg, S., Kenny, T. W., Fearing, R., Israelachvili, J. N. and Full, R. J. (2002). Evidence for van der Waals adhesion in gecko setae. Proc. Natl. Acad. Sci. USA 99, 12252-12256.

Bauer, A. M. (1998). Morphology of the adhesive tail tips of carphodactyline geckos (Reptilia: Diplodactylidae). Journal of Morphology 235, 41-58.

Chen, B., Wu, P. and Gao, H. (2008a). Pre-tension generates strongly reversible adhesion of a spatula pad on substrate. J. R. Soc. Interface 6, 529-537.

Chen, B., Wu, P. D. and Gao, H. (2008b). Hierarchical modelling of attachment and detachment mechanisms of gecko toe adhesion. Proc. R. Soc. A 464, 1639-1652.

Elstrott, J. and Irschick, D. J. (2004). Evolutionary correlations among morphology, habitat use and clinging performance in Caribbean Anolis lizards. Biological Journal of the Linnean Society 83, 389-398.

Federle, W. (2006). Why are so many adhesive pads hairy? Journal of Experimental Biology 209, 2611-2621.

Full, R. J. and Koditschek, D. E. (1999). Templates and anchors: neuromechanical hypotheses of legged locomotion on land. J Exp Biol 202, 3325-32.

Gamble, T., Greenbaum, E., Jackman, T. R., Russell, A. P. and Bauer, A. M. (2012). Repeated Origin and Loss of Adhesive Toepads in Geckos. PLoS ONE 7.

Glossip, D. and Losos, J. B. (1997). Ecological correlates of number of subdigital lamellae in anoles. Herpetologica 53, 192-199.

Gravish, N., Wilikinson, M. and Autumn, K. (2008). Frictional and elastic energy in gecko adhesive detachment. J. R. Soc. Interface 5, 339-348.

Hansen, W. R. and Autumn, K. (2005). Evidence for self-cleaning in gecko setae. Proc. Natl. Acad. Sci. USA 102, 385-389.

Hecht, M. K. (1952). Natural Selection in the Lizard Genus Aristelliger. Evolution 6, 112-124.

Huber, G., Gorb, S. N., Hosoda, N., Spolenak, R. and Arzt, E. (2007). Influence of surface roughness on gecko adhesion. Acta Biomater. 3, 607-610.

Irschick, D. J., Austin, C. C., Petren, K., Fisher, R. N., Losos, J. B. and Ellers, O. (1996). A comparative analysis of clinging ability among pad-bearing lizards. Biol. J. Linn. Soc. 59, 21-35.

Irschick, D. J., Herrel, A. and Vanhooydonck, B. (2006). Whole-organism studies of adhesion in pad-bearing lizards: creative evolutionary solutions to functional problems. J. Comp. Physiol. A 192, 1169-1177.

Johnson, M. K. and Russell, A. P. (2009). Configuration of the setal fields of Rhoptropus (Gekkota: Gekkonidae): functional, evolutionary, ecological and phylogenetic implications of observed pattern. J Anat 214, 937-55.

Losos, J. B. (2009). Lizards in an evolutionary tree : the ecology of adaptive radiation in anoles. Berkeley: University of California Press.

Maderson, P. F. A. (1964). Keratinized Epidermal Derivatives as an Aid to Climbing in Gekkonid Lizards. Nature 203, 780-781.

McCool, J. I. (2012). Using the Weibull distribution: Reliability, modeling and inference: Wiley.

Peattie, A. M. (2007). The Function and Evolution of Gekkotan Adhesive Feet, vol. Doctor of Philosophy, pp. 61. Berkeley: University of California, Berkeley.

Peattie, A. M. (2009). Functional demands of dynamic biological adhesion: an integrative approach. Journal of Comparative Physiology B-Biochemical Systemic and Environmental Physiology 179, 231-239.

Persson, B. N. J. (2003). On the mechanism of adhesion in biological systems. J. Chem. Phys. 118, 7614-7621.

Pesika, N. S., Gravish, N., Wilkinson, M., Zhao, B., Zeng, H., Tian, Y., Israelachvili, J. and Autumn, K. (2009). The Crowding Model as a Tool to Understand and Fabricate Gecko-Inspired Dry Adhesives. J. Adhesion 85, 512-525.

Pugno, N. M. and Lepore, E. (2008a). Living Tokay Geckos Display Adhesion Times Following Weibull Statistics. J. Adhesion 84, 949-962.

Pugno, N. M. and Lepore, E. (2008b). Observation of optimal gecko's adhesion on nanorough surfaces. BioSystems 94, 218-222.

Puthoff, J. B., Prowse, M. S., Wilkinson, M. and Autumn, K. (2010). Changes in materials properties explain the effects of humidity on gecko adhesion. J Exp Biol 213, 3699-704.

Ruibal, R. and Ernst, V. (1965). The structure of the digital setae of lizards. J. Morphol. 117, 271-293.

Russell, A. P. (1979). Parallelism and Integrated Design in the Foot Structure of Gekkonine and Diplodactyline Geckos. Copeia 1979, 1-21.

Russell, A. P. (2002). Integrative Functional Morphology of the Gekkotan Adhesive System (Reptilia: Gekkota). Integr. Comp. Biol. 42, 1154-1163.

Russell, A. P. and Higham, T. E. (2009). A new angle on clinging in geckos: incline, not substrate, triggers the deployment of the adhesive system. Proc. R. Soc. B 276, 3705-3709.

Russell, A. P. and Johnson, M. K. (2007). Real-world challenges to, and capabilities of, the gekkotan adhesive system: contrasting the rough and the smooth. Can. J. Zoolog. 85, 1228-1238.

Spezzano, L. C., Jr. and Jayne, B. C. (2004). The effects of surface diameter and incline on the hindlimb kinematics of an arboreal lizard (Anolis sagrei). J Exp Biol 207, 2115-31.

Tian, Y., Pesika, N., Zeng, H., Rosenberg, K., Zhao, B., McGuiggan, P., Autmn, K. and Israelachvili, J. (2006). Adhesion and friction in gecko toe attachment and detachment. Proc. Natl. Acad. Sci. USA 103, 19320-19325.

Williams, E. E. and Peterson, J. A. (1982). Convergent and Alternative Designs in the Digital Adhesive Pads of Scincid Lizards. Science 215, 1509-1511.

Wilson, D. M. (1997). Statistical tensile strength of Nextel(TM) 610 and Nextel(TM) 720 fibres. Journal of Materials Science 32, 2535-2542.

Yamaguchi, T., Gravish, N., Autumn, K. and Creton, C. (2009). Microscopic Modeling of the Dynamics of Frictional Adhesion in the Gecko Attachment System. Journal of Physical Chemistry B 113, 3622-3628.

Yang, Z. L. and Xie, M. (2003). Efficient estimation of the Weibull shape parameter based on a modified profile likelihood. Journal of Statistical Computation and Simulation 73, 115-123.

**Chapter 3. Modeling the Evolution of Adhesive Performance across Padded Lizards**

Travis J. Hagey, Jonathan B. Puthoff, Kristen E. Crandell, Jorn Cheney, Kellar Autumn, and Luke J. Harmon

Abstract

We measured adhesive performance, quantified as the angle of toe detachment, of 55 species of geckos and anoles to examine how performance varies across independent origins of adhesive pads. Angle of toe detachment describes the maximum amount of adhesion (i.e., negative normal force) a toe pad can generate relative to friction. We used an estimate of three independent origins of adhesive pads with anoles, Diplodacylidae geckos, and the clade containing Gekkonidae and Phyllodactylidae geckos representing independent cases. We found broad differences between these clades, with anoles having lower detachment angles then most geckos, Gekkonidae and Phyllodactylidae geckos having the highest detachment angles, and Diplodactylidae geckos exhibiting an intermediate range of detachment angles. We fit Brownian and Ornstein-Uhlenbeck models of trait evolution to our data and found our best-supported model allowed anoles, Diplodacylidae geckos, and the clade containing Gekkonidae and Phyllodactylidae geckos to each have their own OU trait mean, suggesting performance of our chosen clades cluster around different values. We also investigated correlations between adhesive performance, setal morphology and pad type and found setal length to be negatively correlated with adhesive performance in Gekkonidae and Phyllodactylidae geckos. We also found pad type to be associated with performance across padded lizards, however this relationship was not significant after accounting for phylogenetic relationships. Variation in adhesive performance is likely important for geckos

in an ecological context, where species with higher detachment angles may use inverted perches or rougher surfaces more often than species that produce less adhesion (i.e., species with lower detachment angles). Our results illustrate the extensive variation in adhesive performance across padded lizards and the need for additional studies of comparative setal mechanics as well as further studies considering the relationships between habitat use and the adhesive abilities of geckos.

## Introduction

How gecko toe pads adhere to surfaces has been the subject of intense research over the last decade (Autumn et al., 2002; Hansen and Autumn, 2005; Huber et al., 2007; Prowse et al., 2011; Pugno and Lepore, 2008; Russell and Johnson, 2007; Vanhooydonck et al., 2005). Most of these studies considered data from a single gecko species, *Gekko gecko*, yet adhesive toe pads likely evolved twice outside of Gekkota, in anoles and skinks (Irschick et al., 1996; Pyron et al., 2013), and multiple times among the 1400+ described species of geckos, with Gamble et al. (2012) suggesting 11 origins and nine losses of adhesive toe pads across geckos. Across and within these independent origins, there is considerable diversity in regards to adhesive morphology at the macroscale i.e. toe-pad shape, skeletal features and digital musculature (see Gamble et al., 2012; Russell, 1979). Setal morphology also varies substantially between geckos and anoles (Ruibal and Ernst, 1965) and within geckos (Johnson and Russell, 2009; Peattie, 2007), yet this diversity has rarely been considered from a biomechanical or performance perspective (but see Irschick et al., 1996; Irschick et al., 2006). Adhesive morphology and performance is likely linked to the wide array of habitats occupied by padded lizards, including arboreal, rock, and terrestrial microhabitats in humid

and arid environments (Elstrott and Irschick, 2004; Glossip and Losos, 1997; Harmon et al., 2007; Lamb and Bauer, 2010; Losos, 2009; Macrini et al., 2003; Pianka and Huey, 1978; Pianka and Pianka, 1976; Russell and Johnson, 2007; Zaaf and Van Damme, 2001). It is also unknown how adhesive performance and setal morphology may be associated with the independent origins of adhesive toe pads (but see Ruibal and Ernst, 1965).

In this study, we quantified the diversity of adhesive performance across padded lizards and evaluated the hypothesis that instances of independently evolved adhesive toe pads exhibit unique performance characteristics. In our analyses, we used an estimate of three independent origins of adhesive toe pads in which anoles, Diplodactylidae geckos, and the clade containing Phyllodactylidae and Gekkonidae geckos represent independent cases. We hypothesized that these three clades will have different rates of evolutionary change in regards to their adhesive performance, different performance means, or both.

The adhesive performance of padded lizards can be quantified in multiple ways (TH, unpublished data; Autumn et al., 2006a; Autumn et al., 2006b; Irschick et al., 1996). Irschick et al. (1996) quantified frictional performance of 14 species of padded lizards (six geckos, four anoles, and four skinks) and found substantial variation among species in the absolute amount of friction generated. These authors also found performance to be significantly related to pad area but that the amount of friction generated increased faster than pad area as body size increased. These previous results suggest that performance could not be fully explained by pad area and other factors may also play a role in the generation of friction by padded lizards, such as setal morphology or pad shape. We chose the angle of toe detachment as our measure of adhesive performance (Autumn et al., 2006a). The angle of toe detachment quantifies the maximum relative proportions of adhesion (negative normal force) and friction

generated by a toe pad (see Methods). Autumn et al. (2006a) showed this assay to be weight independent, where individuals detach at the same angle regardless of experimentally modified mass. The angle of detachment can easily be measured in the laboratory or field with relatively simple equipment. Autumn et al. (2006a) also suggested toe detachment angle may be related to setal morphology. Using our dataset of observed detachment angles, we investigated the relationship between angle of toe detachment, setal length, and adhesive pad morphology.

## Methods

We collected angle of toe detachment observations from over 200 individual lizards from 55 species, including anoles, Diplodactylidae, Phyllodactylidae, and Gekkonidae geckos (Figure 3.3 and Table 3.1). Our angle of toe detachment observations were collected in the lab using captive specimens and in the field using wild caught specimens. We used a variety of equipment setups that included powered rotational stages (Autumn et al., 2006a), stepper motors (including Lego Mindstorm motors), and manual rotational stages. Data were collected in the field from sites in Costa Rica, Panama, Thailand and Australia. To measure the angle of toe detachment, live non-sedated lizards were suspended via their natural adhesive properties from a vertical glass substrate by a single rear toe following Autumn et al. (2006a). Using only a single toe, we eliminated the confounding forces that would be generated by multiple toes acting in different directions. During this assay, the glass substrate is initially vertical and the animal's toe pad generates mostly friction relative to the substrate to prevent the animal from falling. We then slowly invert the glass substrate. When this occurs, the toe pad generates adhesion as well as friction relative to the glass to prevent

detachment. As the angle of inversion increases, more relative adhesion is required to support the animal. At the angle of toe detachment, the maximum ratio of adhesion to friction the toe pad is capable of generating has been reached, and the animal falls onto a cushioned pad (see Figure 3.1).

We used the R statistical software for our analyses (version 3.0.1, R Core Development Team 2013). All detachment observations were analyzed using the same approach. Observations from each individual lizard were fit to a Weibull distribution, which is often used in "time-to-failure" analyses (McCool, 2012; see Appendix). The Weibull scale parameter with standard error was then estimated, representing that individual's estimated detachment angle (see Appendix). To produce a species' mean detachment angle, we calculated a weighted average of estimated Weibull scale values from each individual in that species (see Appendix). In some of our focal species, our observations could not be assigned to individual lizards (see Table 3.1) and were treated as observations from a single individual in our analyses.

We used an ultrametric species-level phylogentic tree of Squamates from Pyron et al. (in press, *Ecology Letters*; see Pyron et al., 2013) to consider how traits may have changed through time as opposed to a scale of molecular change. We modified the phylogeny both by removing unsampled taxa and by replacing closely related unsampled taxa with taxa for which we had measurements. When comparing our phylogeny to other previously published hypotheses, we found a discrepancy in the topology of the *Strophurus* genus. Sadlier et al. (2005) suggest *S. krisalys* is more closely related to *S. williamsi* as compared to *S. ciliaris*, while Brown et al. (2012) suggest *S. krisalys* is most closely related to *S. ciliaris* with low nodal support. In the phylogeny we used from Pyron et al. (in press, *Ecology Letters*), *S.*

*williamsi* is more closely related to *S. ciliaris* with low support. We also had performance observations from three species that were not present in our phylogeny and that we could not substitute for closely related taxa, a currently undescribed species closely related to *Oedura marmorata* (P. Oliver, pers. comm) and two *Afroedura* species (*A. hawequensis* and *A. loveridgei*). We substituted *Oedura sp.* with the sister species to *O. marmorata*, *O. gemmata*. As a result, the divergence between *Oedura marmorata* and *Oedura sp*. may be overestimated, although Oliver et al. (2012) suggested deep divergences between populations of *O. marmorata*, nearly as deep as the divergence between *O. marmorata* and *O. gemmata*. The phylogeny from Pyron et al. also suggested that the *Afroedura* genus is polyphyletic, with *A. pondolia* in the same clade as the *Afrogecko*, *Matoatoa*, *Cryptactites*, *Christinus*, and *Paragehyra* genera, whereas *A. karroica* grouped with the *Geckolepis*, *Homopholis*, and *Blaesodactylus* genera. T. Jackman (unpublished data) suggested *Afroedura* is monophyletic and sister to the *Geckolepis*, *Homopholis*, *Blaesodactylus* clade. As a result, we replaced *A. karroica* and one of the closely related *Geckolepis* species with *A. hawequensis* and *A. loveridgei*. As a result, the divergence between our two sampled *Afroedura* species is likely overestimated.

After natural log transforming our estimated species mean detachment angles, we used the R package OUwie (Beaulieu et al., 2012) and our phylogeny, scaled to a height of one, to fit multiple models of trait evolution to our data. We considered models that assume traits evolve under a random-walk process (Brownian motion with a mean and rate of drift) and models that assume traits evolve under a random-walk process with an additional parameter, α, that draw the traits values back towards a specific value, also known as the OU mean parameter (Ornstein-Uhlenbeck process). We considered seven models in total (see

Table 3.2). One of our Brownian motion models (BM1) and one of our Ornstein-Uhlenbeck models (OU1) each fit a single set of parameters across our entire dataset. Our other five models used clades chosen *a priori* to which different model parameter values would be fit. Anoles, Diplodactylidae geckos, and the clade containing Phyllodactylidae and Gekkonidae geckos represent our estimate of three independent evolutions of toe pads (Gamble et al., 2011; Irschick et al., 1996, see Figure 3.3). Gamble et al. (2012) suggested additional independent evolutions, in Phyllodactylidae and *Hemidactylus* for example, but our limited sampling within these clades prevented us from treating them separately in our models. Using our chosen clade assignments, we fit the following models: a Brownian motion model with variable evolutionary rate and mean values (BMS), an Ornstein-Uhlenbeck model with single $\alpha$ value, representing the strength of the pull towards the mean parameter, a single $\sigma^2$ parameter value, representing the rate of drift, and multiple mean values (OUM), an Ornstein-Uhlenbeck model with a single $\alpha$ but multiple means ($\theta$) and $\sigma^2$ values (OUMV), an Ornstein-Uhlenbeck model with a single $\sigma^2$ but variable $\theta$ and $\alpha$ values (OUMA), and a Ornstein-Uhlenbeck model in which all three parameters ($\theta$, $\sigma^2$, and $\alpha$) could vary among our assigned clades (OUMVA; see Table 3.2 and Beaulieu et al., 2012). We then compared the fit of our seven models using AICc weights based on relative model likelihoods and the Akaike Information Criterion values with a correction for small sample size (Burnham and Anderson, 2002) and BIC, the Bayesian Information Criterion; estimating a posterior probability for each of our focal models (Raftery, 1995; Schwarz, 1978).

Adhesive morphology may contribute to toe detachment angles across padded lizards. Thus, we also investigated how setal length and pad type may be correlated with adhesive performance. Setal length is known to vary across the toe (Johnson and Russell, 2009) and as

a result, we regard observations of maximum setal length to serve as a representation of a species' setal morphology. We gathered observations of maximum setal length and toe-pad type (undivided, divided and pairs; Table 3.1) from published sources (Bauer, 1998; Peattie, 2007; Ruibal and Ernst, 1965) and personal observations (TH, KC). In cases where measurements of our focal species were not available, we used setal measurements from closely related species. We used setal observations of *Pseudothecadactylus lindneri* in place of *P. australis*, *Ptyodactylus hasselquistii* in place of *P. guttatus*, and *Ptychozoon lionotum* in place of *P. kuhli*.

We also considered the relationship between pad type and detachment angle (Figure 3.5). Within geckos, several toe-pad morphologies have repeatedly evolved (Gamble et al., 2012). We assigned each focal species to an undivided, divided, or paired toe-pad class (TH, pers. obs.; see Table 3.1). These classes represent simplified categories, with each group containing an array of morphological diversity. Our paired class contained species with multiple pairs of adhesive pads such as *Hemidactylus* geckos, species with single pairs of adhesive pads like those found in the *Phyllodactylus* genus, and species with complex pad morphologies like those found in *Afroedura*, *Oedura*, and *Strophurus*. Our divided class also contained morphologically diverse species with the inclusion of one fan toed species *Ptyodactylus guttatus*. We natural log transformed our setal length measurements and observed toe detachment angles to normalize them. Using linear models and phylogenetic generalized least squares analyses (PGLS) with the R libraries caper (version 0.5) and ape (version 3.0-8; Orme et al., 2011; Paradis et al., 2004), we evaluated the affect of setal length and pad type on detachment angle. In our PGLS analyses we estimated Pagel's $\lambda$, bounded between zero and one, using a maximum likelihood approach to adjust our analyses in

accordance with the level of phylogenetic signal in our data (Pagel, 1997; Pagel, 1999; Revell, 2010). A λ value near zero suggests very little phylogenetic signal. In this scenario, our PGLS results will converge on our linear model results, with the phylogeny contributing little to our analyses. A λ value near one suggests strong phylogenetic signal and our PGLS analyses will be similar to a phylogenetic independent contrasts approach (Blomberg et al., 2012; Felsenstein, 1985).

Results

Toe detachment angle varied widely across padded lizards (Figure 3.2, Table 3.1), ranging from 15° to over 40°. When we consider detachment angle among clades (Figure 3.2, 3.3), we see detachment angle in anoles ranged from 15° to nearly 25°, lower than most gecko species. Gekkonidae and Phyllodactylidae geckos had the most variation, with detachment angles near 25° to over 40° (Figure 3.2, 3.3). Diplodactyline geckos were intermediate in performance between anoles and Gekkonidae and Phyllodactylidae, with detachment angles between 20° and 30° (Figure 3.2, 3.3).

When considering the multiple models of trait evolution we fit to our data, we found the Ornstein-Uhlenbeck model with multiple means and single $\sigma^2$ and α (OUM) to be the best supported model with an AICc weight of 0.84 and the next best supported model having a ΔAICc of over five (Table 3.2). Our BIC results were similar, with the OUM model having an estimated posterior probability of 0.84, and the next best model having a ΔBIC of over five (Table 3.2). Together, these results suggest considerable support for the OUM model (Burnham and Anderson, 2002; Raftery, 1995; Schwarz, 1978). Our OUM model estimated α to be 18.0 and $\sigma^2$ of 0.63 for our entire dataset. The estimated OU mean of our anole clade

was 19.16° (95% CI: 17.81 – 20.62). The mean parameter of the Gekkonidae and Phyllodactylidae clade was estimated at 31.52° (95% CI: 30.07 – 33.05). Lastly, we estimated a mean parameter value of 24.41° (95% CI: 22.60 – 26.36) for the Diplodactylidae clade. Using these values, we calculated the phylogenetic half-life of our trait (calculated as ln[2]/α; Hansen, 1997) to be 0.039. In other words, the time a species would take to move halfway towards the mean parameter value is 3.9% of our total tree depth. With a total tree depth of 168.8 million years, we estimated the phylogenetic half-life of our trait to be 6.51 million years, much shorter than our total tree length suggesting our model predicted a strong pull towards each clade's mean parameter value.

When we compared angle of toe detachment angle and morphology, we found setal length and detachment angle to be significantly negatively correlated for Gekkonidae and Phyllodactylidae geckos in both our linear model ($p = 0.02$) and PGLS analyses ($\lambda = 1$, $p = 0.01$; see Figure 3.4 and Table 3.3). Anoles and Diplodactylidae geckos showed no significant relationship. Within our small sample of setal lengths and detachment angles from Diplodactyidae geckos, we observed species that differed from anoles and the trend observed in Gekkonidae and Phyllodactylidae gecko including *Pseudothecadactylus australis* (detachment angle of 29.9° and setal length from P. lindneri of 37μm), *Strophurus williamsi* (detachment angle of 24.0° and setal length of 50μm), and *Rhacodactylus ciliatus* (18.8° and 47μm, see Figure 3.4). We also found that pad type was significantly correlated with detachment angle in our linear model analysis ($p = 0.01$, Table 3.3) but when we accounted for the relationships between species, estimating Pagel's λ at 0.9, this relationship was no longer significant ($p = 0.2$, Table 3.3).

Discussion

In this study, we showed that toe detachment angle is variable across species of padded lizards and may be influenced by setal morphology and pad type. We found support for our hypothesis in which our chosen clades, representing independent origins, were predicted to have unique OU mean parameter values. Our results suggest that our three chosen clades of padded lizards exhibit different performance capabilities. The performance values of our chosen clades tended to cluster around each clade's unique estimated OU mean. The performance of each clade may be distinct due to the idiosyncratic evolutionary history of each clade. In other words, since each clade may have evolved adhesive pads independently, each instance of adhesive pads may have different performance capabilities as compared to other independent origins due to historical contingency or constrains inherent in each clade.

We also observed correlations between toe detachment angle, setal length, and pad type. The observed association of setal length and detachment angle may vary across clades due to the clades differences in setal morphology. While anole setae are typically shorter then gecko setae (Peattie, 2007; Ruibal and Ernst, 1965), anole setae are also distinct in that they are not branched and have much larger terminal ends (called spatulae) as compared to most geckos (Ruibal and Ernst, 1965). Other setal characteristics, such as density, curvature, and diameter may also play a role in adhesive performance. Comparative micromechanics considering anoles and multiple families of geckos would be informative to determine how setal mechanics may vary between groups of padded lizards. Additional sampling of setal length and detachment angle of Diplodatylidae geckos would also be valuable to investigate

how Diplodactylidae geckos may differ from other geckos and anoles in regards to their relationship between setal length and adhesive performance.

Our analyses also found a significant relationship between pad type and toe detachment angle prior to accounting for the phylogenetic relationships between species. Similar toe-pad types have evolved multiple times between geckos and anoles as well as within geckos. Pad structure likely influences how padded lizards control their adhesive system as well as how setae interact with a substrate. Divided pads and paired adhesive pads, both divided along the sagittal plane (divided into left and right sections), may allow the toe-pad halves to work independently on rough surfaces. Toe-pad structure may also influence how geckos detach their feet during locomotion. Russell and Higham (2009) showed geckos changed their body posture when deploying their adhesive pads on inclined surfaces. To detach their toes during locomotion, geckos hyperextend their toes, curling their pads up and away from a substrate (Hu et al., 2012; Russell and Bels, 2001). The shape and orientation of the adhesive pads may influence this action. Comparative studies considering closely related species with dissimilar pad types, such as species with divided and undivided pads in the *Gehyra* genus, would be informative regarding how adhesive morphologies beyond the setal level, such as pad type, influence the adhesive abilities and kinematics of padded lizards.

While we considered the angle of toe detachment as a measure of adhesive performance in this study, performance of padded lizards has previously been quantified in different ways such as the generation of friction (Irschick et al., 1996; Irschick et al., 2006). Comparative studies considering how different measures of adhesive performance co-vary with setal morphology or microhabitat across species would be very informative. Toe-pad area has also previously been shown to correlate with the amount of friction generated by

anole toe pads (Irschick et al., 1996), presumably due to the fact that larger pads have more setae interacting with the substrate. This relationship has not been investigated regarding toe detachment angle. While we would not predict toe-pad area to be correlated with the angle of toe detachment due to the fact that detachment angle is likely related to setal morphology (Autumn et al., 2006a) and not the absolute number of setae contacting the surface, this relationship still requires evaluation.

Our observed variation in adhesive performance likely has ecological and biomechanical consequences for our focal species. Species with the lowest detachment angles (near 15°) only produced a maximum of 0.27 units of adhesion for one unit of friction (using tangent[detachment angle] = adhesion/friction; Autumn et al., 2006a), whereas our best performing species, with detachment angles over 40°, produced up to 0.84 units of adhesion for every unit of friction, over three times as much as our lowest performing species. This variation in performance may be correlated with ecological variables, including perching behavior or foraging style. Within anoles, variation in detachment angle appears to be higher in mainland species. This may be related to ecological differences between these groups (Losos, 2009; Macrini et al., 2003), or divergent pad morphology (Macrini et al., 2003). Lizards with higher detachment angles are likely capable of using highly angled or inverted perches with little risk of detachment. In contrast, species with lower detachment angles cannot generate as much adhesion relative to friction and thus may use different microhabitats. Extremely rough surfaces offer a reduced surface area for a gecko to attach to, and as a result, higher detachment angles may be able to compensate for surface texture. In addition, there may exist a trade-off in high and low detachment angles regarding the production of friction vs. adhesion. Species with a high detachment angle likely have setae

and spatuale shaped to maintain proper contact with a substrate under high setal shaft angles, producing some amount of both adhesion and friction, but less friction than if the setal shaft angle was near parallel with the substrate, translating the applied force into only friction. Although additional research considering the setal mechanics underlying detachment angle would be necessary to further describe this potential trade-off. Further work exploring the relationship between adhesive performance and habitat use of padded lizards is also crucial to place the performance continuum reported here in an ecological context. Our results also highlight the need to conduct more biomechanical studies of padded lizards with an explicit consideration of the variation in adhesive morphological diversity across species.

Acknowledgements

We would like to thank the National Science Foundation in collaboration with Aaron Bauer and Todd Jackman (Award #0844523), the National Geographic Society/Waitts Institute (Grant #W216-12), and Sigma XI (#G200803150489) for funding, Matt Pennell for helpful discussions, Jon Eastman and Josef Uyeda for help with figures and analyses, Jon Boone for access to animals, Bobby Espinoza, JR Wood, Jesse Grismer, and Mat Vickers for field logistics, and Andrew Schnell, Scott Harte, Jonathan Losos, Anthony Herrel, Shane Campbell-Staton, Kristi Fenstermacher, Hannah Frank, Martha Munoz, and Paul VanMiddlesworth for help collecting data in the lab and field.

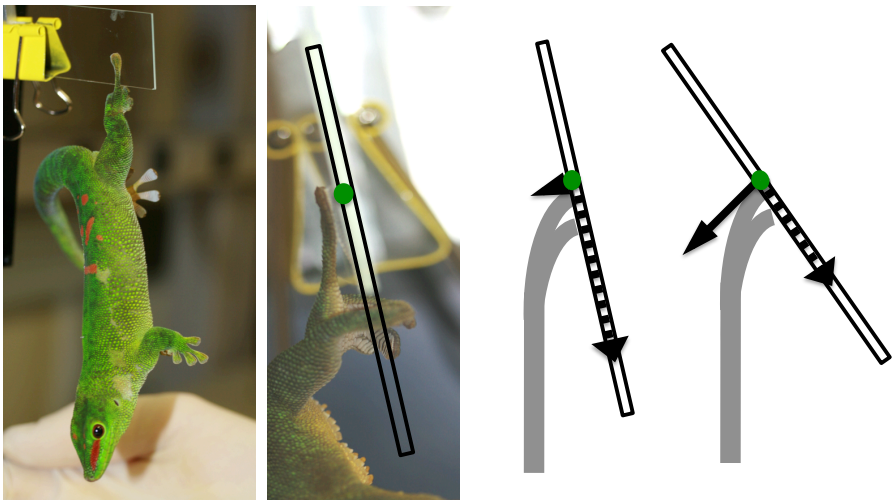

Figure 3.1. Angle of Toe Detachment Assay

To quantify toe detachment angle, a padded lizard is suspended from a glass microscope slide by a single rear toe (left images). When the glass substrate is near vertical, the lizard's toe pad, and hence setae, are generating predominantly friction (dashed arrow) relative to the substrate. As the substrate is slowly inverted, the setae generate less friction (dashed arrow) and more adhesion (negative normal force, solid arrow) relative to the substrate. At the angle of toe detachment, the setae (seen in gray) can no longer maintain the proper orientation with the substrate to remain attached and the animal falls onto a cushioned base. As a result, the angle to toe detachment quantifies the maximum amount of adhesion, relative to friction, a toe pad is capable of generating.

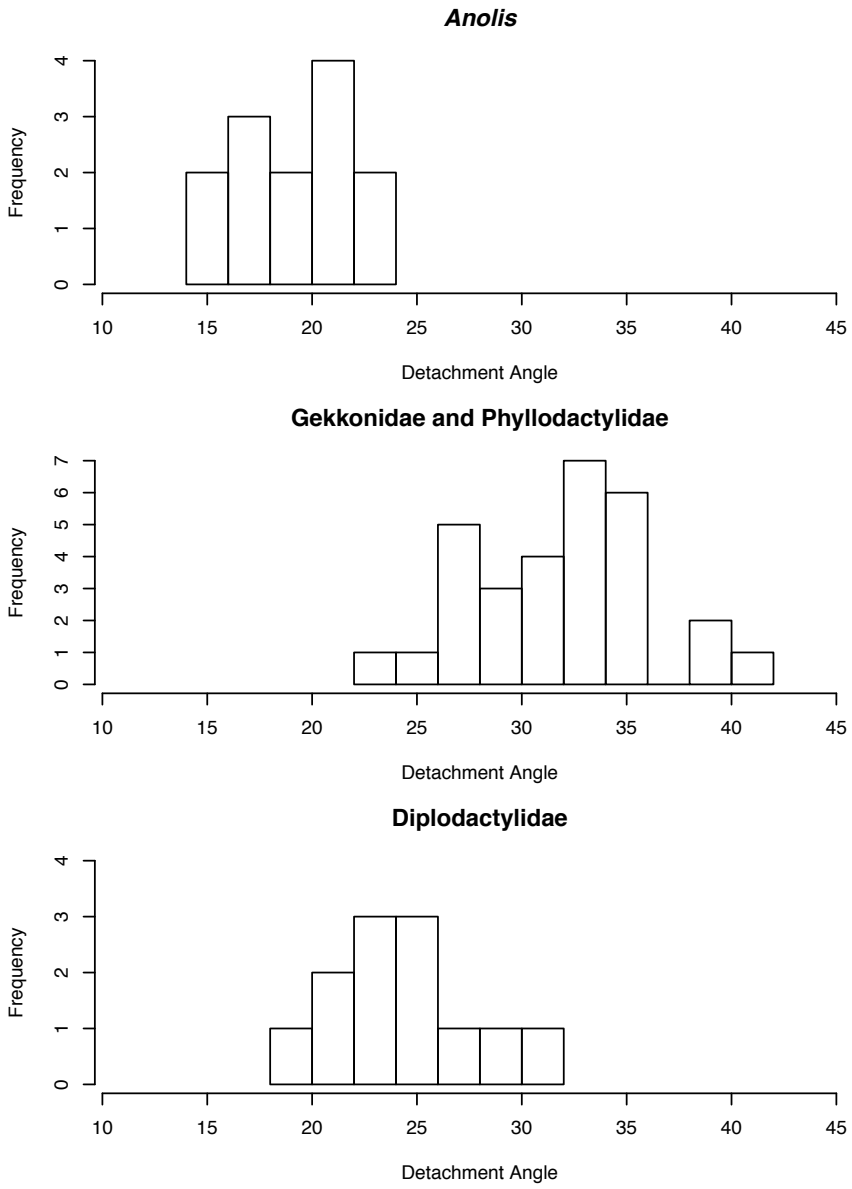


Figure 3.2. Variation in Detachment Angle

We measured toe detachment angle across 55 species of geckos and anoles. Of the three clades considered, anoles had the lowest detachment angles, followed by Diplodactylidae geckos. Gekkoinidae and Phyllodactylidae geckos had the highest and broadest range of detachment angles.

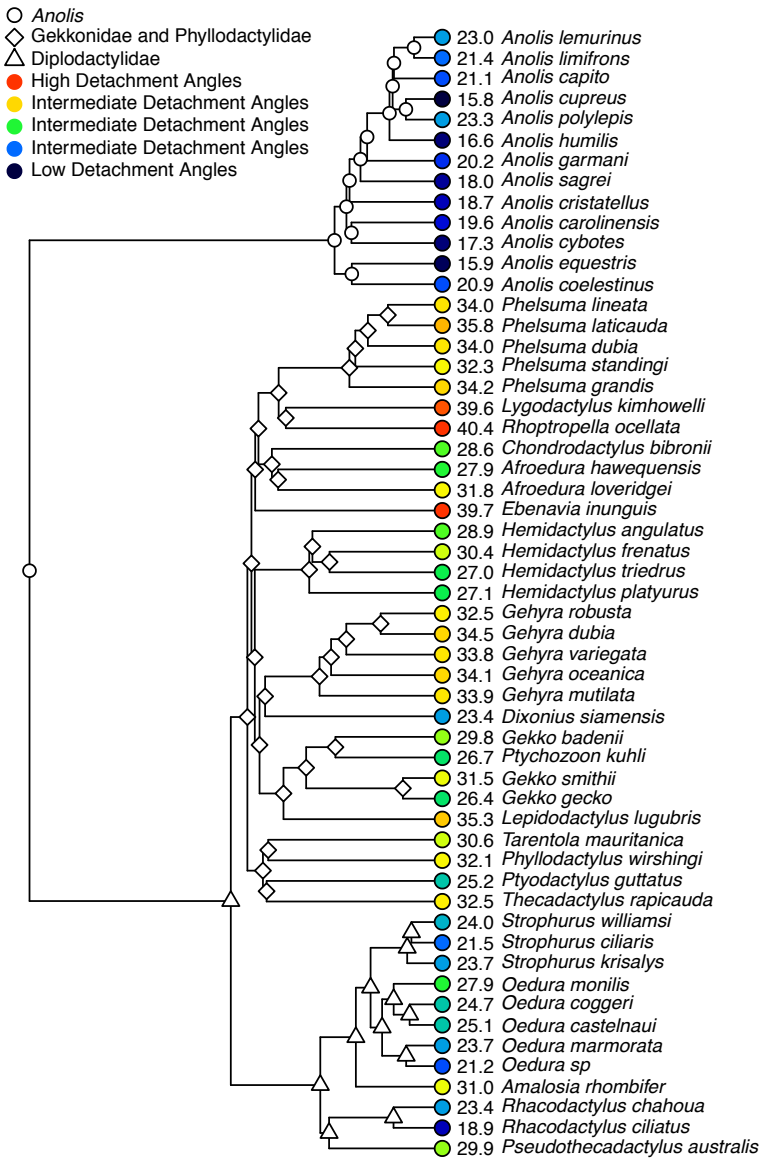


Figure 3.3. Phylogeny of Padded Lizards with Performance and Regime Assignments

We quantified toe detachment angle across 55 species of geckos and anoles. Colored circles and numbers at the tips of the tree represent each species estimated detachment angle. Warmer colors represent higher detachment angles. We fit our estimated detachment angles to multiple models of trait evolution, some of which required *a priori* clade assignments to fit multiple parameter regimes. In these analyses we chose three clades representing independent origins of adhesive toe pads. Our clades consisted of anoles (nodes with circles), Gekkonidae and Phyllodactylidae geckos (nodes with diamonds), and Diplodactylidae geckos (nodes with triangles).

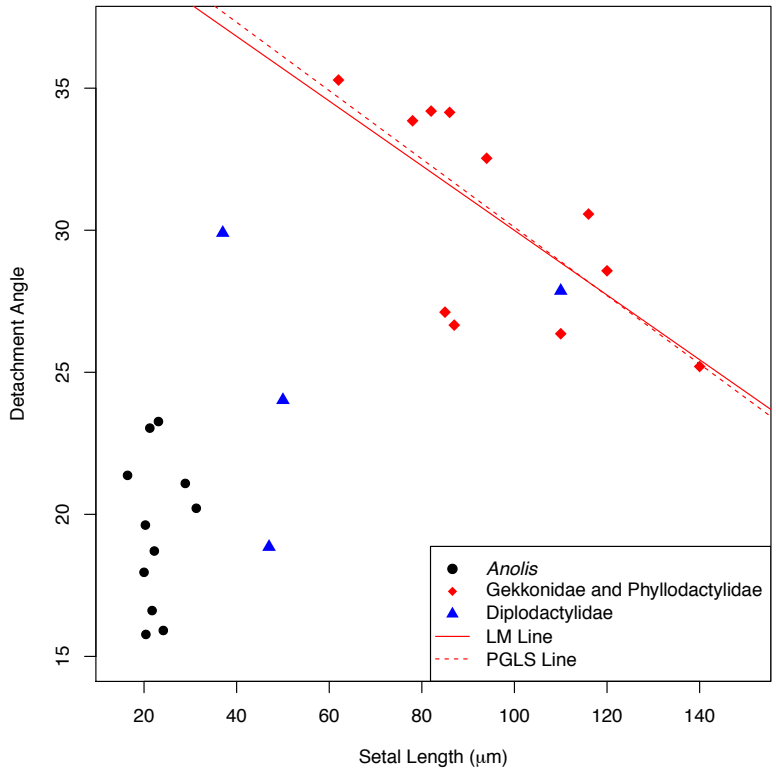


Figure 3.4. Setal Length vs. Toe Detachment Angle

We compared our estimated toe detachment angles to measurements of setal length, gathered from the literature and personal observations. We found setal length to be negatively correlated with detachment angle in Gekkonidae and Phyllodactylidae geckos using both a linear model analysis (red solid line) and a phylogenetic generalized least squares approach (red dashed line). Anoles do not have such a relationship. Our limited sampling of Diplodacylidae geckos also appear to diverge from the pattern seen in Gekkonidae and Phyllodacylidae.

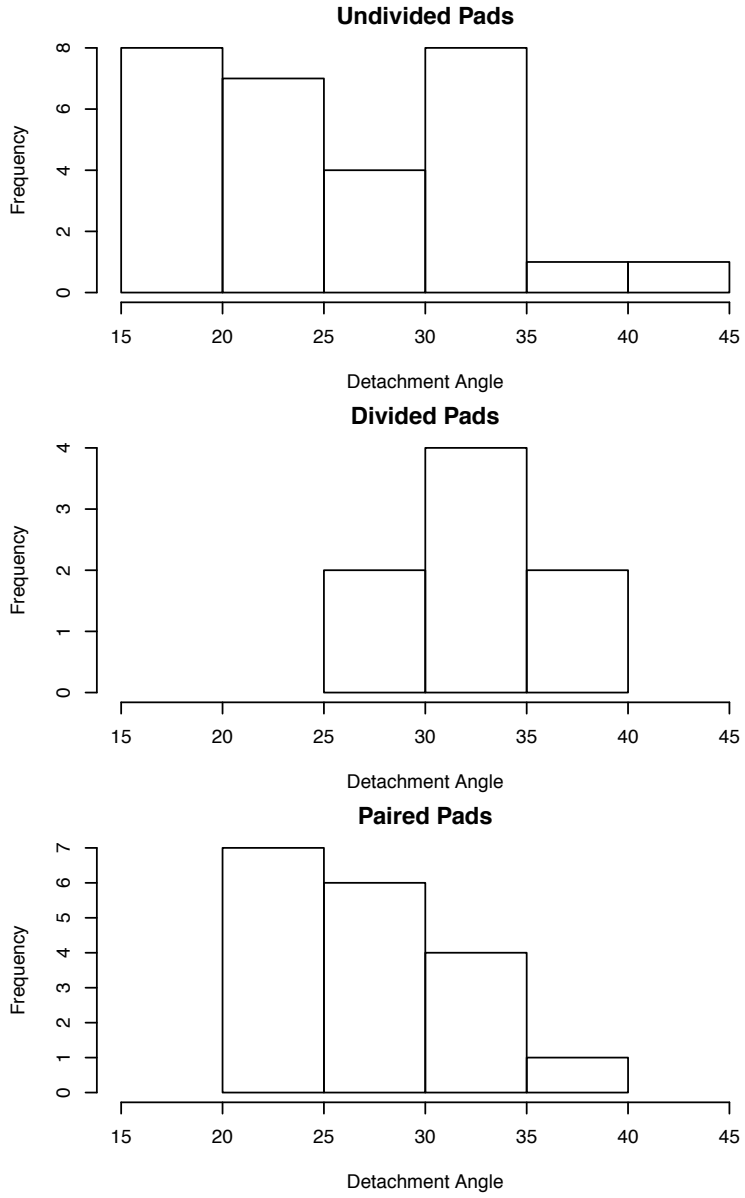


Figure 3.5. Toe Detachment Angle and Pad Type

Using pad type assignments of undivided, divided and paired, we compared pad type to our observed toe detachment angles across padded lizards.

| Species | Clade | Species Mean | Species Variance | Number of Individuals | Pad Type Assignment |
|---|---|---|---|---|---|
| *Anolis capito* | *Anolis* | 21.09 | 0.43 | NA | Undivided |
| *Anolis carolinensis* | *Anolis* | 19.62 | 0.81 | 6 | Undivided |
| *Anolis coelestinus* | *Anolis* | 20.89 | 0.06 | 3 | Undivided |
| *Anolis cristatellus* | *Anolis* | 18.71 | 0.71 | 7 | Undivided |
| *Anolis cupreus* | *Anolis* | 15.77 | 0.31 | NA | Undivided |
| *Anolis cybotes* | *Anolis* | 17.35 | 0.79 | 3 | Undivided |
| *Anolis equestris* | *Anolis* | 15.91 | 0.76 | 1 | Undivided |
| *Anolis garmani* | *Anolis* | 20.21 | 0.44 | 1 | Undivided |
| *Anolis humilis* | *Anolis* | 16.61 | 0.38 | NA | Undivided |
| *Anolis lemurinus* | *Anolis* | 23.04 | 0.41 | NA | Undivided |
| *Anolis limifrons* | *Anolis* | 21.37 | 0.51 | NA | Undivided |
| *Anolis polylepis* | *Anolis* | 23.27 | 0.28 | NA | Undivided |
| *Anolis sagrei* | *Anolis* | 17.96 | 0.78 | 7 | Undivided |
| *Amalosia rhombifer* | Diplodactylidae | 30.96 | 0.33 | 6 | Pairs |
| *Oedura castelnaui* | Diplodactylidae | 25.13 | 0.80 | 4 | Pairs |
| *Oedura coggeri* | Diplodactylidae | 24.72 | 0.02 | 4 | Pairs |
| *Oedura marmorata* | Diplodactylidae | 23.68 | 0.82 | 4 | Pairs |
| *Oedura monilis* | Diplodactylidae | 27.87 | 0.45 | 3 | Pairs |
| *Oedura sp.* | Diplodactylidae | 21.24 | 1.76 | 1 | Pairs |
| *Pseudothecadactylus australis* | Diplodactylidae | 29.91 | 1.00 | 2 | Divided |
| *Rhacodactylus chahoua* | Diplodactylidae | 23.43 | 0.12 | 6 | Undivided |
| *Rhacodactylus ciliatus* | Diplodactylidae | 18.85 | 0.22 | 3 | Undivided |
| *Strophurus ciliaris* | Diplodactylidae | 21.54 | 0.25 | 4 | Pairs |
| *Strophurus krisalys* | Diplodactylidae | 23.68 | 2.02 | 7 | Pairs |
| *Strophurus williamsi* | Diplodactylidae | 24.02 | 0.35 | 1 | Pairs |
| *Afroedura hawequensis* | Gekkonidae and Phyllodactylidae | 27.89 | 0.31 | 6 | Pairs |
| *Afroedura loveridgei* | Gekkonidae and Phyllodactylidae | 31.77 | 0.88 | 5 | Pairs |
| *Chondrodactylus bibronii* | Gekkonidae and Phyllodactylidae | 28.57 | 0.41 | 3 | Undivided |
| *Dixonius siamensis* | Gekkonidae and Phyllodactylidae | 23.38 | 0.71 | 3 | Pairs |
| *Ebenavia inunguis* | Gekkonidae and Phyllodactylidae | 39.71 | 0.08 | 4 | Pairs |
| *Gehyra dubia* | Gekkonidae and Phyllodactylidae | 34.48 | 0.31 | 8 | Undivided |
| *Gehyra mutilata* | Gekkonidae and Phyllodactylidae | 33.85 | 1.36 | 7 | Divided |
| *Gehyra oceanica* | Gekkonidae and Phyllodactylidae | 34.15 | 1.88 | 3 | Divided |
| *Gehyra robusta* | Gekkonidae and Phyllodactylidae | 32.50 | 0.98 | 7 | Undivided |
| *Gehyra variegata* | Gekkonidae and Phyllodactylidae | 33.84 | 0.33 | 8 | Divided |
| *Gekko badenii* | Gekkonidae and Phyllodactylidae | 29.84 | 1.19 | 6 | Undivided |
| *Gekko gecko* | Gekkonidae and Phyllodactylidae | 26.36 | 0.14 | 13 | Undivided |
| *Gekko smithii* | Gekkonidae and Phyllodactylidae | 31.49 | 0.97 | 5 | Undivided |
| *Hemidactylus angulatus* | Gekkonidae and Phyllodactylidae | 28.88 | 0.43 | 4 | Pairs |
| *Hemidactylus frenatus* | Gekkonidae and Phyllodactylidae | 30.37 | 2.04 | 4 | Pairs |
| *Hemidactylus platyurus* | Gekkonidae and Phyllodactylidae | 27.12 | 3.35 | 9 | Pairs |
| *Hemidactylus triedrus* | Gekkonidae and Phyllodactylidae | 26.96 | 0.50 | 4 | Pairs |
| *Lepidodactylus lugubris* | Gekkonidae and Phyllodactylidae | 35.29 | 0.33 | 6 | Divided |
| *Lygodactylus kimhowelli* | Gekkonidae and Phyllodactylidae | 39.58 | 1.31 | 5 | Divided |
| *Phelsuma dubia* | Gekkonidae and Phyllodactylidae | 34.02 | 0.43 | 4 | Undivided |
| *Phelsuma grandis* | Gekkonidae and Phyllodactylidae | 34.19 | 0.16 | 5 | Undivided |
| *Phelsuma laticauda* | Gekkonidae and Phyllodactylidae | 35.85 | 0.13 | 5 | Undivided |
| *Phelsuma lineata* | Gekkonidae and Phyllodactylidae | 33.96 | 0.21 | 5 | Undivided |
| *Phelsuma standingi* | Gekkonidae and Phyllodactylidae | 32.30 | 0.70 | 7 | Undivided |
| *Phyllodactylus wirshingi* | Gekkonidae and Phyllodactylidae | 32.13 | 0.61 | 4 | Pairs |
| *Ptychozoon kuhli* | Gekkonidae and Phyllodactylidae | 26.66 | 1.85 | 2 | Undivided |
| *Ptyodactylus guttatus* | Gekkonidae and Phyllodactylidae | 25.20 | 2.71 | 8 | Divided |
| *Rhoptropella ocellata* | Gekkonidae and Phyllodactylidae | 40.45 | 0.52 | 6 | Undivided |
| *Tarentola mauritanica* | Gekkonidae and Phyllodactylidae | 30.57 | 0.25 | 3 | Undivided |
| *Thecadactylus rapicauda* | Gekkonidae and Phyllodactylidae | 32.53 | 0.43 | 4 | Divided |

Table 3.1. Table of Focal Species

Species mean toe detachment angle and variance were estimated using the Weibull distribution (see Appendix). The number of individuals represents the number of lizards observed to measure each species angle of detachment. Observations from some species could not be grouped by individual (number of individuals = NA) and were treated as observations from a single individual in our analyses. The clade column represents the multi-rate regime assignments used in our analyses. Pad type assignment illustrates the pad type class we assigned to each focal species to investigate the relationship between performance and pad morphology.

| | LogLik | K | N | AICc | ΔAICc | Relative Model Likelihood | AICc Weights |
|---|---|---|---|---|---|---|---|
| OUM (multiple θ, single α, single $\sigma^2$) | 33.354 | 5 | 55 | -55.483 | 0.000 | 1.000 | 0.838 |
| OUMV (multiple θ, single α, multiple $\sigma^2$) | 33.378 | 7 | 55 | -50.373 | 5.110 | 0.078 | 0.065 |
| OUMA (multiple θ, multiple α, single $\sigma^2$) | 33.361 | 7 | 55 | -50.340 | 5.143 | 0.076 | 0.064 |
| BMS (single μ, multiple $\sigma^2$) | 28.607 | 4 | 55 | -48.414 | 7.069 | 0.029 | 0.024 |
| BM1 (single μ, single $\sigma^2$) | 24.770 | 2 | 55 | -45.310 | 10.173 | 0.006 | 0.005 |
| OU1 (single θ, single α, single $\sigma^2$) | 25.099 | 3 | 55 | -43.728 | 11.755 | 0.003 | 0.002 |
| OUMVA (multiple θ, multiple α, multiple $\sigma^2$) | 31.344 | 9 | 55 | -40.687 | 14.796 | 0.001 | 0.001 |

| | LogLik | K | N | BIC | Posterior Probability |
|---|---|---|---|---|---|
| OUM (multiple θ, single α, single $\sigma^2$) | 33.354 | 5 | 55 | -46.671 | 0.839 |
| BM1 (single μ, single $\sigma^2$) | 24.770 | 2 | 55 | -41.526 | 0.064 |
| BMS (single μ, multiple $\sigma^2$) | 28.607 | 4 | 55 | -41.185 | 0.054 |
| OUMV (multiple θ, single α, multiple $\sigma^2$) | 33.378 | 7 | 55 | -38.704 | 0.016 |
| OUMA (multiple θ, multiple α, single $\sigma^2$) | 33.361 | 7 | 55 | -38.672 | 0.015 |
| OU1 (single θ, single α, single $\sigma^2$) | 25.099 | 3 | 55 | -38.176 | 0.012 |
| OUMVA (multiple θ, multiple α, multiple $\sigma^2$) | 31.344 | 9 | 55 | -26.621 | 0.000 |

Table 3.2. OUwie Model Comparisons

We evaluated multiple models of trait evolution using our estimated toe detachment angles including Brownian motion with a single set of parameter values (BM1), Brownian motion with unique parameter values for each regime (BMS), an Ornstein-Uhlenbeck (OU) model with a single set of parameter values (OU1), an OU model with a single α and $\sigma^2$ across our data and unique means for each regime (OUM), an OU model with multiple means and $\sigma^2$ and single α values (OUMV), an OU model with multiple mean and α and single $\sigma^2$ values (OUMA), and lastly an OU model that allowed all three parameters to vary between regimes (OUMVA). K illustrates the number of free parameters each model used and N is our sample size, assumed to be the number of taxa in our phylogeny. We compared how our chosen models of trait evolution fit our data using both AIC (upper table) and BIC (lower table). We found that both model selection approaches support the OUM model with an AIC weight of 0.84 and a posterior probability of 0.84.

LM of Setal Length and Detachment Angle of Gekkonidae and Phyllodactylidae

| | Natural log Setal Length | Residuals |
|---|---|---|
| Sum of Squares | 0.073 | 0.082 |
| Degrees of Freedom | 1 | 9 |
| F | 7.979 | |
| p | **0.020** | |

LM of Pad Type and Detachment Angle

| | Pad Type | Residuals |
|---|---|---|
| Sum of Squares | 0.505 | 2.785 |
| Degrees of Freedom | 2 | 52 |
| F | 4.719 | |
| p | **0.013** | |

PGLS of Setal Length and Detachment Angle of Gekkonidae and Phyllodactylidae

Estimated λ 1.0

| | Intercept | Natural log Setal Length |
|---|---|---|
| Estimate | 5.177 | -0.388 |
| Standard Error | 0.577 | 0.126 |
| t | 8.977 | -3.076 |
| p | **0.000** | **0.013** |

PGLS of Pad Type and Detachment Angle

Estimated λ 0.9

| | Intercept | Pad Type |
|---|---|---|
| Degrees of Freedom | 1 | 2 |
| F | 707.109 | 1.471 |
| p | **0.000** | 0.239 |

Table 3.3. Linear Model and PGLS Results

We evaluated the relationship between toe detachment angle, setal length and pad type using linear models (LM) and phylogenetic generalized least squares (PGLS) analyses. Our PGLS analyses estimated Pagel's λ, where a λ value near 0 represents little phylogenetic signal in the data. A λ value near one suggests Brownian motion like evolution of our traits.

**Chapter 3. Bibliography**

Autumn, K., Dittmore, A., Santos, D., Spenko, M. and Cutkosky, M. (2006a). Frictional adhesion: a new angle on gecko attachment. J. Exp. Biol. 209, 3569-3579.

Autumn, K., Hsieh, S. T., Dudek, D. M., Chen, J., Chitaphan, C. and Full, R. J. (2006b). Dynamics of geckos running vertically. J. Exp. Biol. 209, 260-272.

Autumn, K., Sitti, M., Liang, Y. A., Peattie, A. M., Hansen, W. R., Sponberg, S., Kenny, T. W., Fearing, R., Israelachvili, J. N. and Full, R. J. (2002). Evidence for van der Waals adhesion in gecko setae. Proc. Natl. Acad. Sci. USA 99, 12252-12256.

Bauer, A. M. (1998). Morphology of the adhesive tail tips of carphodactyline geckos (Reptilia: Diplodactylidae). Journal of Morphology 235, 41-58.

Beaulieu, J. M., Jhwueng, D. C., Boettiger, C. and O'Meara, B. C. (2012). Modeling Stabilizing Selection: Expanding the Ornstein-Uhlenbeck Model of Adaptive Evolution. Evolution 66, 2369-2383.

Blomberg, S. P., Lefevre, J. G., Wells, J. A. and Waterhouse, M. (2012). Independent Contrasts and PGLS Regression Estimators Are Equivalent. Systematic Biology 61, 382-391.

Brown, D., Wilmer, J. W. and Macdonald, S. (2012). A revision of Strophurus taenicauda (Squamata; Diplodactylidae) with the description of two new subspecies from central Queensland and a southerly range extension. Zootaxa, 1-28.

Burnham, K. P. and Anderson, D. R. (2002). Model selection and multi-model inference: a practical information-theoretic approach: Springer Verlag.

Elstrott, J. and Irschick, D. J. (2004). Evolutionary correlations among morphology, habitat use and clinging performance in Caribbean Anolis lizards. Biological Journal of the Linnean Society 83, 389-398.

Felsenstein, J. (1985). Phylogenies and the comparative method. American Naturalist, 1-15.

Gamble, T., Bauer, A. M., Colli, G. R., Greenbaum, E., Jackman, T. R., Vitt, L. J. and Simons, A. M. (2011). Coming to America: multiple origins of New World geckos. Journal of Evolutionary Biology 24, 231-244.

Gamble, T., Greenbaum, E., Jackman, T. R., Russell, A. P. and Bauer, A. M. (2012). Repeated Origin and Loss of Adhesive Toepads in Geckos. PLoS ONE 7.

Glossip, D. and Losos, J. B. (1997). Ecological correlates of number of subdigital lamellae in anoles. Herpetologica 53, 192-199.

Hansen, T. F. (1997). Stabilizing selection and the comparative analysis of adaptation. Evolution 51, 1341-1351.

Hansen, W. R. and Autumn, K. (2005). Evidence for self-cleaning in gecko setae. Proc. Natl. Acad. Sci. USA 102, 385-389.

Harmon, L. J., Harmon, L. L. and Jones, C. G. (2007). Competition and community structure in diurnal arboreal geckos (genus Phelsuma) in the Indian Ocean. Oikos 116, 1863-1878.

Hu, S. H., Lopez, S., Niewiarowski, P. H. and Xia, Z. H. (2012). Dynamic self-cleaning in gecko setae via digital hyperextension. Journal of the Royal Society Interface 9, 2781-2790.

Huber, G., Gorb, S. N., Hosoda, N., Spolenak, R. and Arzt, E. (2007). Influence of surface roughness on gecko adhesion. Acta Biomater. 3, 607-610.

Irschick, D. J., Austin, C. C., Petren, K., Fisher, R. N., Losos, J. B. and Ellers, O. (1996). A comparative analysis of clinging ability among pad-bearing lizards. Biol. J. Linn. Soc. 59, 21-35.

Irschick, D. J., Herrel, A. and Vanhooydonck, B. (2006). Whole-organism studies of adhesion in pad-bearing lizards: creative evolutionary solutions to functional problems. J. Comp. Physiol. A 192, 1169-1177.

Johnson, M. K. and Russell, A. P. (2009). Configuration of the setal fields of Rhoptropus (Gekkota: Gekkonidae): functional, evolutionary, ecological and phylogenetic implications of observed pattern. J Anat 214, 937-55.

Lamb, T. and Bauer, A. M. (2010). Footprints in the sand: independent reduction of subdigital lamellae in the Namib–Kalahari burrowing geckos. Proc. R. Soc. B 273, 855-864.

Losos, J. B. (2009). Lizards in an evolutionary tree : the ecology of adaptive radiation in anoles. Berkeley: University of California Press.

Macrini, T. E., Irschick, D. J. and Losos, J. B. (2003). Ecomorphological differences in toepad characteristics between mainland and island anoles. Journal of Herpetology 37, 52-58.

McCool, J. I. (2012). Using the Weibull distribution: Reliability, modeling and inference: Wiley.

Oliver, P. M., Bauer, A. M., Greenbaum, E., Jackman, T. and Hobbie, T. (2012). Molecular phylogenetics of the arboreal Australian gecko genus Oedura Gray 1842 (Gekkota: Diplodactylidae): Another plesiomorphic grade? Molecular Phylogenetics and Evolution 63, 255-264.

Orme, C. D. L., Freckleton, R. P., Thomas, G. H., Petzoldt, T. and Fritz, S. A. (2011). caper: Comparative Analyses of Phylogenetics and Evolution in R. (http://R-Forge.R-project.org/projects/caper/).

Pagel, M. (1997). Inferring evolutionary processes from phylogenies. Zoologica Scripta 26(4), 331-348.

Pagel, M. (1999). Inferring the historical patterns of biological evolution. Nature 401, 877-884.

Paradis, E., Claude, J. and Strimmer, K. (2004). APE: Analyses of Phylogenetics and Evolution in R language. Bioinformatics 20, 289-290.

Peattie, A. M. (2007). The Function and Evolution of Gekkotan Adhesive Feet, vol. Doctor of Philosophy, pp. 61. Berkeley: University of California, Berkeley.

Pianka, E. R. and Huey, R. B. (1978). Comparative Ecology, Resource Utilization and Niche Segregation among Gekkonid Lizards in the Southern Kalahari. Copeia 691-701.

Pianka, E. R. and Pianka, H. D. (1976). Comparative Ecology of 12 Species of Nocturnal Lizards (Gekkonidae) in Western Australian Desert. Copeia 125-142.

Prowse, M. S., Wilkinson, M., Puthoff, J. B., Mayer, G. and Autumn, K. (2011). Effects of humidity on the mechanical properties of gecko setae. Acta Biomaterialia 7, 733-738.

Pugno, N. M. and Lepore, E. (2008). Observation of optimal gecko's adhesion on nanorough surfaces. BioSystems 94, 218-222.

Pyron, R. A., Burbrink, F. T. and Wiens, J. J. (2013). A phylogeny and revised classification of Squamata, including 4161 species of lizards and snakes. Bmc Evolutionary Biology 13, 93.

Raftery, A. E. (1995). Bayesian model selection in social research. Sociological methodology, 25, 111-164.

Revell, L. J. (2010), Phylogenetic signal and linear regression on species data. Methods in Ecology and Evolution, 1, 319–329.

Ruibal, R. and Ernst, V. (1965). The structure of the digital setae of lizards. J. Morphol. 117, 271-293.

Russell, A. P. (1979). Parallelism and Integrated Design in the Foot Structure of Gekkonine and Diplodactyline Geckos. Copeia 1979, 1-21.

Russell, A. P. and Bels, V. (2001). Digital hyperextension in Anolis sagrei. Herpetologica 57, 58-65.

Russell, A. P. and Higham, T. E. (2009). A new angle on clinging in geckos: incline, not substrate, triggers the deployment of the adhesive system. Proc. R. Soc. B 276, 3705-3709.

Russell, A. P. and Johnson, M. K. (2007). Real-world challenges to, and capabilities of, the gekkotan adhesive system: contrasting the rough and the smooth. Can. J. Zoolog. 85, 1228-1238.

Sadlier, R. A., O'Meally, D. and Shea, G. M. (2005). A New Species of Spiny-Tailed Gecko (Squamata: Diplodactylidae: Strophurus) from Inland Queensland. Memoirs of the Queensland Museum 51, 573-582.

Schwarz, G. (1978). Estimating the dimension of a model. Ann Stat 6,461–464.

Vanhooydonck, B., Andronescu, A., Herrel, A. and Irschick, D. J. (2005). Effects of substrate structure on speed and acceleration capacity in climbing geckos. Biological Journal of the Linnean Society 85, 385-393.

Zaaf, A. and Van Damme, R. (2001). Limb proportions in climbing and ground-dwelling geckos (Lepidosauria, Gekkonidae): a phylogenetically informed analysis. Zoomorphology 121, 45-53.

**Chapter 3. Appendix**

The angle of toe detachment assay was first described by Autumn et al. (2006). The goal of this assay is to measure a maximum value, the highest angle in which a toe pad can adhere to. Autumn et al. (2006) calculated mean observed detachment angle in their analyses. We feel that using the mean observed detachment angle may be misleading due to the fact that the assay represents a maximum value as well as the increasing probability of detachment through the course of the assay. Using our large dataset of observed detachment angles from 55 species of padded lizards as well as simulations, we evaluated the best technique to estimate a species' detachment angle and also considered how to incorporate detachment observations from multiple individuals. In addition, we conducted a power analysis to identify the minimum number of trials per individual and number of individuals needed to detect small differences between species. We summarize these results below. In short, we found the Weibull distribution to fit empirical observations better than the normal distribution. We also found the best approach to estimating toe detachment angle using observations from multiple individuals is to allow each individual to have its own set of Weibull parameter values. To estimate a species' mean detachment angle, we describe a technique to calculate a weighted average and variance using estimates from multiple individuals. Lastly, using the above-described method to estimate mean species toe detachment angle, we simulated multiple toe detachment datasets using the Weibull distribution and conducted a power analysis. We found our approach to have high levels of power, with the ability to detect small differences of one to two degrees between species with relatively weak sampling. We recommend a goal of collecting ten observations per individual to assure the ability to fit the Weibull distribution to each individual lizard's set of

observations, collecting data from at least two individual lizards per species. In conclusion, by using the Weibull distribution as an expected distribution of observed angles, we have more confidence in our experimental design and conclusions. We feel this approach is a superior technique to estimate the angle of toe detachment as opposed to simply averaging observed detachment angles (Autumn et al., 2006) or only using a subset of the highest observed angles.

The Weibull Distribution

The Weibull distribution is a two-parameter distribution often used to investigate material failure rates (McCool, 2012). One and three parameter versions of the Weibull distribution exist, but here we considered the two-parameter version. The Weibull distribution differs from the normal distribution in that in the Weibull distribution, the probability of an event occurring increases with some factor, usually time but in our case angle (Yang and Xie, 2003). This characteristic of the Weibull distribution compliments our toe detachment assay, where a lizard is suspended from a slowing inverting glass surface. The angle of the glass substrate increases with time. A more highly angled glass surface requires the generation of more adhesion, i.e., negative normal force relative to the surface, for a padded lizard to stay attached, and so assuming the probability of detachment increases with surface angle is appropriate.

The two-parameter Weibull distribution has a shape parameter ($k$, also known as Weibull modulus) and a scale parameter ($\lambda$). The Weibull probability distribution function is

$$f(x;k,\lambda) = \frac{k}{\lambda}\left(\frac{x}{\lambda}\right)^{k-1} e^{-\left(\frac{x}{\lambda}\right)^{k}} \text{ for } x > 0, \qquad \text{Eq. 3A.1}$$

with $x$ representing observed failure measurements. The Weibull cumulative distribution function is

$$F(x;k,\lambda) = 1 - e^{-\left(\frac{x}{\lambda}\right)^{k}}. \qquad \text{Eq. 3A.2}$$

The dimensionless shape parameter ($k$) dictates the shape of the distribution (see Figure 3A.1).

When $k < 1$, the probability of failure decreases with time.

When $k = 1$, the distribution simplifies into the exponential distribution with a constant relationship between failure and time.

When $k = 2$, the distribution simplifies into the Rayleigh distribution

When $1 < k < 4$, the distribution is right skewed, with failure rate increasing rapidly and then slowly decreasing with time

When $k > 4$, the distribution is left skewed, with failure rate slowly increasing with time and then rapidly decreasing.

The scale parameter ($\lambda$), with the same units as the data, pushes the distribution along the x-axis. When the shape parameter is held constant, a larger scale parameter will stretch the distribution, moving its peak farther down the x-axis and decreasing the distribution's height. When the scale value increases, a relatively larger shape parameter is needed to narrow the distribution and increase the distribution's height (see Figure 3A.1).

Evaluating the Weibull Distribution

To evaluate the use of the Weibull distribution with toe detachment data, we conducted multiple analyses. We first compared the fit of the Weibull distribution to the normal distribution using empirical data. We then expanded this comparison to include the gamma and log-normal distributions. We then considered the goodness of fit of our data to the Weibull distribution. Based on our results comparing our data to different distributions, we then evaluated the best technique to incorporate toe detachment observations from multiple individual lizards using the Weibull distribution. We also identified an approach to combine estimates of toe detachment angle from multiple individuals to arrive at a weighted species mean and variance. Lastly, we conducted simulations to perform a power analysis to investigate the effect of sample size, i.e., the number of trials per individual and the number of individual lizards sampled, on our ability to detect small differences in detachment angle between species.

We first compared the fit of the Weibull distribution to the normal distribution using two empirical datasets, both considering toe detachment observations from *Gekko gecko*. Our first dataset included 206 observations from multiple individual lizards (n = 13). Our second dataset, a subset of the first, used 40 observations from a single lizard. We found that, qualitatively, the Weibull distribution appears to fit our empirical data better than the normal distribution (note the small deviations from the line y = x in the left QQ plots; Figure 3A.2). The estimated Weibull scale parameter also estimated a more accurate overall angle of detachment (blue solid vertical lines in right histograms, Figure 3A.2) as compared to the estimated mean (red dashed vertical line in right histograms, Figure 3A.2).

Previous studies have shown that the Weibull distribution can sometimes be difficult to distinguish from other distributions such as the gamma distribution so we compared the fit of the normal, Weibull, gamma, and log-normal distributions to our two empirical datasets to evaluate what distribution our data is most similar to (Bain and Engelhardt, 1980; Fearn and Nebenzahl, 1991; Table 3A.1). We found that the Weibull distribution was the best fitting model of the models we considered with an AICc weight (Akaike Information Criterion with a correction for small sample sizes) and estimated posterior probability of 0.94 for our large dataset (Burnham and Anderson, 2002; Raftery, 1995; Schwarz, 1978; Table 3A.1). Using our smaller dataset, we calculated an AICc weight and posterior probability of 0.81 for the Weibull distribution (Table 3A.1). These values suggest considerable support for the Weibull distribution as compared to the other distributions we considered (Burnham and Anderson, 2002, Raftery, 1995; Schwarz, 1978). We then evaluated the goodness of fit of the Weibull distribution to our data using a bootstrap version of the Kolmogorov-Smirnov test to evaluate the probability that our data could have drawn from the Weibull distribution. This modified test allows for the multiple instances of the same value in a dataset (Sekhon, 2008). We found our large dataset to be significantly different than predicted by the Weibull distribution ($p = 0.005$), while our smaller dataset was not ($p = 0.7$). These results suggest that the Weibull distribution fits our data well compared to other selected distributions, but may not perfectly describe our observations. In addition, our larger distribution represents a collection of observations from multiple individuals; possibly each with their own unique performance parameters, and this may be why we found it to be significantly different then predicted by the Weibull distribution.

To investigate the variation between individuals and how best to analyze observations from multiple individuals, we again used the previously mentioned complete *G. gecko* dataset with 206 observations from multiple individuals. We fit the Weibull distribution to all of our observations lumped together and calculated the log likelihood score (our null model). We also allowed each individual lizard (n = 13) to have their own set of parameters and summed the log likelihood scores from each individual lizard's model fit (our alternative model). We then conducted a likelihood ratio test and found a delta of 100.3. Using the chi squared distribution and 24 degrees of freedom; we found a p value of $< 0.0001$, suggesting it is significantly better to allow each individual lizard its own set of parameter values. We also fit a parametric survival regression model using the Weibull distribution where individual predicted detachment angle using the R library survival (Therneau, T. 2013. *A Package for Survival Analysis in S*). We found individual significantly predicted detachment angle ($p < 0.0001$), again suggesting it is better to treat each individual lizard separately. Individual lizards may perform differently due to variation in shed cycle, individual performance, equipment, operator, or environmental factors.

Using a set of estimated detachment angles for each observed lizard (i.e., scale parameter estimates and standard deviations), we proposed calculating a weighted species average detachment angle, weighting each individual lizard's estimate by the confidence in that estimate. To calculate the weights, *w*, we used the following equation, where $\sigma_i^2$ is the error around the scale parameter for individual *i*:

$$w_i = \frac{1}{\sigma_i^2}. \qquad \text{Eq. 3A.3}$$

We then calculated a weighted mean, $\bar{x}$, using the following equation, where $n$ is the number of individuals and $x_i$ is the estimated scale value for individual $i$:

$$\bar{x} = \frac{\sum_{i=1}^{n}\left(x_i w_i\right)}{\sum_{i=1}^{n} w_i}. \qquad \text{Eq. 3A.4}$$

To calculate the variance around our weighted mean, $\sigma_{\bar{x}}^2$, incorporating within and between individual variation, we used the following equation:

$$\sigma_{\bar{x}}^2 = \frac{1}{\sum_{i=1}^{n}\left(\frac{1}{\sigma_i^2}\right)} * \frac{1}{(n-1)} * \sum_{i=1}^{n}\frac{\left(x_i - \bar{x}\right)^2}{\sigma_i^2}. \qquad \text{Eq. 3A.5}$$

It is worth noting that this equation for the variance of a weighted mean is one of many options for calculating the error around a weighted mean. In addition, when the individual errors ($\sigma_i^2$) are all equal, the above equation simplifies into the standard error around an unweighed mean.

Power analyses

Using the above described technique to estimate a species' mean detachment angle with observations from multiple individual lizards, we investigated the trade-off between the number of detachment trials per individual and the number of individuals tested regarding its affect on our ability to detect differences between species. When conducting research using live animals, it is necessary to know how many individuals will be needed to infer significant results as well as the testing procedure for each individual. This information is necessary for

multiple reasons. The number of individual animals needed for an experiment and specific experimental protocols are required for the approval of the project from ethics committees and field collection permit agencies. From a financial and logistics perspective, animals need to be purchased and housed in the proper facilities and the length of time spent in the field to secure the proper number of individuals needs to be known. These factors all depend on the number of individual lizard to be tested, the expected time spent testing each individual, and the sensitivity of the results desired.

In order to simulate the data necessary for a power analysis, we first needed to obtain realistic shape and scale parameter values. We chose a range of scale parameters (15° to 35°) based our empirical observations of toe detachment angle across padded lizards. Because the Weibull distribution is heteroscedastic (McCool, 2012), i.e., inconsistent variances, the shape parameter is affected by changes to the scale parameter and simulating datasets with various scale parameters, yet similar overall form and skew is difficult. In addition, an estimated shape parameter is sensitive to sample size, with smaller datasets predicting larger shape values (narrower distributions). As a result, we chose to use empirical data to estimate realistic shape parameters for a given scale value and number of samples as part of our power analysis.

Using a dataset of toe detachment observations from 55 species of gecko and anole species, excluding species lacking individual assignments of detachment observations, we extracted the estimated shape, scale and number of trials for all individuals observed (see Table 3.1). We fit these data to a linear model where shape was predicted by scale, number of trials, and the interaction between these terms. We found both scale ($p < 0.0001$) and number of trials ($p < 0.0001$) to significantly predict shape. The interaction term was not significant

and removed from the analysis. We used the following coefficients to estimate realistic shape values for a given scale value and number of trials:

$$Shape = 0.6286 * Scale - 0.5142 * N + 9.1317. \quad \text{Eq. 3A.6}$$

We produced multiple datasets of simulated toe detachment data using the Weibull distribution. We first held the total number of trials constant at 20, distributed across one individual (with 20 trials), two individuals (with 10 trials each), and four individuals (with five trials each). We evaluated datasets with low detachment angles i.e. drawn from distributions with low scale parameters, and datasets with high detachment angles i.e. simulating data with high scale values. In each dataset we considered effect sizes of one, two, three, five, and ten. In total, we compared detachment angles of 15° vs. 16°, 15° vs. 17°, 15° vs. 18°, 15° vs. 20°, 15° vs. 25°, 25° vs. 26°, 25° vs. 27°, 25° vs. 28°, 25° vs. 30°, and 25° vs. 35°. We also conducted a second set of analyses using 50 total trials distributed across two individuals (25 trials each), five individuals (ten trials each), and ten individuals (five trials each) using the same high and low datasets and effect sizes as described above. To compare our estimated weighted averages between species, we tested whether either of the species' means were within 1.96 standard deviations (square root of the estimated mean variance multiplied by 1.96) of the other species. We then calculated the percentage of our 1000 replicate trials produced significantly different comparisons (Figure 3A.3).

We found abundant power to detect small differences in the scale parameter (effect sizes of one to two) even with relatively small datasets, i.e., few total trials, few individuals, or few trials per individual. Datasets with more individuals and fewer trials per individual appear to have more power for a given total amount of data, yet fitting the Weibull distribution to datasets with five or fewer observations per individual, especially if there is

little variation among the observations, can be problematic and cause the operation to fail. In our simulations using 50 total observations, we observed an overall increase in power, as to be expected with an increase in the amount of data regardless of partitioning. In addition, we did not observe differences between datasets considering low detachment angles and high detachment angles. We believe this is due to the fact that we chose our shape parameter with regard to the scale and the number of trials per individual. We conducted similar analyses where the shape parameter was held constant regardless of the scale value and number of trials per individual and found power to decrease when considering higher scale values. This is because at higher scale values, with a constant shape parameter, the Weibull distribution is relatively wider with a larger variance, reducing the power to detect differences between species.

## Conclusions

In light of our analyses, we feel using the Weibull distribution and weighted averages to estimate mean species toe detachment angle is a significant improvement over previously used simpler approaches (Autumn et al., 2006). In addition to our above-described method, a Bayesian approach estimating species level meta parameters is conceivable, but we felt such an approach was beyond the scope of this project. With regards to experimental design, we recommend ten trials per individual to assure a successful fit of the Weibull distribution. We found it problematic to fit the distribution to datasets with fewer than five trials per individual, and occasionally more if there was little variation among the observations. We then recommend collecting observations from as many individuals as the experiment allows.

Even when only considering data from two individual lizards with ten trials each, we consistently had enough power to detect a difference of one degree in 80% of the time.

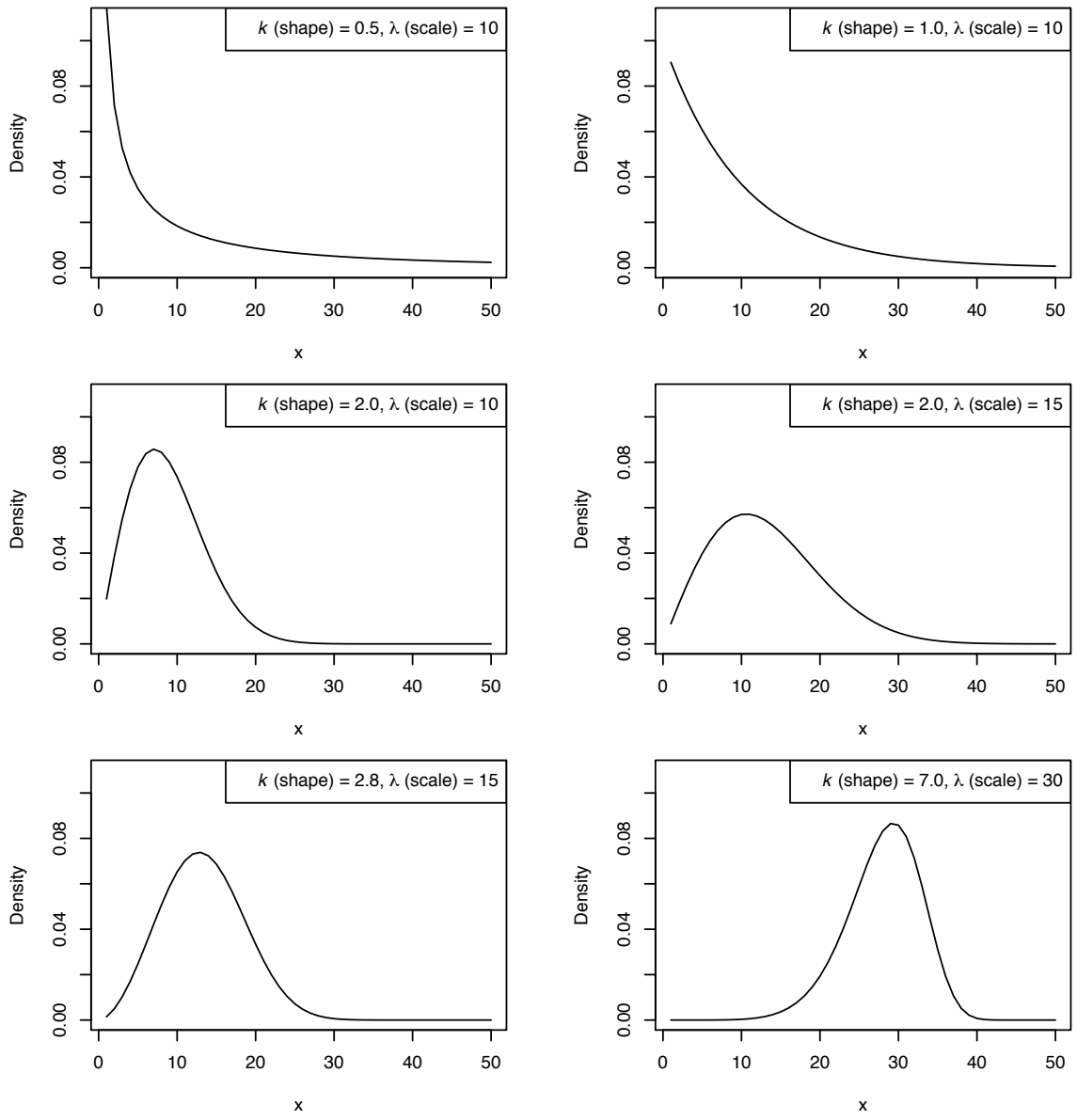


Figure 3A.1. Variation in Weibull Parameters and Distribution

The shape and scale parameters of the Weibull distribution interact to dictate the shape and location of the curve. Here we display multiple distributions with various parameter values illustrating the variation possible.

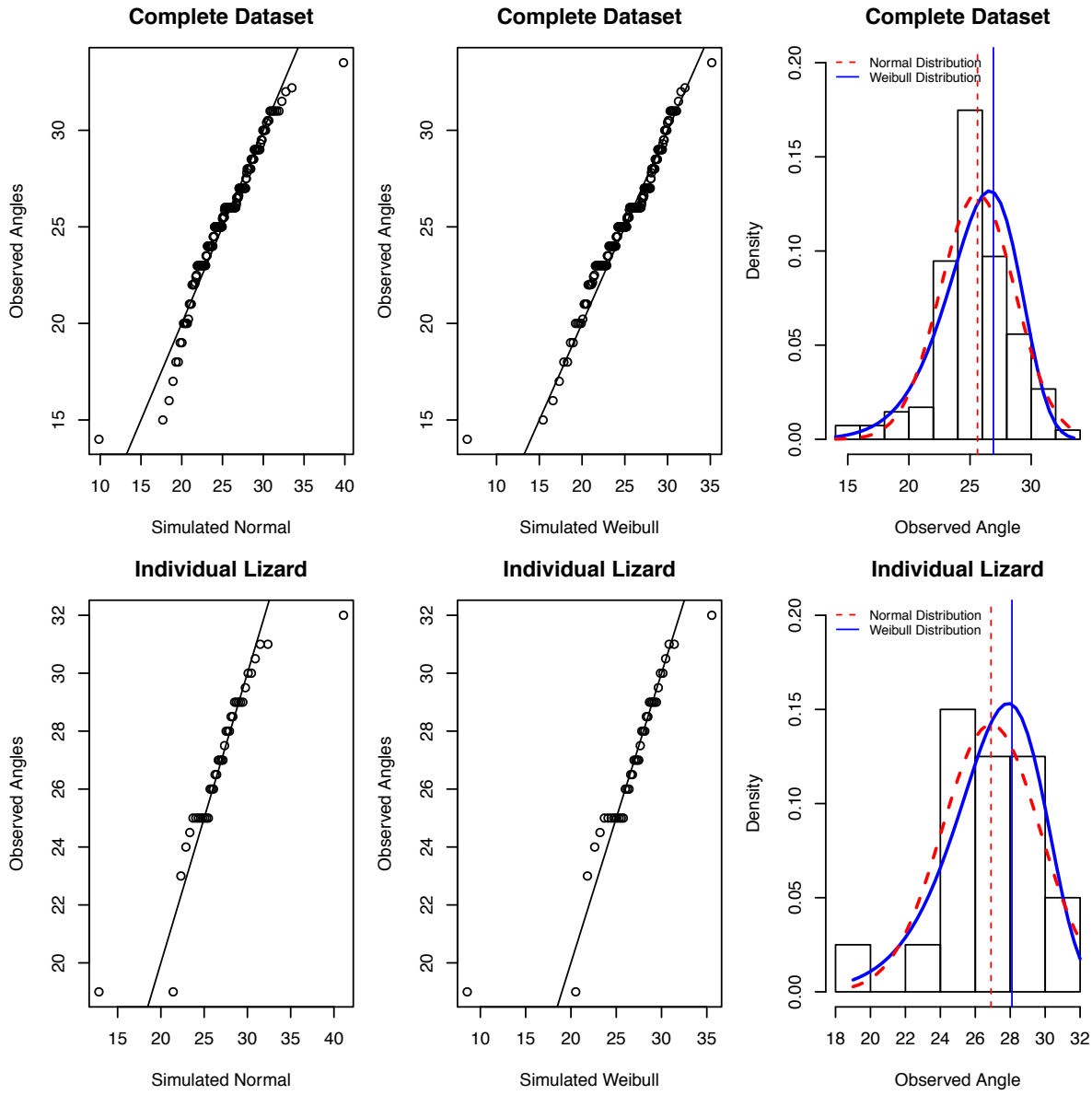


Figure 3A.2. Fit of Empirical Data to the Weibull

To determine the qualitative fit of the Weibull distribution to empirical data; we generated QQ plots using our complete dataset from *Gekko gecko* (top plots) and a subset of the data from only one individual lizard (lower plots). The QQ plots also contain a line at y = x as reference. The histograms on the right display our raw data with the two fitted distributions (Weibull in solid blue and normal in dashed red). The vertical lines illustrate the estimated Weibull scale parameter value (blue solid line) and mean (red dashed line)

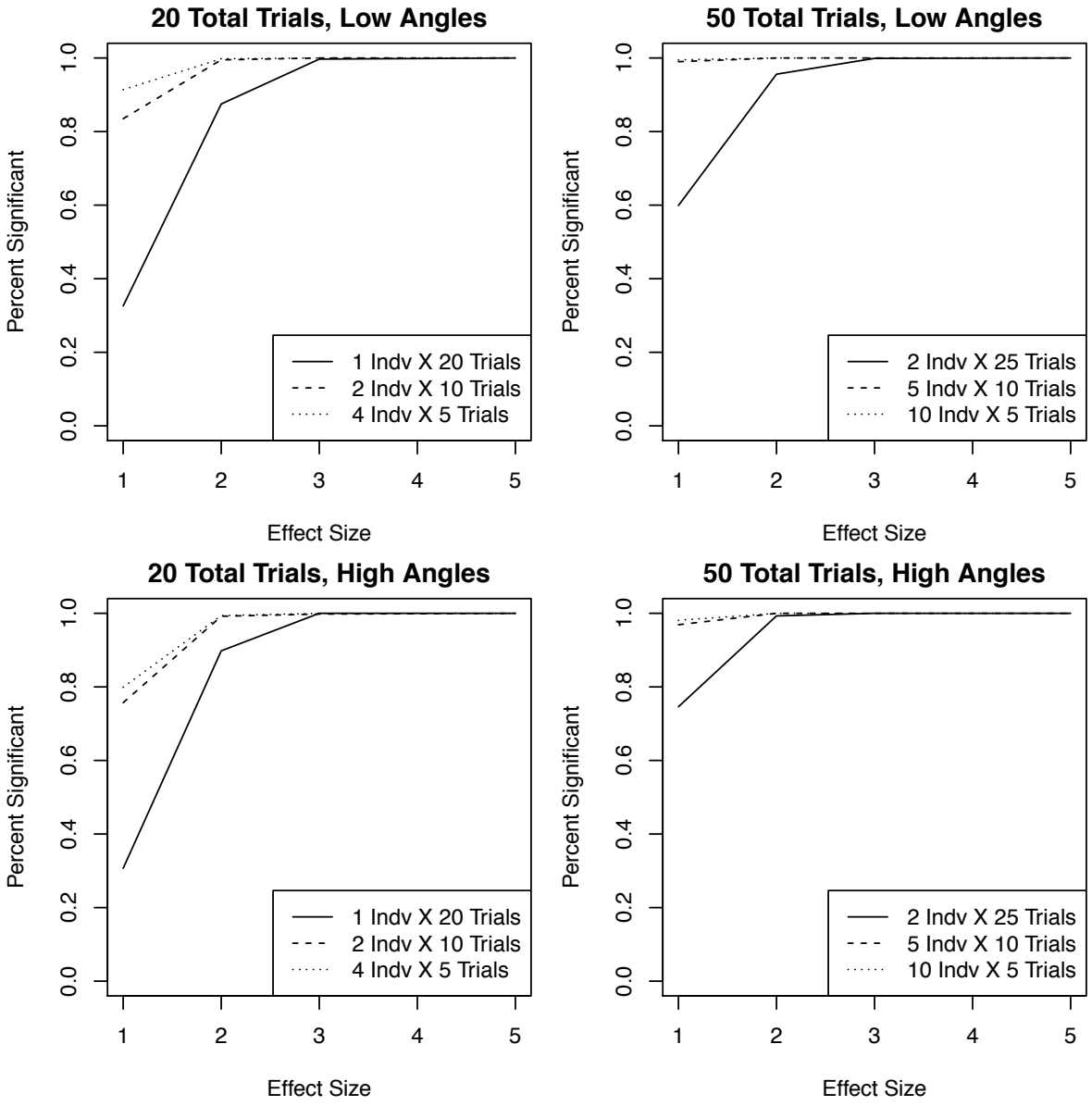


Figure 3A.3. Weibull Power Analyses

In our power analysis, we considered two sets of effect sizes (low detachment angles from 15° to 25° in the upper plots, and high detachment angles from 25° to 35° in the lower plots) as well as datasets using 20 total trials (left plots) and 50 total trials (right plots). The y-axes represent the percentage of our 1000 replications that were significantly different for a given set of parameters and effect size.

**Large Dataset**

| Distribution | N | K | Log Likelyhood | AICc | AICc Weight | BIC | Posterior Probability |
|---|---|---|---|---|---|---|---|
| Normal | 206 | 2 | -522.56 | 1049.18 | 0.061 | 1055.78 | 0.061 |
| Weibull | 206 | 2 | -519.83 | 1043.73 | 0.939 | 1050.32 | 0.939 |
| Gamma | 206 | 2 | -530.51 | 1065.09 | 0.000 | 1071.69 | 0.000 |
| Log-Normal | 206 | 2 | -535.80 | 1075.67 | 0.000 | 1082.27 | 0.000 |

**Single Individual**

| Distribution | N | K | Log Likelyhood | AICc | AICc Weight | BIC | Posterior Probability |
|---|---|---|---|---|---|---|---|
| Normal | 40 | 2 | -98.07 | 200.46 | 0.137 | 203.52 | 0.137 |
| Weibull | 40 | 2 | -96.29 | 196.91 | 0.813 | 199.96 | 0.813 |
| Gamma | 40 | 2 | -99.45 | 203.23 | 0.034 | 206.29 | 0.034 |
| Log-Normal | 40 | 2 | -100.25 | 204.83 | 0.015 | 207.89 | 0.015 |

Table 3A.1. Toe Detachment Angle and Model Selection

We fit out data to multiple distributions to determine which focal distribution was most similar to our observed toe detachment angles. We considered a large dataset with 206 observations (N) from 13 individuals and a smaller dataset composed of 40 observations from a single individual. K illustrates the number of free parameters each model had. We found the Weibull distribution to be the most similar to our observed dataset of toe detachment angles.

**Chapter 3. Appendix Bibliography**

Autumn, K., Dittmore, A., Santos, D., Spenko, M. and Cutkosky, M. (2006). Frictional adhesion: a new angle on gecko attachment. J. Exp. Biol. 209, 3569-3579.

Bain, L. J., & Engelhardt, M. (1980). Probability of correct selection of Weibull versus gamma based on livelihood ratio. Communications in statistics-theory and methods, 9(4), 375-381.

Burnham, K. P. and Anderson, D. R. (2002). Model selection and multi-model inference: a practical information-theoretic approach: Springer Verlag.

Fearn, D. H., & Nebenzahl, E. (1991). On the maximum likelihood ratio method of deciding between the Weibull and Gamma distributions. Communications in Statistics-Theory and Methods, 20(2), 579-593.

McCool, J. I. (2012). Using the Weibull distribution: Reliability, modeling and inference: Wiley.

Raftery, A. E. (1995). Bayesian model selection in social research. Sociological methodology, 25, 111-164.

Schwarz, G. (1978). Estimating the dimension of a model. Ann Stat 6,461–464.

Sekhon, J. (2008). Multivariate and propensity score matching software with automated balance optimization: the matching package for R. Journal of Statistical Software, Forthcoming.

Yang, Z. L. and Xie, M. (2003). Efficient estimation of the Weibull shape parameter based on a modified profile likelihood. Journal of Statistical Computation and Simulation 73, 115-123.

**Chapter 4. How Geckos Stick in Nature: Ecology and Biomechanics of Gecko Feet**

Travis J. Hagey, Scott Harte, Mathew Vickers, Luke J. Harmon, Lin Schwarzkopf

Abstract

Phenotype and performance play a fundamental role in evolution and ecology. Studies of form and function often use correlations between morphology, performance, and habitat use to examine patterns of ecomorphology and morphological adaptation. Geckos, of the taxonomic group Gekkota, are an understudied yet diverse clade of lizards in which studies of form and function would greatly improve our understanding of their evolution. Geckos have the rather unique trait of adhesive toe pads, enabling them to use arboreal and rocky environments in a way few other animals can. Gecko toe-pad morphology and adhesive abilities are highly variable across species, suggesting ecological adaptations may have driven their evolution, yet few studies has considered gecko adhesive morphology and performance in an ecological context. In this study, we quantified morphology, adhesive performance, and habitat use of 13 gecko species from Queensland, Australia including tropical, arid, arboreal, and rock-dwelling species. We found toe detachment angle to be correlated with residual limb length. We also found residual limb length to be correlated with the use of arboreal and rock microhabitats as well as negatively correlated with perch diameter. This study is one of the first examples investigating gecko adhesive performance and specific microhabitat parameters. We suggest additional comparative studies investigating gecko limb kinematics and setal mechanics to corroborate our observational results.

Introduction

The processes of evolution and adaptation link a species' phenotype and ecology. Habitat use is one facet of ecology that is typically strongly related to morphology, where particular microhabitats may select for specialized phenotypic structures. Studies of form and function often focus on the relationships between an organism's morphology, performance capabilities, and ecology, quantifying correlations between these traits to suggest adaptation (Autumn et al., 2002a; Losos, 1994; Losos, 2009; Wainwright and Reilly, 1994).

Geckos are an excellent group to apply such an approach. They are a diverse group of lizards that live in a wide array of environments including arboreal, rocky, and terrestrial microhabitats. Geckos are also well known for their adhesive toe pads. The ventral surface of a gecko's toe pad has millions of microscopic hair-like structures called setae (Russell, 2002). A gecko's setae interact with a substrate using van der Waal's forces to generate strong adhesion (negative normal force) and friction (Autumn et al., 2002b). Gecko toe-pad morphology is highly variable across species and genera, including simple undivided pads, complex divided or fan-like pads, paired adhesive pads, and feet without pads (Gamble et al., 2012; Peattie, 2007; Ruibal and Ernst, 1965; Russell, 2002). There are also many examples of convergent toe-pad shapes between distantly related genera (Gamble et al., 2012; Russell, 1979). Setal morphology is also highly variable across species, with species exhibiting a variety of setal lengths, diameters, and densities (Bauer, 1998; Peattie, 2007; Ruibal and Ernst, 1965). Together, this variation suggests the gecko adhesive system may have evolved adaptively, but this variation has not yet been considered in an ecological context (but see; Hecht, 1952; Huber et al., 2007; Pugno and Lepore, 2008; Russell and Johnson, 2007). In addition, there has been much research investigating the biomechanical properties of gecko

adhesion (Autumn et al., 2006a; Autumn et al., 2006b; Huber et al., 2007; Pesika et al., 2009; Pugno and Lepore, 2008; Yamaguchi et al., 2009). Thus, geckos provide an excellent opportunity to test hypotheses regarding form and function relationships.

The frictional adhesion model (Autumn et al., 2006a) describes how geckos generate adhesion and friction. As part of this model, Autumn et al. (2006a) described a single parameter, toe detachment angle, which captures the performance abilities of a gecko toe pad. The angle of toe detachment is a whole-animal performance assay that quantifies the maximum ratio of adhesion and friction a gecko's toe pad can generate, which is likely mechanically linked to setal orientation and morphology (Autumn et al., 2006a; Hagey et al., in review; Tian et al., 2006). The angle of toe detachment can easily be measured in the field with minimal equipment (Figure 4.1). If particular species' toe detachment angle has been influenced by selection imposed by microhabitat, then this measure of performance may be correlated with particular ecological parameters. For example, species with low detachment angles produce less adhesion relative to friction, requiring more applied force to produce similar levels of adhesion. As a result, species with low detachment angles may not be able to suspend themselves from inverted perches or obtain strong purchase on surfaces with extreme texture (i.e. limited usable surface area), and hence may be limited to particular microhabitats. By contrast, species with superior adhesive capabilities, predicted by higher detachment angles, may use a wider range of microhabitats or be able to exploit novel microhabitats.

Additional hypotheses regarding gecko morphology and microhabitat relationships can be drawn from previous research considering *Anolis* lizards, a distantly related group of arboreal lizards with convergent adhesive toe pads. Toe-pad area in both South American and

Caribbean anoles has been found to increase significantly with perch height (Elstrott and Irschick, 2004; Macrini et al., 2003). In addition, anole toe-pad area is significantly positively related to the amount of friction generated (Elstrott and Irschick, 2004; Irschick et al., 1996; Zani, 2000). As a result, *Anolis* lizards with larger toe pads have better clinging abilities and perch higher. Here we used toe detachment angle as a direct measure of adhesive performance to evaluate performance-microhabitat relationships in geckos. *Anolis* lizards have also been studied extensively regarding other, non-toe pad related, morphological and habitat relationships. For example, anole species with relatively shorter legs often use narrower perches presumably due to a trade-off between speed and balance (Jones and Jayne, 2012; Losos and Irschick, 1996; Losos and Sinervo, 1989). Based on the above-mentioned previous research considering the mechanics of our toe detachment assay and habitat use correlations in *Anolis* lizards, we hypothesized that the following relationships will be present in geckos.

1. Gecko species with a higher toe detachment angle will use more highly angled perches.
2. Gecko species with a higher toe detachment angle will use higher perches.
3. Gecko species with shorter legs will use narrower perches.

Methods

In this project, we considered the functional morphology and ecology of Australian geckos with an emphasis on relationships between adhesive capabilities, limb length, and microhabitat. We conducted field research in Queensland, Australia during September and

October 2012, sampling tropical gecko species on the Cape York Peninsula and arid species in western Queensland totaling 70 individuals from 13 species and two families (Figure 4.2 and Table 4.1). One species we observed is a putatively new species of *Oedura* found in western Queensland and the Northern Territory. This species has previously been considered a subpopulation of *Oedura marmarota*. We referred to it as *Oedura sp.* (P. Oliver, pers. comm.; Oliver et al., 2012).

All field techniques were approved by the University of Idaho animal care and use committee (protocol #2012-14), James Cook University ethics committee (JCU-A1813), and the Queensland Department of Environment and Heritage Protection Department (scientific collection permit #WISP11483112). Individual gecko specimens were located between sunset and midnight, during their activity period, using headlamps to reflect eyeshine. Live specimens were captured by hand and microhabitat measurements were collected from the perch on which the animal was first sighted. We recorded perch type, using the categories vegetation, rock, and ground. Perch height and diameter were measured with a tape measure. Perch angle was recorded using a digital goniometer with measurements ranging from 0° i.e., a flat surface, 90° representing a vertical surface, and more then 90° indicating an inverted surface.

Performance and morphology were quantified the day following capture. Morphological measurements, collected with a ruler and digital calipers, included snout vent length, tail length (original and regrown portions), pelvic width, upper hindlimb length (from hip joint to knee), mid-hindlimb length (knee to ankle), and lower hindlimb length (from ankle to tip of longest toe), interlimb length, upper forelimb length (axilla to elbow), mid-forelimb length (elbow to wrist), and lower forelimb length (wrist to top of longest toe), head

length (jaw joint to tip of lower jaw), head width at widest point, head depth at deepest point, and vertical eye diameter.

Measurements of toe-pad performance, i.e. toe detachment angle, were collected using purpose built field equipment consisting of a Pacific Scientific Powermax 1.8° stepper motor (model #P21NRXB-LNN-NS-00), Vernier dual-range force sensor, Vernier three-axis accelerometer (Figure 4.1), Vernier sensorDAQ data-acquisition interface, and a Phidget bipolar stepper control board (#1063_1). Operation and data collection occurred via a custom LabVIEW program (2011 version 11.0.1f2, National Instruments, Austin, TX, USA) running on a Gateway LT series netbook (LT2805u). The frame of our toe detachment equipment acts as a lever with a fulcrum in the center, force sensor at one end, and the lizard suspended from the other end.

Ten toe detachment trials were performed for each individual lizard. Live, non-sedated lizards were suspended by a hind toe from a glass microscope slide via their natural adhesive properties following established protocols (Figure 4.1; Autumn et al., 2006a). The glass slide was rotated one degree per second. As the glass slide was slowly inverted, the force generated by the animals toe pad transitioned from mostly friction to a combination of adhesive and frictional forces relative to the glass slide. At the angle of toe detachment, the animals' single toe cannot generate the required adhesion to support the animal's mass, and the toe detaches from the glass, dropping the lizard onto a cushioned base pad. When the lizard detaches, the force sensor records the corresponding change in force, allowing us to pinpoint the time in which the lizard detaches. Our accelerometer, attached to the rotating glass surface, allowed us to determine the angle of the substrate. Autumn et al. (2006a) illustrated toe detachment angle to be a weight-independent assay, where individuals with

weighted backpacks constantly detached at the same angle regardless of total mass. To eliminate extraneous variation, we limited our measurements to only the longest rear toe. While geckos rarely hang by a single toe in the wild, limiting our test to a single toe eliminates confounding force vectors generated by multiple toes pulling in different directions. This allows a more precise measure of performance and limits within individual variation. Additionally, the longest rear toe has been shown to be important for ecologically relevant performance capabilities in other lizard groups (Schulte et al., 2004; Zani, 2000).

After performance and morphological measurements were collected, specimens were euthanized using MS-222 (tricaine methanesulfonate; Conroy et al., 2009), formalin fixed, and prepared as museum specimens. A center rear toe was collected for future imaging. 50 preserved specimens were submitted to the Queensland Museum at the end of the field portion of this project. The remaining 20 individual lizards were not euthanized and released at their original point of capture.

All analyses were conducted in the R statistical software (version 3.0.1, R Core Development Team 2013). We first fit a three parameter broken regression model to our force output data from our toe detachment equipment. We estimated the y-intercept of a horizontal line fit to the data before the lizard fell, the time point in which the lizard fell, and the y-intercept of a horizontal line fit to the force data after the lizard detached. We then converted our accelerometer data into a measure of angle using the two axis of our accelerometer that were perpendicular to the axis of rotation. We set the ratio of these two channels equal the tangent of the substrate's angle. Using our estimated time point that the lizard fell and our converted angle data, we were able to pinpoint the angle of the glass at the point of toe detachment. We then fit each individual lizard's set of ten observed detachment

angles to the Weibull distribution and estimated the distribution's scale parameter with error (see Chapter 3). To calculate the overall species detachment angle, we calculated a weighted average for each species, weighting each individual's estimated detachment angle by one over the standard deviation of that individual's estimated scale parameter. We then calculated the variance around each weighted species average using the formula

$$\sigma_{\bar{x}}^2 = \frac{1}{\sum_{i=1}^{n} \frac{1}{\sigma_i^2}} * \frac{1}{n-1} * \sum_{i=1}^{n} \frac{\left(x_i - \bar{x}\right)^2}{\sigma_i^2}, \qquad \text{Eq. 4.1}$$

where $\sigma_{\bar{x}}^2$ is the variance of the weighted mean, $n$ is the number of individuals, $\sigma_i^2$ is the individual error, $x_i$ is the individual estimate, and $\bar{x}$ is the weighted average. Size independent morphological measurements were calculated using each species mean morphological measurements and mean snout vent length. All morphological measurements were natural log transformed and fit to a linear model in which snout vent length predicted the trait of interest. The residuals from this model fit were extracted and used as our size-adjusted measurements. We also calculated the number of individuals observed on vegetation and rocks, dividing by the total number of ecological observations for each species to calculate the percent of our observations that occurred on vegetation and rocks for each species.

Linear models and phylogenetic generalized least squares (PGLS) were used to evaluate if morphological, performance, or ecological variables, chosen *a priori*, were significantly correlated. Ecological and performance observations were natural log transformed (or arcsine square root transformed in the case of percentages) to assure normality. In our analyses considering performance, we considered both toe detachment measurements as an angle as well as transformed into a force ratio by calculating the tangent

of the angle (Eq. 2.1). Observations of *Pseudothecadactylus australis* were removed from our analyses due to the variation in our limited observations and unique perch characteristics. We accounted for phylogenetic relatedness across species using the caper library in R (Orme et al., 2011; Paradis et al., 2004). The caper library estimates Pagel's λ (Pagel, 1999) using a maximum likelihood approach; bounding λ between zero (no phylogenetic relationship in the data) and one (traits appear to evolve under a Brownian Motion model). Using a likelihood ratio test, caper also evaluates whether the estimated λ values are significantly different from zero and one.

We used an ultrametric cropped Squamate phylogeny from Pyron et al. (in press, *Ecology Letters*; see Pyron et al. 2013) assuming it more appropriate to consider phylogenetic relationships through time as opposed to molecular distance. We removed taxa that lack measurements (Figure 4.2). We also assumed a similar age of divergence between *Oedura marmorata* and our observed *Oedura sp.* species as Pyron et al. (in press, *Ecology Letters*) observed between *O. marmorata* and its current sister species *O. gemmata*. Oliver et al. (2012) hypothesized deep divergences within *O. marmorata*, divergences nearly as large as the distance between *O. marmorata* and *O. gemmata*. We also observed topological differences within the *Strophurus* genus in our phylogeny. Sadlier et al. (2005) hypothesized *S. krisalys* is more closely related to *S. williamsi*, then as to *S. ciliaris* . Brown et al. (2012) suggested *S. krisalys* and *S. ciliaris* are sister species, but with low nodal support. The phylogeny from Pyron el al. (in press, *Ecology Letters*) suggests yet a different topology, with *S. williamsi* and *S. ciliaris* closely related with low support. We kept the topology from Pyron et al. and suggest additional sampling to resolve these conflicting hypotheses.

## Results

### *Adhesive performance and microhabitat*

We did not find significant relationships between our measures of performance and perch height, angle, or diameter (Figure 4.3) possibly due to our small sample sizes. When we consider toe detachment angle, genera, and habitat use, qualitative patterns can be observed (Figure 4.3). *Strophurus* species had low detachment angles and appeared to use low, narrow and horizontal perches. *Gehyra* species had high detachment angles and often used high, wide, and vertical perches. Rock dwelling *Oedura* typically had lower detachment angles than arboreal *Oedura*, *Amalosia* and *Gehyra*. In addition, one arboreal *Oedura* species, *O. monilis*, used lower, more narrow and horizontal perches as compared to other species. This pattern is consistent with our frequent observations of this species on the ground (Figure 4.10).

### *Morphology and microhabitat*

We found residual upper and mid hind and forelimb lengths to be significantly negatively correlated with perch diameter in both our linear model and PGLS analyses (Figure 4.4 and Table 4.2). We also found support for a weak relationship between residual mid-hindlimb length and perch angle in both our linear model ($p = 0.06$) and PGLS analyses ($p = 0.06$, Figure 4.5 and Table 4.2). Within only our PGLS analyses we found multiple relationships between limb length and percent perch type observed (Figure 4.5 and Table 4.2), with residual upper hind and forelimb lengths significantly negatively correlated with the use of vegetation and significantly positively correlated to the use of rock perches, except the relationship between residual upper forelimb and rock use, which was only weakly

significant ($p = 0.054$). In addition, we found weak support for a positive relationship between lower forelimb length and the use of rock perches ($p = 0.07$).

*Morphology and adhesive performance*

We found significant negative relationships between residual upper hind and forelimb lengths and toe detachment angle as well as a significant negative relationship between residual mid forelimb length and toe detachment angle in both our linear models and PGLS analyses (Figure 4.7 and Table 4.2). When comparing residual lower limb lengths, we found the opposite relationship, with a significant positive relationship between residual lower hindlimb length and toe detachment angle in both our linear model and PGLS analyses. The positive relationship between residual lower forelimb length and toe detachment angle was only significant in our linear model analysis ($p = 0.04$, PGLS $p = 0.7$). Lastly, we evaluated the relationship between snout vent length and toe detachment angle (Figure 4.8 and Table 4.2). We found a significant negative correlation using a linear model ($p = 0.02$), but this relationship was not significant in our PGLS analysis ($p = 0.1$). When these analyses were conducted with toe detachment angle as a force ratio (Eq. 2.1), we observed very similar p-values.

## Discussion

In this study, we evaluated relationships between gecko adhesive performance, morphology, and ecology. Our study represents one of the first examples investigating specific ecological parameters and gecko adhesive capabilities, while posing additional questions regarding the trade-off between limb length and perch diameter and intra-limb

lengths and their relationship with adhesive abilities within geckos. Our results also illustrate ecomorphological patterns that may underlie morphological variation across geckos.

*Adhesive performance and microhabitat*

While we did not find support for our first two hypotheses considering gecko toe detachment angle, perch height, and perch angle, we did observe qualitative differences between genera. This may be due to our small sample sizes. In addition, our result may be related to how we quantified adhesive performance. In previous studies of anoles in which toe-pad performance, pad area, and microhabitat were considered, authors measured the friction generated by the lizard's toe pads (Irschick et al., 1996). This measure of performance was found to be positively correlated with pad area. In addition, pad area has been found it to be positively correlated with perch height (Elstrott and Irschick, 2004; Macrini et al., 2003). As a result, the absolute amount of friction generated by an anole is likely directly used by the animal to increase traction while climbing and may provide species a larger safety margin to prevent falling (Losos, 2009). Conversely, our angle of toe detachment is a relative measure of adhesion to friction and does not quantify any absolute forces generated by a lizard's adhesive pads. As a result, a species could conceivably generate small amounts of both friction and adhesion, but if the amount of adhesion were high relative to friction, we would consider this species to have a high toe detachment angle. Additional studies comparing how the generation of friction and toe detachment angle are associated with each other as well as pad area would be very valuable (see Chapter 5).

In addition, lizards in the wild may use friction and adhesion differently. The generation of friction by padded lizards likely serves to increase traction, possibly as a

supplement to claws on smooth surfaces. This ability can be used in many microhabitats to assist locomotion. Conversely, adhesion as we've defined it here, is the generation of negative normal force relative to a substrate. This ability is presumably useful to traverse inverted surfaces and overhangs, although we did not observe a significant relationship between perch angle and detachment angle, or to possibly prevent the animal from being removed from a substrate by a predator or competitor. As a result, adhesion could be conceived to assist the animal in staying in place.

Lastly, much theoretical work has been done considering surface texture and gecko performance (Huber et al., 2005; Pugno and Lepore, 2008; Russell and Johnson, 2007; Vanhooydonck et al., 2005), yet few studies have treated the generation of friction and adhesion separately in regards to how it may be related to texture and microhabitat use. Here we observe rock dwelling species (*Oedura sp*. and *O. coggeri*) to have lower toe detachment angles, possibly suggesting adhesion is not strongly selected for in these habitats. Additional studies quantifying gecko microhabitat texture and their biomechanical relationship with adhesive and frictional performance would be valuable to determine if performance-microhabitat relationships are present within or across different gecko communities. Noteworthy communities include rock dwelling, palm, and non-palm specialist *Phelsuma* geckos of Madagascar and the surrounding islands (Glaw and Vences, 2007; Harmon et al., 2007) and the rock dwelling gecko species found in southern Africa (Russell and Johnson, 2007).

*Morphology and microhabitat*

Our results did not support our third hypothesis considering gecko limb length and perch diameter. Our data suggest the opposite pattern is present, with limb length negatively related to perch diameter, so that species with relatively longer legs use narrower perches. These results are different than limb length and perch diameter relationships in *Anolis* (Jones and Jayne, 2012; Losos, 2009; Losos and Irschick, 1996; Losos and Sinervo, 1989). Zaaf and Van Damme (2001) hypothesized arboreal geckos should have shorter legs than terrestrial geckos but did not find any clear relationship. They suggest our understanding of the biomechanics of climbing may be insufficient. Additional analyses would be very valuable to determine if geckos truly do exhibit a unique relationship between limb length and perch diameter. The use of residuals from a linear regression of snout vent length and limb length to determine relative limb length is influenced by the species included in the analysis. In our analysis, we only included geckos and as a result, our residual limb length values illustrate deviations from the expected limb length of a gecko for a given snout vent length. If geckos tend to have short legs as a group, our linear regression and residuals will illustrate this. We found that *Strophurus* geckos had the longest relative limbs in our dataset and used the narrowest perches, and while they may have relatively long limbs for a gecko, this may not be the case when considering a wider range of lizard species (see Chapter 5). A comparative analysis including other groups of lizards, specifically anoles and chameleons for which leg length and perch diameter data are available (Butler, 2005; Fischer et al., 2010; Hagey et al., 2010; Losos, 2009; Losos et al., 1993), may show convergent ecomorphological relationships. In addition, broader comparisons between geckos and other arboreal lizards may shed light on how leg length and perch diameter affect locomotion speed, balance and

clinging ability (Fischer et al., 2010; Higham et al., 2001; Losos and Irschick, 1996; Losos and Sinervo, 1989; Losos et al., 1993; Sinervo and Losos, 1991).

In addition, we found significant correlations between relative upper limb length and perch type, where species that are found more often on rock have longer limbs. While these results seem at odds with our results suggesting species with shorter limbs use broader perches, they compliment previous studies of non-gecko rock dwelling lizards (Goodman et al., 2008; Revell et al., 2007). The rocky microhabitats we observed geckos using were typically vertical and very broad. The correlations we observed may be a result of the adhesive requirements of using rock as compared to arboreal perches; additional data would be needed to investigate this hypothesis. Our results linking limb length and the use of rock perches, when considered with our results linking limb length and toe detachment angle, may suggest species that use rocky perches have lower detachment angles. Although we did not find this relationship to be significant in our analyses (but see Figure 4.3), it is consistent with the textures of the rock and arboreal perches we observed geckos using. We often observed geckos using ironbark *Eucalyptus* trees and paperbark *Melaleuca* trees. Clinging to either of these trees would be difficult because the bark of ironbark trees is very rough, with large topological features including valleys, fissures, and ridges, greatly limiting the available surface area for a toe pad to adhere. Conversely, the bark of paperbark trees is smooth, but dusty and flaky, again limiting a species clinging ability and quickly contaminating a gecko's toe pad (see Cole et al., 2005). As a result of the difficulties associated with using these arboreal perches, gecko species that use these perches may have evolved higher detachment angles to compensate and hence have shorter upper limbs and longer lower limbs as compared to rock dwelling geckos. Future studies quantifying the surface texture of observed

gecko perches and setal morphology would be invaluable in furthering our understanding of how gecko adhesive morphology, performance, and microhabitat texture are related (but see Huber et al., 2007; Pugno and Lepore, 2008; Russell and Johnson, 2007; Vanhooydonck et al., 2005).

*Morphology and adhesive performance*

When considering limb length and toe detachment angle, we found relative upper and mid limb lengths were negatively correlated with toe detachment angle, while lower limb length was positively correlated with toe detachment angle. These results may suggest the presence of other morphological adaptations that compliment the use of toe pads in conjunction with modified locomotion kinematics. Having adhesive pads may require some geckos to adopt locomotion kinematics that are different than lizards without pads or other gecko species with less adhesive pads. Russell and Higham (2009) describe changes in body and leg posture when a gecko with adhesive pads deploys its pads during a transition from a horizontal surface to an incline surface. These changes were less pronounced in a second focal gecko species without toe pads. In addition, our other findings suggest geckos with different adhesive abilities may use different kinds of perches (Figure 4.3), and so as a result, geckos with different adhesive abilities may have also undergone other complimentary morphological changes to assist with the use of adhesive toe pads in specific microhabitats. Further research investigating the kinematics of geckos with different adhesive abilities, limb morphologies, and microhabitat preferences would be informative regarding gecko ecology, specifically regarding patterns of character displacement and microhabitat partitioning as has

been seen in anoles and *Phelsuma* geckos (Gardner, 1984; Hagey et al., in review; Harmon et al., 2007; Losos, 2009).

Lastly, we found a significant negative relationship between gecko snout vent length and toe detachment angle in our linear model analysis. While snout vent length is correlated with mass, Autumn et al. (2006a) illustrated that the toe detachment assay is independent of mass. As a result, this relationship may suggest that larger lizards rely less on their adhesive system and more on other structures such as claws while climbing. There may also exist constraints in the gecko locomotion system that limit a large-bodied gecko from heavily relying on their adhesive toes to support their body weight. Additional ecological observations focusing on how large and small-bodied geckos move through their environment as well as kinematic studies of how different sized geckos use their adhesive system and claws would be intriguing.

*Conclusions*

In this study, we examined patterns of gecko adhesive abilities, limb morphology, and microhabitat use, investigating how geckos may have adapted to particular environments. Our results are among the first to consider how toe-pad characteristics and habitat use of geckos are associated. While we did not find support for our hypotheses, many of our results suggest additional form and function relationships within geckos that had not previously been identified. Broader assessments of ecomorphology across arboreal and rock dwelling lizards may illustrate convergent suites of traits and microhabitats, similar to previous work comparing North American and Australian desert agamid and iguanid lizards (Melville et al., 2006). The data gathered in this study suggests ecomorphological patterns may be present in

geckos (Figure 4.3, 4.9, 4.10), with some groups specialized to use low and narrow arboreal perches (*Strophurus*, and *Oedura monilis*) or rocky microhabitats (*O. coggeri* and *Oedura sp*.), while observations of *Pseudothecadactylus australis* suggest it may be an arboreal canopy specialist.

Although similar ecomorphological patterns may be present in geckos as have been previously seen in other lizard groups, geckos likely have unique kinematic and locomotion patterns that compliment their adhesive toe pads and specific microhabitats. Adhesive toe pads have likely evolved multiple times within lizards and within geckos (Gamble et al., 2012; Irschick et al., 1996), allowing for interesting form and function comparisons between independent origins. In addition, our taxonomic sampling in this study was limited to species found in Queensland, Australia and this non-random sampling may have influenced our findings. As a result, we encourage additional sampling of geckos from different locations and clades. Additional studies would strengthen our understanding of evolution and adaptation as well as foster interdisciplinary collaborations between ecologists, biomechanics, evolutionary biologists, and engineers; integrating the fields of functional morphology and ecology through the study of biomechanics.

Acknowledgements

Many people assisted with the design and execution of this project. We would like to thank James Cook University and University of Idaho animal ethics committees and the Queensland Government for providing collection permits. We received funding from the National Geographic Society and the Waitt Institute (#W216-12) via University of Idaho's Institute for Bioinformatics and Evolutionary Studies (IBEST). Neely's Travel assisted with

trip logistics. We received assistance building equipment for the field from Matt Wilkinson (LCC), Mitch Day, Craig McGowan (UI), Missy Thompson (UI), Alan Odenborg (UI Facilities Dept), BJ Schenck (UI Facilities Dept), Russ Porter (UI), Terry Soule (UI), and Eric Wolbrecht (UI). While in Australia, we received assistance from Richard Duffy (JCU), Matt Vucko (JCU), and the entire Schwarzkopf lab (JCU), the JCU Biology department staff and motor pool, the Australian Wildlife Conservancy, and lastly we would like to thank the Queensland landowners of whom allowed us access to their properties.

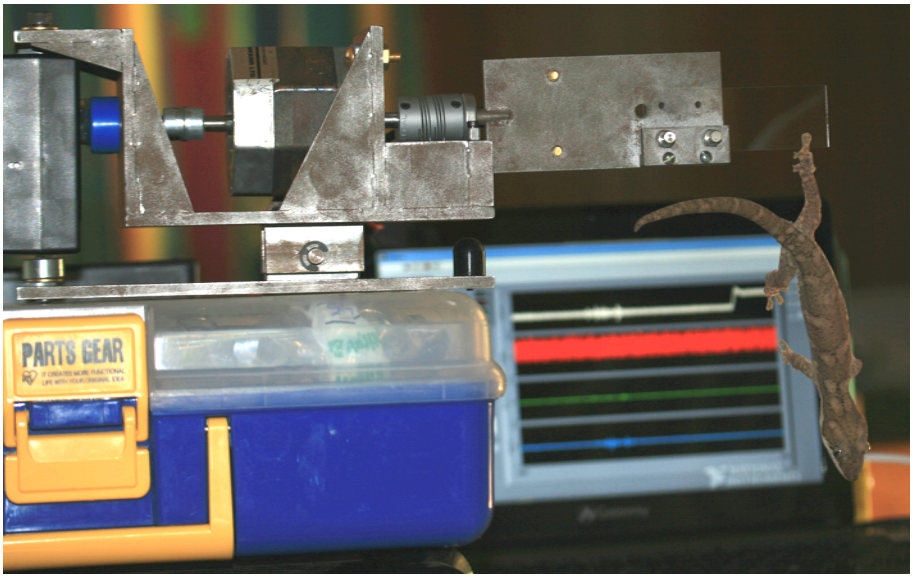


Figure 4.1. Angle of Toe Detachment Field Equipment

To measure toe detachment angle in the field, we used purpose-built equipment consisting of a stepper motor, force sensor, and three-axis accelerometer. The frame of our apparatus acted as a lever with the fulcrum in the center, allowing the force sensor to detect when the animal detached.

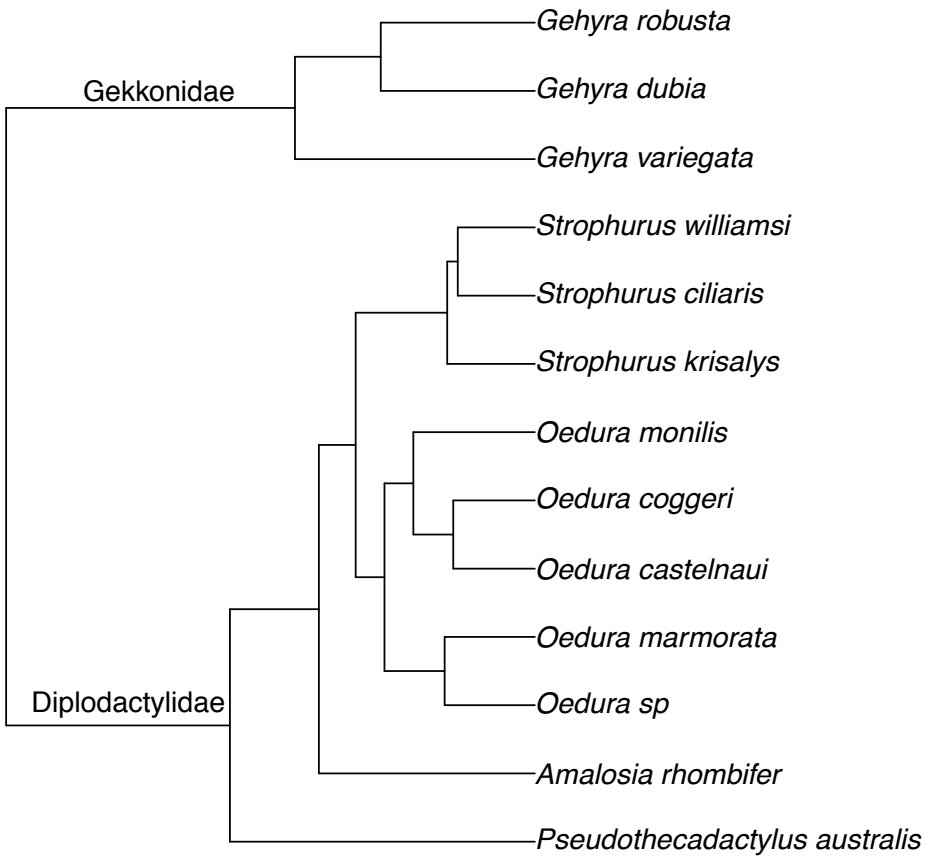


Figure 4.2. Phylogeny of Focal Species

As part of our PGLS analyses, we used an ultrametic phylogeny modified Pyron et al. (in press, *Ecology Letters*; see Pyron et al. 2013), removing taxa for which we didn't have data. We sampled species from both the Gekkonidae and the Diplodactylidae families. The currently unnamed *Oedura* species (*Oedura sp.*) was assumed to have a similar date of divergence as *Oedura marmorata* and *Oedura gemmata* (see Oliver et al., 2012). Topology discrepancies were observed within the *Strophurus* genus that differed from previous hypotheses (Brown et al., 2012; Sadlier et al., 2005), although we maintained the topology from Pyron et al (in press, *Ecology Letters*) for our analyses.

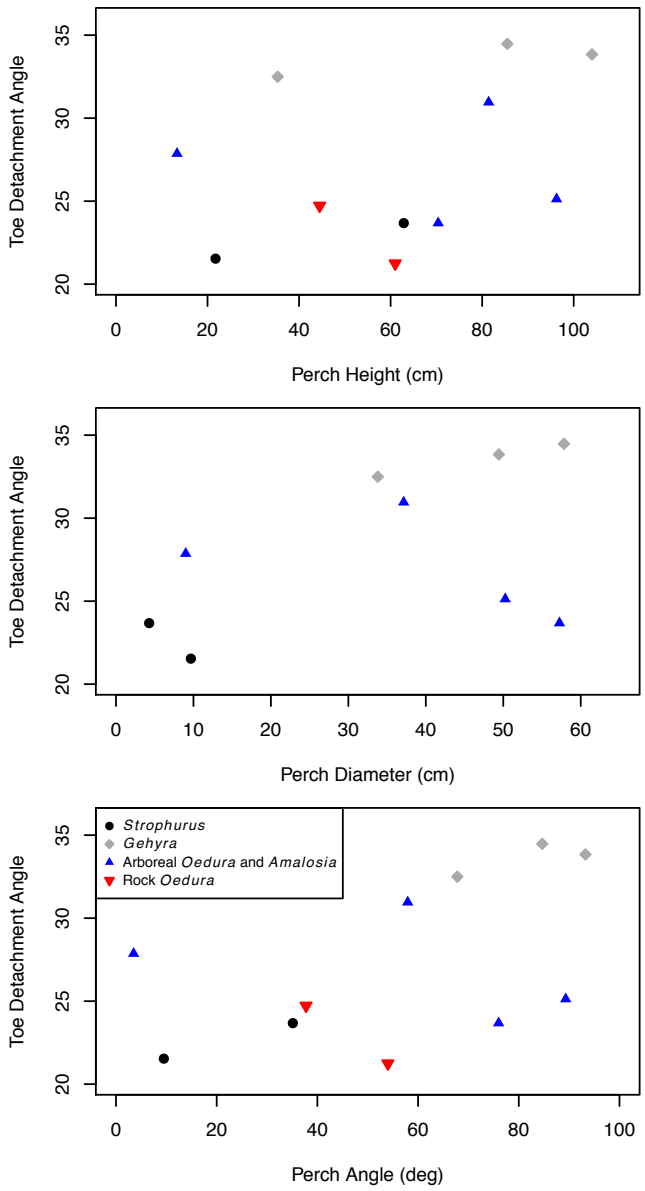


Figure 4.3. Toe Detachment Angle vs. Microhabitat

We investigated relationships between toe detachment angle and three perch measurements; height, diameter, and angle. Our linear model and PGLS analyses did not reveal significant relationships, yet when species are separated by genera and ecology (*Strophurus* in black circles, *Gehyra* in gray diamonds, Arboreal *Oedura* and *Amalosia* in blue triangles, and rock dwelling *Oedura* in red inverted triangles) qualitative patterns appear. *Pseudothecadactylus* was omitted from this plot due to its large observed perch height. In addition, perch diameter was not quantified for rock dwelling species.

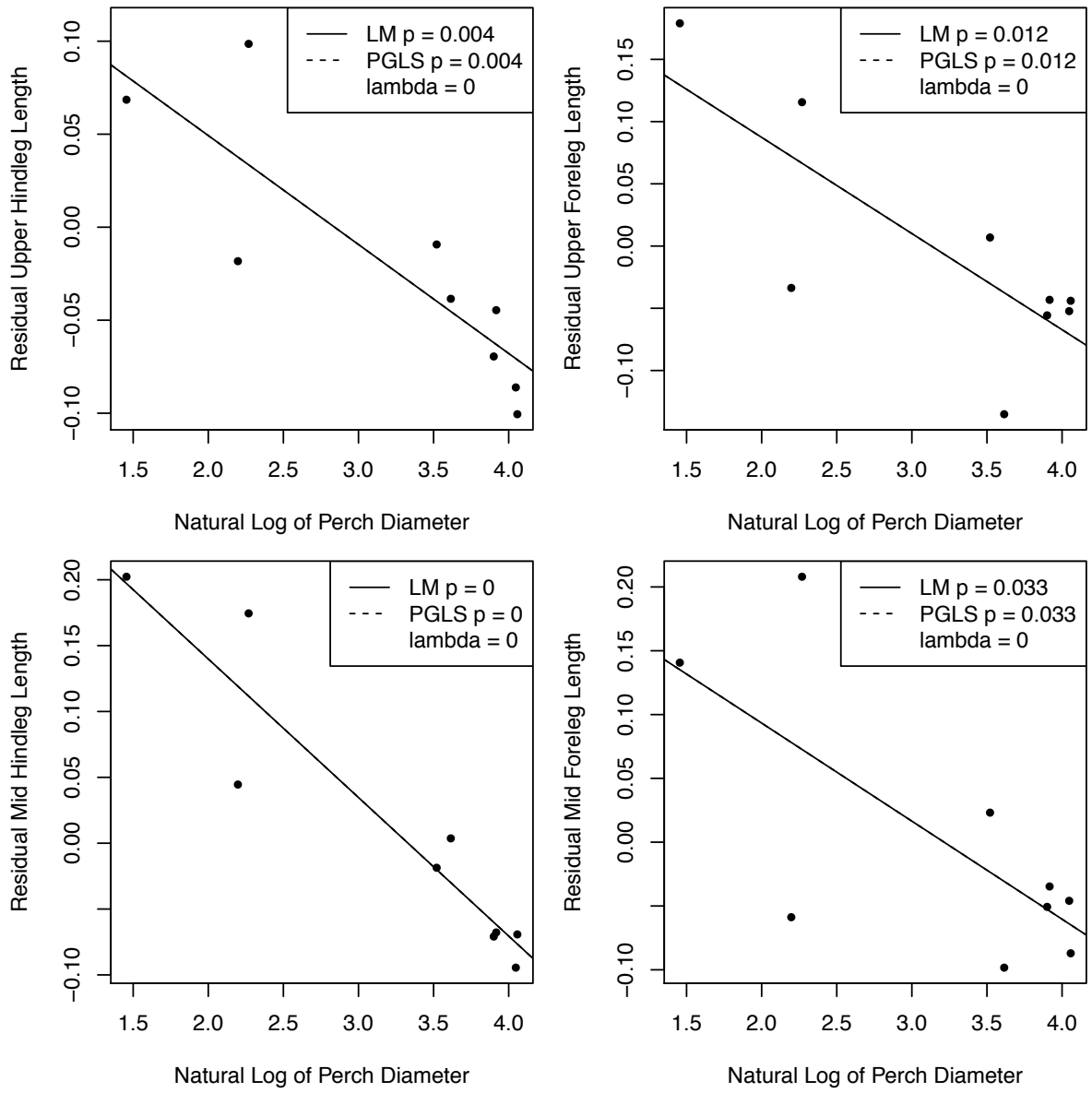


Figure 4.4. Limb Length vs. Perch Diameter

We observed significant negative correlations between residual upper and mid fore and hindlimb lengths and perch diameter for both our linear model and PGLS analyses. In these analyses, the estimated λ parameter was found to be zero, a case in which no phylogenetic signal was present and our linear model and PGLS analyses are equivalent.

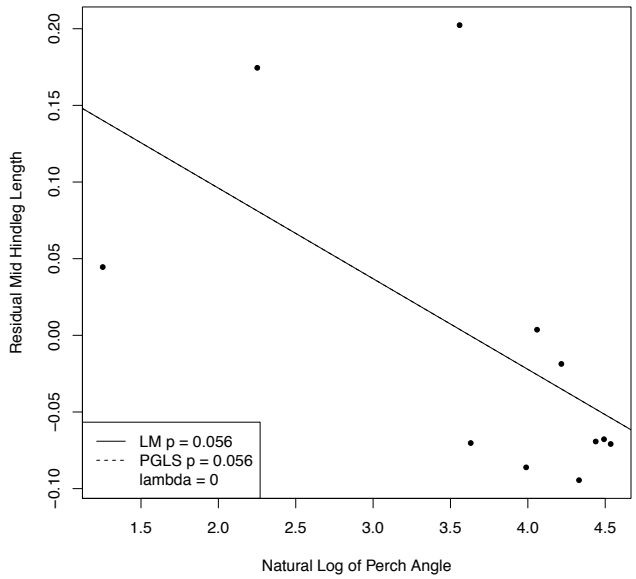


Figure 4.5. Limb Length vs. Perch Angle

We found residual mid hindlimb length to be weakly correlated ($p = 0.056$) with perch angle in both our linear model and PGLS analyses. The $\lambda$ parameter in our PGLS analysis was again zero, making our linear model and PGLS analyses equivalent.

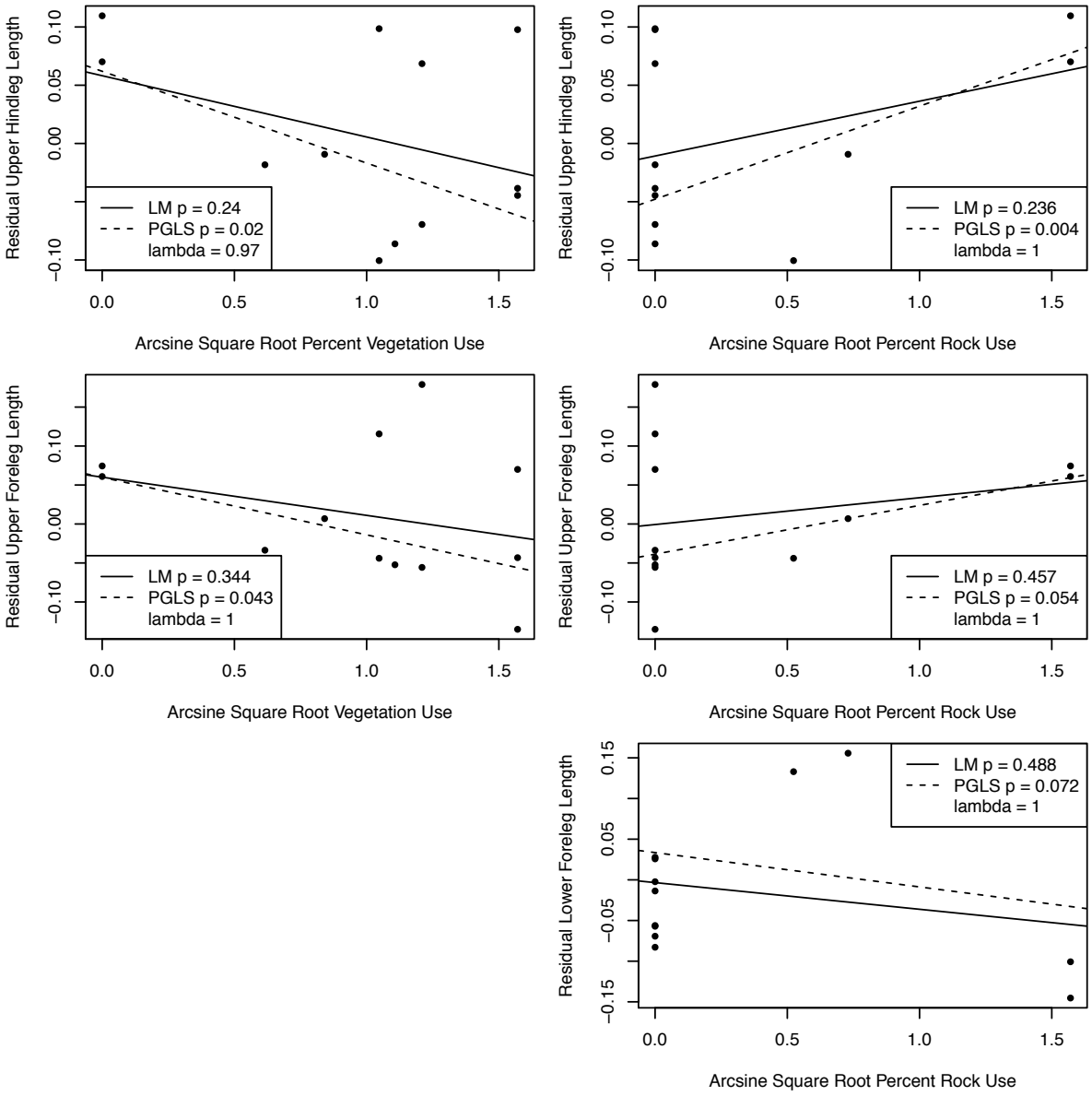


Figure 4.6. Limb Length vs. Perch Type

When comparing limb length and perch type, we found residual upper fore and hindlimb to be significantly negatively correlated with the use of vegetation and positively related to the use of rock perches in our PGLS analyses, yet residual upper forelimb length was only weakly significant ($p = 0.054$). We also found residual lower forelimb length to be weakly negatively correlated with the use of rock perches ($p = 0.07$). The $\lambda$ values of these analyses were all at or near one, suggesting our traits are consistent with a Brownian motion model of evolution.

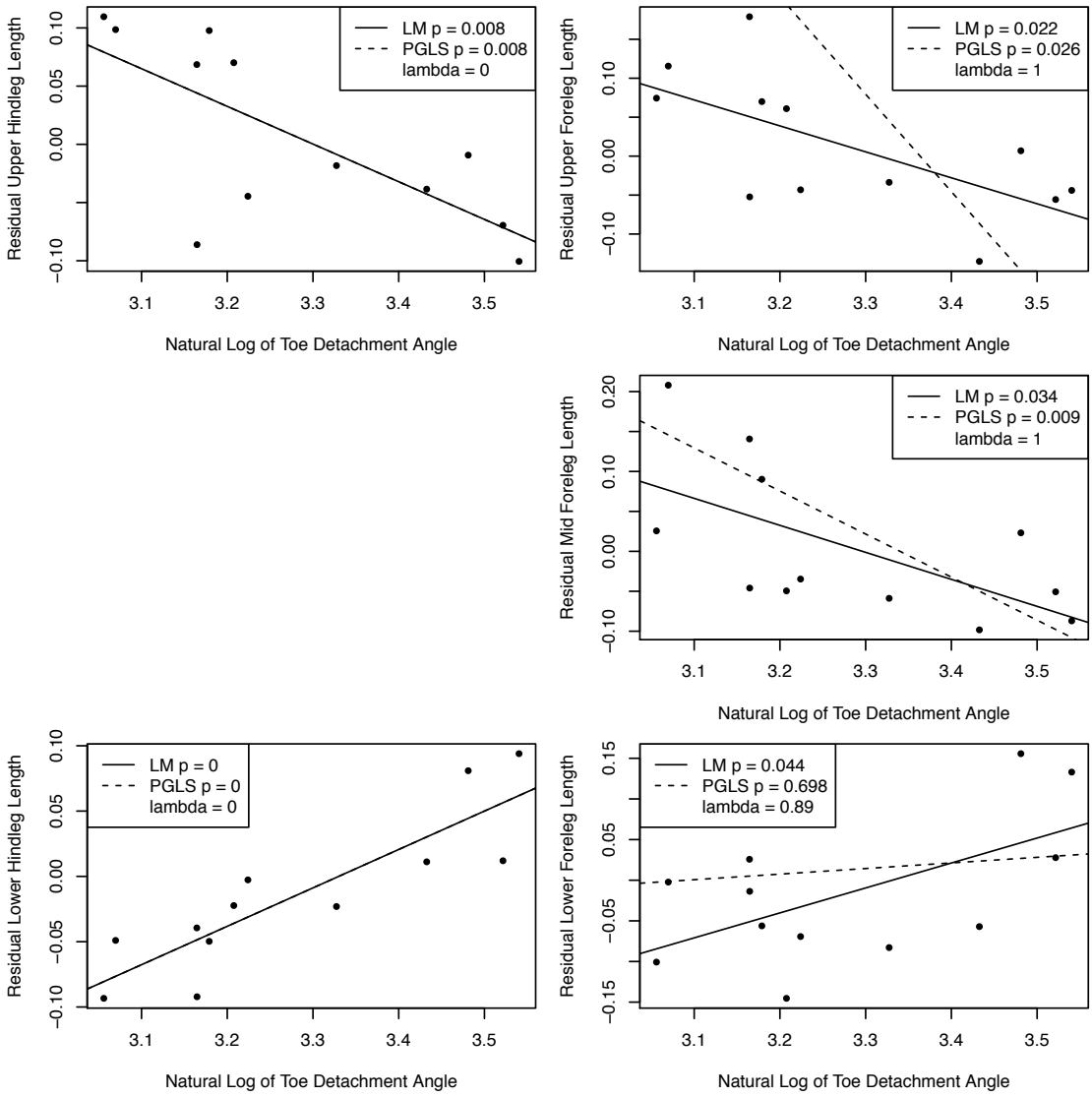


Figure 4.7. Toe Detachment Angle vs. Limb Length

We found leg length to have a complex relationship with toe detachment angle, where residual upper fore and hindlimb lengths were significantly negatively related to toe detachment angle as well as residual mid forelimb length in both our linear model and PGLS analyses. Residual lower hindlimb length was found to be significantly positively correlated to toe detachment angle in both analyses, with residual lower forelimb length only significantly positively correlated to toe detachment angle in our linear model analysis. We estimated λ to be zero when considering hindlimb length, suggesting no phylogenetic signal, yet λ was estimated as one or near one in our analyses considering forelimb length.

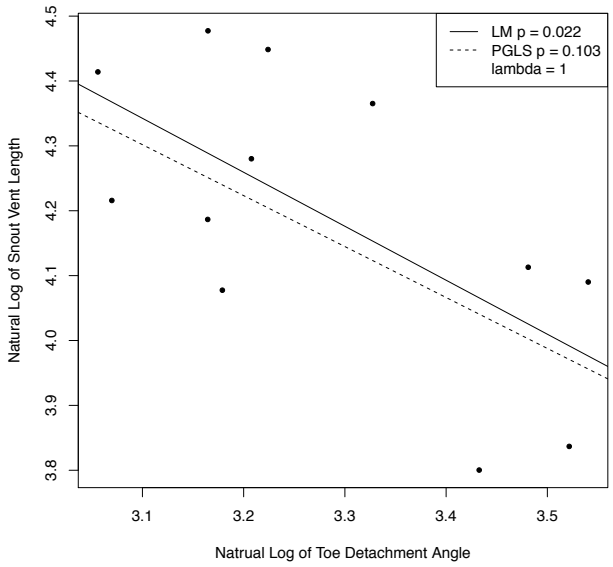


Figure 4.8. Toe Detachment Angle vs. Snout Vent Length

We found snout vent length to be significantly negatively correlated with toe detachment angle in our linear model analysis, yet this relationship was not significant when we accounted for the phylogenetic relationships of our species ($p = 0.1$).

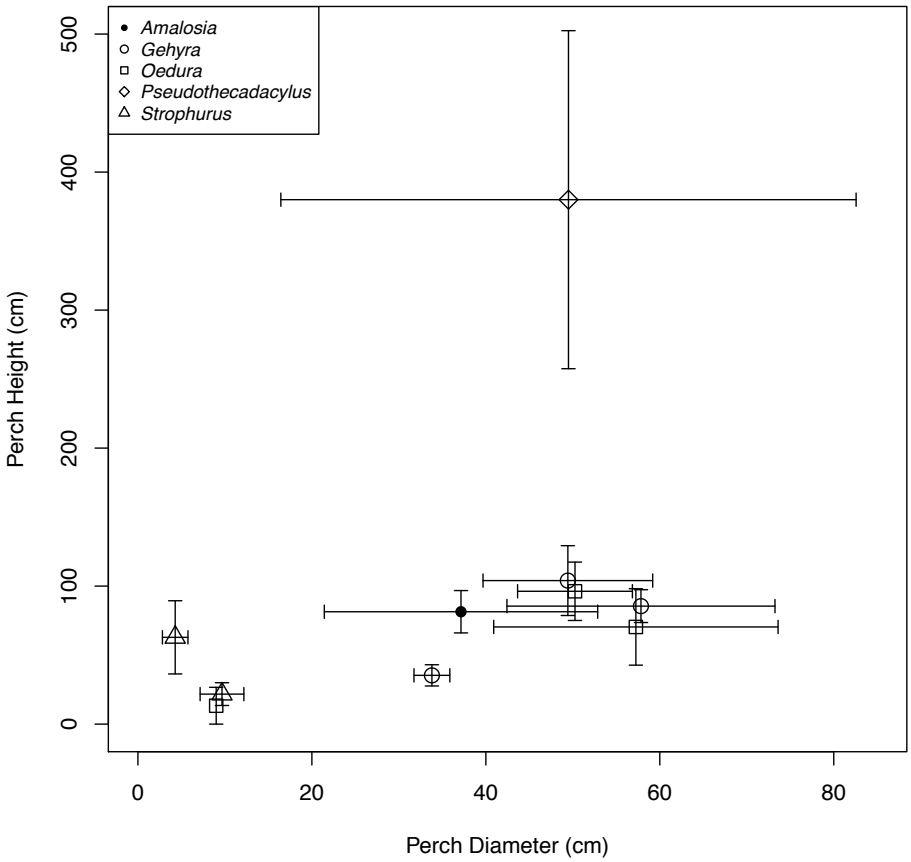


Figure 4.9. Perch Height vs. Perch Diameter

When comparing our observed perch diameter and perch height measurements, ecomorphological patterns appear to be present among our focal species. Error bars represent standard errors around the each species mean observation. *Strophurus* geckos and *Oedura monilis* appear to only use low narrow perches. Considering additional limited data, we suggest *Pseudothecadactylus* may be a canopy specialist using a variety of perch diameters well above the ground.

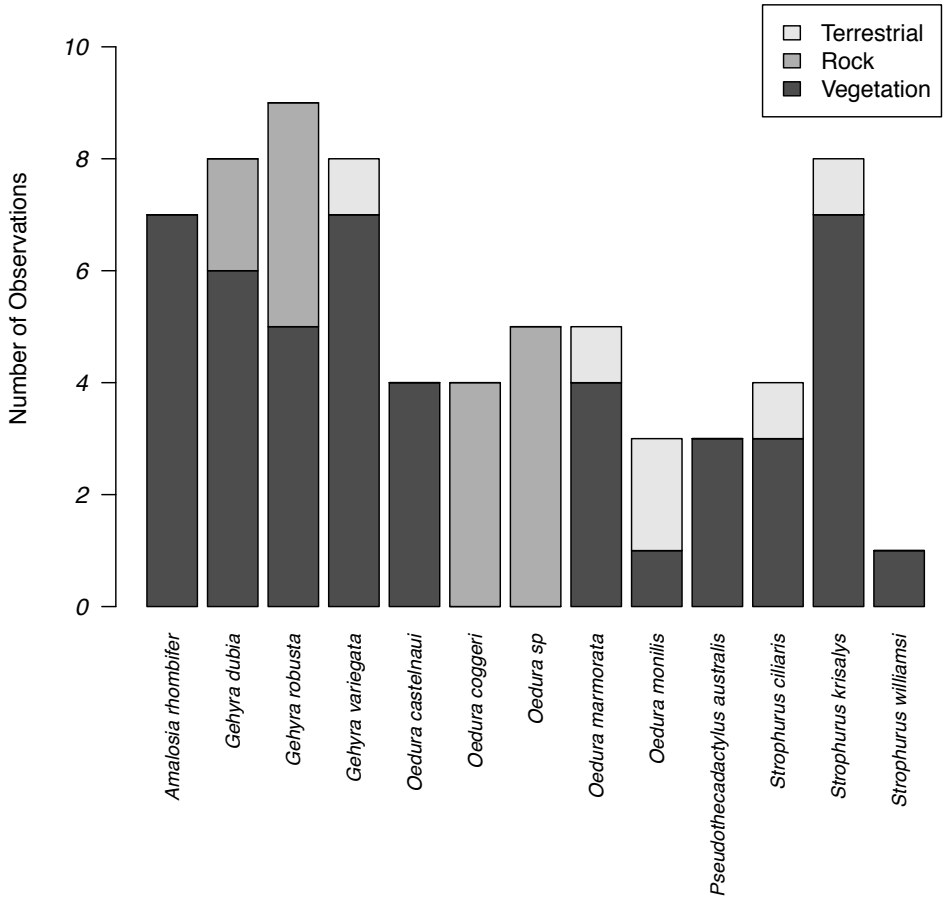


Figure 4.10. Perch Type Across Species

Considering the types of perches we observed geckos using (terrestrial, vegetation, and rock), we can again observe ecomorpholoigcal patterns, with two species of *Oedura* (*O. coggeri* and *Oedura sp*.) using only rock perches.

| Species | Family | Sites Observed | Biome | Number of Individuals |
|---|---|---|---|---|
| *Amalosia rhombifer* | Diplodactylidae | Mt. Carbine | tropical | 7 |
| *Gehyra dubia* | Gekkonidae | Mingela, Magnetic Island | tropical | 8 |
| *Gehyra robusta* | Gekkonidae | Winton | arid | 9 |
| *Gehyra variegata* | Gekkonidae | Winton | arid | 8 |
| *Oedura castelnaui* | Diplodactylidae | Mt. Carbine, Coen | tropical | 4 |
| *Oedura coggeri* | Diplodactylidae | Chillagoe | arid | 4 |
| *Oedura sp.* | Diplodactylidae | Mt. Isa | arid | 5 |
| *Oedura marmorata* | Diplodactylidae | Winton | arid | 5 |
| *Oedura monilis* | Diplodactylidae | Magnetic Island | tropical | 3 |
| *Pseudothecadactylus australis* | Diplodactylidae | Iron Range National Park | tropical | 3 |
| *Strophurus ciliaris* | Diplodactylidae | Bedourie | arid | 4 |
| *Strophurus krisalys* | Diplodactylidae | Winton, Mt. Isa | arid | 8 |
| *Strophurus williamsi* | Diplodactylidae | Mingela | tropical | 2 |
| | | | | Total: 70 |

Table 4.1. Table of Focal Species

We collected data from 13 gecko species found in tropical and arid sites in Queensland, Australia including species from both the Gekkonidae and Diplodactylidae families. The sites observed describe the nearest town or common name of the area in which we collected our specimens. Biome highlights the distinction between the tropical and arid species we observed. Lastly, the number of individuals illustrates the number of individuals of each species in which we collected data for.

| **Linear Model Results** | **PGLS Results** |
|---|---|
| Limb Length and Habitat | Limb Length and Habitat |
| *Perch Diameter* | *Perch Diameter* |
| residual upper hindleg length~ natural log perch diameter | residual upper hindleg length~ natural log perch diameter |
| F(1, 7) = 18.38 , p = 0.004 | F(2, 7) = 18.38 , p = **0.004** , λ = 0.00 , ( 1.000 , **0.012** ) |
| residual mid hindleg length ~ natural log perch diameter | residual mid hindleg length ~ natural log perch diameter |
| F(1, 7) = 52.67 , p = **0.000** | F(2, 7) = 52.67 , p = **0.000** , λ = 0.00 , ( 1.000 , 0.053 ) |
| residual upper foreleg length ~ natural log perch diameter | residual upper foreleg length ~ natural log perch diameter |
| F(1, 7) = 11.26 , p = **0.012** | F(2, 7) = 11.26 , p = **0.012** , λ = 0.00 , ( 1.000 , 0.089 ) |
| residual mid foreleg length ~ natural log perch diameter | residual mid foreleg length ~ natural log perch diameter |
| F(1, 7) = 7.01 , p = **0.033** | F(2, 7) = 7.01 , p = **0.033** , λ = 0.00 , ( 1.000 , **0.027** ) |
| *Perch Angle* | *Perch Angle* |
| residual mid hindleg length ~ natural log perch angle | residual mid hindleg length ~ natural log perch angle |
| F(1, 9) = 4.80 , p = 0.056 | F(2, 9) = 4.80 , p = 0.056 , λ = 0.00 , ( 1.000 , 1.000 ) |
| *Perch Type* | *Perch Type* |
| residual upper hindleg length ~ arcsine square root percent vegetation use | residual upper hindleg length ~ arcsine square root percent vegetation use |
| F(1, 10) = 1.56 , p = 0.240 | F(2, 10) = 7.66 , p = **0.020** , λ = 0.97 , ( 0.165 , 0.892 ) |
| residual upper foreleg length ~ arcsine square root percent vegetation use | residual upper foreleg length ~ arcsine square root percent vegetation use |
| F(1, 10) = 0.99 , p = 0.344 | F(2, 10) = 5.37 , p = **0.043** , λ = 1.00 , ( 0.134 , 1.000 ) |
| residual upper hindleg length ~ arcsine square root percent rock use | residual upper hindleg length ~ arcsine square root percent rock use |
| F(1, 10) = 1.59 , p = 0.236 | F(2, 10) = 13.90 , p = **0.004** , λ = 1.00 , ( **0.026** , 1.000 ) |
| residual upper foreleg length ~ arcsine square root percent rock use | residual upper foreleg length ~ arcsine square root percent rock use |
| F(1, 10) = 0.60 , p = 0.457 | F(2, 10) = 4.75 , p = 0.054 , λ = 1.00 , ( 0.140 , 1.000 ) |
| residual lower foreleg length ~ arcsine square root percent rock use | residual lower foreleg length ~ arcsine square root percent rock use |
| F(1, 10) = 0.52 , p = 0.488 | F(2, 10) = 4.05 , p = 0.072 , λ = 1.00 , ( **0.001** , 1.000 ) |
| Limb Length and Performance | Limb Length and Performance |
| residual upper hindleg length ~ natural log toe detachment angle | residual upper hindleg length ~ natural log toe detachment angle |
| F(1, 10) = 10.89 , p = **0.008** | F(2, 10) = 10.89 , p = **0.008** , λ = 0.00 , ( 1.000 , **0.005** ) |
| residual lower hindleg length ~ natural log toe detachment angle | residual lower hindleg length ~ natural log toe detachment angle |
| F(1, 10) = 31.47 , p = **0.000** | F(2, 10) = 31.47 , p = **0.000** , λ = 0.00 , ( 1.000 , 0.372 ) |
| residual upper foreleg length ~ natural log toe detachment angle | residual upper foreleg length ~ natural log toe detachment angle |
| F(1, 10) = 7.35 , p = **0.022** | F(2, 10) = 6.78 , p = **0.026** , λ = 1.00 , ( **0.004** , 0.987 ) |
| residual mid foreleg length ~ natural log toe detachment angle | residual mid foreleg length ~ natural log toe detachment angle |
| F(1, 10) = 6.00 , p = **0.034** | F(2, 10) = 10.33 , p = **0.009** , λ = 1.00 , ( **0.042** , 1.000 ) |
| residual lower foreleg length ~ natural log toe detachment angle | residual lower foreleg length ~ natural log toe detachment angle |
| F(1, 10) = 5.32 , p = **0.044** | F(2, 10) = 0.16 , p = 0.698 , λ = 0.89 , ( 0.154 , 0.591 ) |
| Snout Vent Length and Performance | Snout Vent Length and Performance |
| natural log snout vent length ~ natural log toe detachment angle | natural log snout vent length ~ natural log toe detachment angle |
| F(1, 10) = 7.30 , p = **0.022** | F(2, 10) = 3.21 , p = 0.103 , λ = 1.00 , ( 0.551 , 1.000 ) |

Table 4.2. Linear Model and PGLS Results

We fit our data to multiple linear models and conducted multiple PGLS analyses using the caper R package, evaluating relationships between traits chosen *a priori*, including comparisons between limb morphology and perch characteristics and limb morphology and toe detachment angle. We also estimated the λ parameter of our PGLS analyses, which was bounded between zero (no phylogenetic signal) and one (Brownian motion trait evolution). We also compared the λ parameter to one and zero, reporting the p values from these comparisons (in parentheses following our estimated λ value).

**Chapter 4. Bibliography**

Autumn, K., Dittmore, A., Santos, D., Spenko, M. and Cutkosky, M. (2006a). Frictional adhesion: a new angle on gecko attachment. J. Exp. Biol. 209, 3569-3579.

Autumn, K., Majidi, C., Groff, R. E., Dittmore, A. and Fearing, R. (2006b). Effective elastic modulus of isolated gecko setal arrays. J. Exp. Biol. 209, 3558-3568.

Autumn, K., Ryan, M. J. and Wake, D. B. (2002a). Integrating historical and mechanistic biology enhances the study of adaptation. Q Rev Biol 77, 383-408.

Autumn, K., Sitti, M., Liang, Y. A., Peattie, A. M., Hansen, W. R., Sponberg, S., Kenny, T. W., Fearing, R., Isrealachvili, J. N. and Full, R. J. (2002b). Evidence for van der Waals adhesion in gecko setae. Proc. Natl. Acad. Sci. USA 99, 12252-12256.

Bauer, A. M. (1998). Morphology of the adhesive tail tips of carphodactyline geckos (Reptilia: Diplodactylidae). Journal of Morphology 235, 41-58.

Brown, D., Wilmer, J. W. and Macdonald, S. (2012). A revision of Strophurus taenicauda (Squamata; Diplodactylidae) with the description of two new subspecies from central Queensland and a southerly range extension. Zootaxa, 1-28.

Butler, M. A. (2005). Foraging mode of the chameleon, Bradypodion pumilum: a challenge to the sit-and-wait versus active forager paradigm? Biological Journal of the Linnean Society 84, 797-808.

Cole, N. C., Jones, C. G. and Harris, S. (2005). The need for enemy-free space: The impact of an invasive gecko on island endemics. Biological Conservation 125, 467-474.

Conroy, C. J., Papenfuss, T., Parker, J. and Hahn, N. E. (2009). Use of Tricaine Methanesulfonate (MS222) for Euthanasia of Reptiles. Journal of the American Association for Laboratory Animal Science 48, 28-+.

Elstrott, J. and Irschick, D. J. (2004). Evolutionary correlations among morphology, habitat use and clinging performance in Caribbean Anolis lizards. Biological Journal of the Linnean Society 83, 389-398.

Fischer, M. S., Krause, C. and Lilje, K. E. (2010). Evolution of chameleon locomotion, or how to become arboreal as a reptile. Zoology (Jena) 113, 67-74.

Gamble, T., Greenbaum, E., Jackman, T. R., Russell, A. P. and Bauer, A. M. (2012). Repeated Origin and Loss of Adhesive Toepads in Geckos. PLoS ONE 7.

Gardner, A. S. (1984). The evolutionary ecology and population systematics of day geckos (Phelsuma) in the Seychelles, vol. Ph.D.: University of Aberdeen.

Glaw, F. and Vences, M. (2007). A field guide to the amphibians and reptiles of Madagascar: Vences & Glaw.

Goodman, B. A., Miles, D. B. and Schwarzkopf, L. (2008). Life on the Rocks: Habitat Use Drives Morphological and Performance Evolution in Lizards. Ecology 89, 3462-3471.

Hagey, T. J., Losos, J. B. and Harmon, L. J. (2010). Cruise foraging of invasive chameleon (Chamaeleo jacksonii xantholophus) in Hawai'i. Cambridge: Museum of Comparative Zoology.

Harmon, L. J., Harmon, L. L. and Jones, C. G. (2007). Competition and community structure in diurnal arboreal geckos (genus Phelsuma) in the Indian Ocean. Oikos 116, 1863-1878.

Hecht, M. K. (1952). Natural Selection in the Lizard Genus Aristelliger. Evolution 6, 112-124.

Higham, T. E., Davenport, M. S. and Jayne, B. C. (2001). Maneuvering in an arboreal habitat: the effects of turning angle on the locomotion of three sympatric ecomorphs of Anolis lizards. Journal of Experimental Biology 204, 4141-4155.

Huber, G., Gorb, S. N., Hosoda, N., Spolenak, R. and Arzt, E. (2007). Influence of surface roughness on gecko adhesion. Acta Biomater. 3, 607-610.

Huber, G., Gorb, S. N., Spolenak, R. and Arzt, E. (2005). Resolving the nanoscale adhesion of individual gecko spatulae by atomic force microscopy. Bio. Lett. 1, 2-4.

Irschick, D. J., Austin, C. C., Petren, K., Fisher, R. N., Losos, J. B. and Ellers, O. (1996). A comparative analysis of clinging ability among pad-bearing lizards. Biol. J. Linn. Soc. 59, 21-35.

Irschick, D. J., Herrel, A. and Vanhooydonck, B. (2006). Whole-organism studies of adhesion in pad-bearing lizards: creative evolutionary solutions to functional problems. J. Comp. Physiol. A 192, 1169-1177.

Jones, Z. M. and Jayne, B. C. (2012). Perch diameter and branching patterns have interactive effects on the locomotion and path choice of anole lizards. Journal of Experimental Biology 215, 2096-2107.

Losos, J. B. (1994). Integrative Approaches to Evolutionary Ecology - Anolis Lizards as Model Systems. Annual Review of Ecology and Systematics 25, 467-493.

Losos, J. B. (2009). Lizards in an evolutionary tree : the ecology of adaptive radiation in anoles. Berkeley: University of California Press.

Losos, J. B. and Irschick, D. J. (1996). The effect of perch diameter on escape behaviour of Anolis lizards: Laboratory predictions and field tests. Animal Behaviour 51, 593-602.

Losos, J. B. and Sinervo, B. (1989). The Effects of Morphology and Perch Diameter on Sprint Performance of Anolis Lizards. Journal of Experimental Biology 145, 23-30.

Losos, J. B., Walton, B. M. and Bennett, A. F. (1993). Trade-Offs between Sprinting and Clinging Ability in Kenyan Chameleons. Functional Ecology 7, 281-286.

Macrini, T. E., Irschick, D. J. and Losos, J. B. (2003). Ecomorphological differences in toepad characteristics between mainland and island anoles. Journal of Herpetology 37, 52-58.

Melville, J., Harmon, L. J. and Losos, J. B. (2006). Intercontinental community convergence of ecology and morphology in desert lizards. Proceedings of the Royal Society B-Biological Sciences 273, 557-563.

Oliver, P. M., Bauer, A. M., Greenbaum, E., Jackman, T. and Hobbie, T. (2012). Molecular phylogenetics of the arboreal Australian gecko genus Oedura Gray 1842 (Gekkota: Diplodactylidae): Another plesiomorphic grade? Molecular Phylogenetics and Evolution 63, 255-264.

Orme, C. D. L., Freckleton, R. P., Thomas, G. H., Petzoldt, T. and Fritz, S. A. (2011). caper: Comparative Analyses of Phylogenetics and Evolution in R. (http://R-Forge.R-project.org/projects/caper/).

Pagel, M. (1999). Inferring the historical patterns of biological evolution. Nature 401, 877-884.

Paradis, E., Claude, J. and Strimmer, K. (2004). APE: Analyses of Phylogenetics and Evolution in R language. Bioinformatics 20, 289-290.

Peattie, A. M. (2007). The Function and Evolution of Gekkotan Adhesive Feet, vol. Doctor of Philosophy, pp. 61. Berkeley: University of California, Berkeley.

Pesika, N. S., Gravish, N., Wilkinson, M., Zhao, B., Zeng, H., Tian, Y., Israelachvili, J. and Autumn, K. (2009). The Crowding Model as a Tool to Understand and Fabricate Gecko-Inspired Dry Adhesives. J. Adhesion 85, 512-525.

Pugno, N. M. and Lepore, E. (2008). Observation of optimal gecko's adhesion on nanorough surfaces. BioSystems 94, 218-222.

Pyron, R. A., Burbrink, F. T. and Wiens, J. J. (2013). A phylogeny and revised classification of Squamata, including 4161 species of lizards and snakes. Bmc Evolutionary Biology 13, 93.

Revell, L. J., Johnson, M. A., Schulte, J. A., Kolbe, J. J. and Losos, J. B. (2007). A phylogenetic test for adaptive convergence in rock-dwelling lizards. Evolution 61, 2898-2912.

Ruibal, R. and Ernst, V. (1965). The structure of the digital setae of lizards. J. Morphol. 117, 271-293.

Russell, A. P. (1979). Parallelism and Integrated Design in the Foot Structure of Gekkonine and Diplodactyline Geckos. Copeia 1979, 1-21.

Russell, A. P. (2002). Integrative Functional Morphology of the Gekkotan Adhesive System (Reptilia: Gekkota). Integr. Comp. Biol. 42, 1154-1163.

Russell, A. P. and Higham, T. E. (2009). A new angle on clinging in geckos: incline, not substrate, triggers the deployment of the adhesive system. Proc. R. Soc. B 276, 3705-3709.

Russell, A. P. and Johnson, M. K. (2007). Real-world challenges to, and capabilities of, the gekkotan adhesive system: contrasting the rough and the smooth. Can. J. Zoolog. 85, 1228-1238.

Russell, A. P., Johnson, M. K. and Delannoy, S. M. (2007). Insights from studies of gecko-inspired adhesion and their impact on our understanding of the evolution of the gekkotan adhesive system. J. Adhesion Sci. Technol. 21, 1119-1143.

Sadlier, R. A., O'Meally, D. and Shea, G. M. (2005). A New Species of Spiny-Tailed Gecko (Squamata: Diplodactylidae: Strophurus) from Inland Queensland. Memoirs of the Queensland Museum 51, 573-582.

Schulte, J. A., Losos, J. B., Cruz, F. B. and Nunez, H. (2004). The relationship between morphology, escape behaviour and microhabitat occupation in the lizard clade Liolaemus (Iguanidae : Tropidurinae : Liolaemini). Journal of Evolutionary Biology 17, 408-420.

Sinervo, B. and Losos, J. B. (1991). Walking the Tight Rope - Arboreal Sprint Performance among Sceloporus-Occidentalis Lizard Populations. Ecology 72, 1225-1233.

Tian, Y., Pesika, N., Zeng, H., Rosenberg, K., Zhao, B., McGuiggan, P., Autmn, K. and Israelachvili, J. (2006). Adhesion and friction in gecko toe attachment and detachment. Proc. Natl. Acad. Sci. USA 103, 19320-19325.

Vanhooydonck, B., Andronescu, A., Herrel, A. and Irschick, D. J. (2005). Effects of substrate structure on speed and acceleration capacity in climbing geckos. Biological Journal of the Linnean Society 85, 385-393.

Wainwright, P. C. and Reilly, S. M. (1994). Ecological Morphology. Chicago IL: University of Chicago Press.

Yamaguchi, T., Gravish, N., Autumn, K. and Creton, C. (2009). Microscopic Modeling of the Dynamics of Frictional Adhesion in the Gecko Attachment System. Journal of Physical Chemistry B 113, 3622-3628.

Zaaf, A. and Van Damme, R. (2001). Limb proportions in climbing and ground-dwelling geckos (Lepidosauria, Gekkonidae): a phylogenetically informed analysis. Zoomorphology 121, 45-53.

Zani, P. A. (2000). The comparative evolution of lizard claw and toe morphology and clinging performance. Journal of Evolutionary Biology 13, 316-325.

## Chapter 5. Conclusions

The field of ecological morphology uses data from studies of biomechanics, evolution, and ecology to investigate the relationship between an organism's morphology and environment (Wainwright and Reilly, 1994) with broader applications to habitat partitioning, character displacement, adaptation, and adaptive radiations (Grant and Grant, 2008; Losos, 2009; Wainwright and Reilly, 1994). My dissertation investigated two components of ecological morphology, the relationship between morphology and performance, and the relationship between performance and ecology, with an emphasis on the gecko adhesive system. Previous studies have found interesting patterns of ecological morphology in geckos (Gardner, 1984; Harmon et al., 2007; Zaaf and Van Damme, 2001), yet very few have considered gecko adhesive performance in an ecological morphology framework (but see Irschick et al., 1996; Russell and Johnson, 2007). Overall, my dissertation described multiple ecomorphological patterns present across geckos and padded lizards, suggesting geckos represent an understudied clade in which novel biomechanical and ecological patterns likely exist.

Chapter 2 of my dissertation considered morphology and performance of two gecko species, evaluating the accuracy of three mathematical models relating setal morphology to different aspects of performance. While I did find morphological and performance differences between my focal species, my main conclusions from this chapter focused on the accuracy of the focal mathematical models. The models I considered were capable of predicting some of the performance values I measured, while failing to accurately predict other parameters. With more accurate models, future studies could quickly and easily predict

how gecko species with divergent setal morphology may perform. My results suggest the models I investigated may benefit from the addition of more realistic parameter values. For example, the work of detachment model (Gravish et al., 2008) and the effective modulus model (Autumn et al., 2006b) both consider a single value of setal length, yet previous work by Johnson and Russell (2009) describe the variation in setal length across a toe of *Gekko gecko*. These mathematical models may be more accurate if they drew from a distribution of setal lengths to predict a range of possible performance values. I also found that during vertical compression, setal arrays did not always exhibit distinct phases of compression, as proposed by the crowding model (Pesika et al., 2009). As a result, the effective modulus model may benefit from incorporating a dynamic spring approach.

The use of other predictive approaches beyond mathematical modeling, such as *in silico* physical simulations could also greatly improve our understanding of setal mechanics. Simulations could incorporate setal variation as well as morphological characters beyond the setal level such as lamellae structure, paraphalanges, and internal fluid sinuses (Gamble et al., 2012; Russell, 2002). The use of simulations and the refinement of currently described mathematical models would allow not only for a better understanding of the underlying mechanics of the gecko adhesive system, but improvements to these models would also aid in the design of synthetic gecko-like adhesives (Choi et al., 2006; Gravish et al., 2010; Sitti and Fearing, 2003).

My second research chapter (Chapter 3) investigated the diversity in adhesive performance across padded lizards. In this study I considered adhesive performance quantified by the toe detachment assay. I found a wide range of performance capabilities across padded lizards (Figure 3.2, 3.3). My results also suggest that the independent origins

of adhesive pads in anoles, Diplodactylidae geckos, and the clade containing Gekkonidae and Phyllodactylidae geckos cluster around different performance means, possibly due to historical constraints. In this chapter, I also evaluated the relationship between setal length and performance across species and found a significant negative relationship in Gekkonidae and Phyllodactylidae geckos (see Figure 3.4), with Diplodacylidae geckos and anoles showing no such relationship. Without a mathematical model describing the relationship between setal morphology and toe detachment angle, this result is difficult to explain. Autumn et al. (2006a) suggested toe detachment angle is associated with setal miter angle (see Figure 2.2). However, the relationship between setal morphology and detachment angle may be more complicated with an interplay between spatulae morphology, setal branching morphology, the production of van der Waals forces, and internal stresses in the setal shaft. *In silico* simulations of setal detachment would be very valuable to investigate how different setal morphologies may affect detachment angle.

Another issue in considering the angle of toe detachment is that this assay describes a maximum ratio of forces (adhesion to friction) that a species is capable of generating. This measure of performance does not describe an absolute amount of friction or adhesion. As a result, it may be difficult to predict how species with high or low detachment angles may use their abilities in the wild (see Discussion of Chapter 4). Clinging ability in padded lizards has also been quantified using the amount of friction a gecko's pads generate (Irschick et al., 1996). A study investigating the relationship between friction, toe detachment angle, and pad area would be very informative. Pad area has been shown to be significantly correlated with the absolute amount of friction generated (Irschick et al., 1996), yet I do not predict such as relationship between toe detachment angle and pad area due to the fact that detachment angle

is likely a result of setal mechanics and not related to absolute forces (Autumn et al., 2006a). By comparing the absolute amount of friction generated by a species in conjunction with toe detachment angle, one could investigate the variation in the absolute frictional and adhesive forces generated across species. This relationship between the amount of friction and adhesion a species generates and toe-pad area may be highly variable. For example, using data from Irschick et al., (1996), I calulated the amount of friction generated, adjusted for pad area (absolute amount of friction divided by pad area, see Table 5.1) of five gecko and two anole species. It can be seen that species with larger toe pads tend to produce more absolute friction. When we consider the toe detachment angles of these species (data from Chapter 3), I predicted area-adjusted adhesive forces using Eq. 2.1 (Table 5.1).

These preliminary analyses reveal very interesting and novel patterns (Figure 5.1). *Gehyra mutilata* and *Lepidodactylus lugubris* have similarly high detachment angles, yet I predict them to produce different amounts of adhesion. Conversly, *Hemidactylus frenatus* and *Anolis sagrei* have very different toe detachment angles, yet I predict them to produce similar amounts of adhesion per area, which is unexpected considering how they use their habitat. Anoles typically use veritcal surfaces and do not cling to inverted surfaces, where as *H. frenatus* can often be observed using inverted perches (Irschick et al., 1996). As can be seen by the above calcuations, pad area, friction generated, adhesion generated, and toe detachment angle likely interact in a complicated fashion. A broad study investigating these parameters will likely find many interesting ecomorphological patterns.

My third research chapter (Chapter 4) investigated ecological correlations between limb length, toe detachment angle, and micorhabitat use. We found that our hypotheses, based on the mechanics of the toe detachment assay and previous studies of anoles, were not

supported. Despite this result, we found many other interesting correlations, suggesting potentially novel ecomorphological patterns may be present in geckos. Our results illustrate complex correlations between limb length and adhesive performance, suggesting gecko limb mechanics may be coadapted with the use of adhesive pads. We also found a complex relationship between perch type and limb length, complimenting the relationship we found between detachment angle and limb length. Lastly, we found unexpected negative correlations between perch diameter and limb length. A broad comparative analysis considering limb morphology and microhabitat use across lizard groups would be valuable in interpreting these results (see Figure 5.2).

In addition, we transformed our raw morphological measurements into relative values by extracting residual limb lengths from a regression of limb length on body length (see Chapter 4 methods). Using this approach, our relative morphological measurements represent deviations from an expected limb length for a given body length given our particular set of focal species. As a result, comparing results using our residual limb length measurements to studies using residual limb lengths of other taxa may be misleading if, as a whole, geckos have different limb lengths, possibly as a result of having adhesive pads.

A comparative study investigating how limb length, body length, and ecology may be related across lizards would be very interesting. Using data from previous studies of anoles (Losos, 2009); geckos (Zaaf and Van Damme, 2001; TH, unpublished data); skinks (Goodman et al., 2008); other arboreal, rock dwelling, and terrestrial lizards (Melville et al., 2006; Revell et al., 2007); and chameleons (Bickel and Losos, 2002; Butler, 2005; Fischer et al., 2010; Hagey et al., 2010; Losos et al., 1993), novel ecomorphological patterns may be found (Figure 5.2). Previous studies of both geckos (Zaaf and Van Damme, 2001) and

chameleons (Bickel and Losos, 2002) have found unexpected relationships between limb length and microhabitat, and using a broader comparative approach may highlight additional novel patterns.

Lastly, my hypothesis regarding toe detachment angle and perch angle was not supported. While toe detachment angle alone may be difficult to correlate with perch characteristics due to the lack of an explanatory mathematical model and absolute force values (as noted above), there are additional microhabitat parameters such as perch texture that we did not investigate. Previous studies have investigated the theoretical relationship between setal morphology, spatuale morphology, and substrate textures at different scales (Huber et al., 2007; Pugno and Lepore, 2008; Vanhooydonck et al., 2005), yet very few have considered the textures of perches used by geckos in the wild (but see Russell and Johnson, 2007). Together, these studies suggest a complex relationship between surface roughness and setal morphology, with surface texture interacting with each hierarchical level of the adhesive system to affect performance. A study combining setal morphology, measurements of perch textures used by geckos in the wild, and a measure of adhesive performance (likely both friction generated and toe detachment angle) may be informative as to how geckos may have evolved to live on different textured surfaces. Previous studies of *Phelsuma* geckos have found species in this genus to partition their environment based on perch type, palm-like vs. non-palm like (Harmon et al., 2007), and these perches likely exhibit different textures. In addition to observational data and correlations, an ecomorphological study considering geckos and perch texture would also benefit from the use of simulations to investigate the mechanical relationship between various setal morphologies and surface oscillations.

Based on the results in this dissertation, geckos likely exhibit novel ecomorphological patterns. Together with the unique mechanics of their adhesive system, geckos represent an excellent study system to examine the interplay between biomechanics, evolution, and ecology. As outlined above, there are many more questions regarding how geckos use their toe pads in the wild and how geckos may be convergent or unique when considering morphology and ecology compared to other well studied lizard clades.

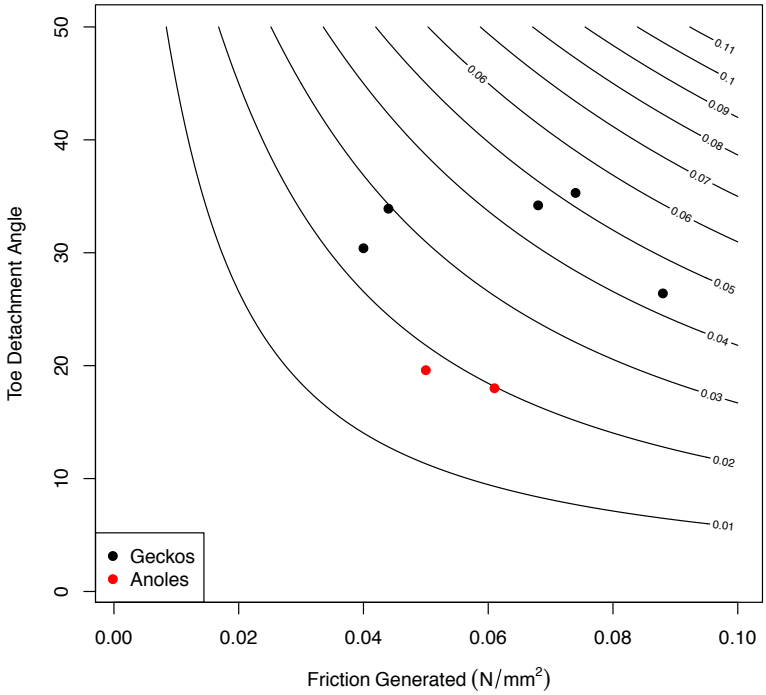


Figure 5.1. Friction, Toe Detachment Angle, and Adhesion Generated by Padded Lizards

Using frictional and pad area data from Irschick et al. (1996), toe detachment measurements from Chapter 3, and Eq. 2.1, I plotted the area-adjusted friction generated by a padded lizard (absolute friction / pad area) against toe detachment angle. Within the plot, I also illustrated the predicted area-adjusted adhesive forces generated by each species ($N/mm^2$) using Eq 2.1.

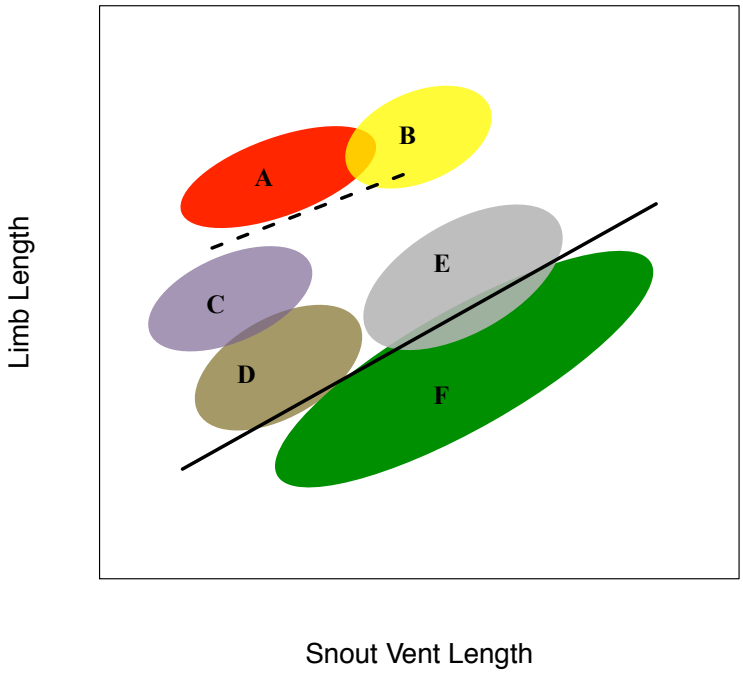


Figure 5.2. Limb Length, Body Length, and Ecology across Lizards

A broad comparative study of the relationship between body size (snout vent length) and limb length across lizards while also considering habitat use would be valuable to investigate convergent and novel ecomorphological patterns (hypothetical data for geckos and anoles shown). In the above plot, a hypothetical regression line of body length and limb length of anoles (dashed line) and geckos (solid line) can be seen. In addition, species in these clades likely group based on their ecology, with hypothetical data from trunk dwelling anoles illustrated in red (A), crown giant anoles in yellow (B), twig anoles in purple (C), geckos that use low, narrow perches in brown (D), rock dwelling geckos in gray (E), and the remaining arboreal geckos in green (F). By using such a broad comparative approach, convergent morphologies may be illustrated, such as the similarities in twig anoles (C) and geckos that use low narrow perches (D). If analyzed separately, in the above illustration, twig anoles would have relatively short limbs and low perching geckos would have relatively long limbs.

| Species | Pad Area ($mm^2$) | Friction (N) | Relative Friction ($N/mm^2$) | Toe Detachment Angle | Predicted Relative Adhesion ($N/mm^2$) |
|---|---|---|---|---|---|
| *Hemidactylus frenatus* | 25.3 | 1.0 | 0.040 | 30.4 | 0.023 |
| *Gehyra oceanica* | 69.1 | 4.7 | 0.068 | 34.2 | 0.046 |
| *Gehyra mutilata* | 18.1 | 0.8 | 0.044 | 33.9 | 0.030 |
| *Lepidodactylus lugubris* | 12.1 | 0.9 | 0.074 | 35.3 | 0.053 |
| *Gekko gecko* | 227.1 | 20.0 | 0.088 | 26.4 | 0.044 |
| *Anolis carolinensis* | 30.1 | 1.5 | 0.050 | 19.6 | 0.018 |
| *Anolis sagrei* | 21.4 | 1.3 | 0.061 | 18.0 | 0.020 |

Table 5.1. Friction, Toe Detachment Angle, and Adhesion Generated by Padded Lizards

Using frictional and pad area data from Irschick et al. (1996), toe detachment measurements from Chapter 3, and Eq. 2.1, I calculated the area adjusted friction generated by a padded lizard (absolute friction / pad area) and the predicted size adjusted adhesive forces ($\tan[\bar{\alpha}^*]\ F_{\parallel} \geq F_{\perp}$).

**Chapter 5. Bibliography**

Autumn, K., Dittmore, A., Santos, D., Spenko, M. and Cutkosky, M. (2006a). Frictional adhesion: a new angle on gecko attachment. J. Exp. Biol. 209, 3569-3579.

Autumn, K., Majidi, C., Groff, R. E., Dittmore, A. and Fearing, R. (2006b). Effective elastic modulus of isolated gecko setal arrays. J. Exp. Biol. 209, 3558-3568.

Bickel, R. and Losos, J. B. (2002). Patterns of morphological variation and correlates of habitat use in chameleons. Biological Journal of the Linnean Society 76, 91-103.

Butler, M. A. (2005). Foraging mode of the chameleon, Bradypodion pumilum: a challenge to the sit-and-wait versus active forager paradigm? Biological Journal of the Linnean Society 84, 797-808.

Choi, P., Kim, J. and Guo, L. J. (2006). Fabrication of Synthetic Gecko Tape and Characterization of Adhesion Forces. In Proceedings of the 50th International Conference on Electron, Ion, and Photon Beam Technology and Nanofabrication.

Fischer, M. S., Krause, C. and Lilje, K. E. (2010). Evolution of chameleon locomotion, or how to become arboreal as a reptile. Zoology (Jena) 113, 67-74.

Gamble, T., Greenbaum, E., Jackman, T. R., Russell, A. P. and Bauer, A. M. (2012). Repeated Origin and Loss of Adhesive Toepads in Geckos. PLoS ONE 7.

Gardner, A. S. (1984). The evolutionary ecology and population systematics of day geckos (Phelsuma) in the Seychelles, vol. Ph.D.: University of Aberdeen.

Goodman, B. A., Miles, D. B. and Schwarzkopf, L. (2008). Life on the Rocks: Habitat Use Drives Morphological and Performance Evolution in Lizards. Ecology 89, 3462-3471.

Grant, P. R. and Grant, B. R. (2008). How and why species multiply : the radiation of Darwin's finches. Princeton: Princeton University Press.

Gravish, N., Wilikinson, M. and Autumn, K. (2008). Frictional and elastic energy in gecko adhesive detachment. J. R. Soc. Interface 5, 339-348.

Gravish, N., Wilkinson, M., Sponberg, S., Parness, A., Esparza, N., Soto, D., Yamaguchi, T., Broide, M., Cutkosky, M., Cretin, C. et al. (2010). Rate-dependent frictional adhesion in natural and synthetic gecko setae. J. R. Soc. Interface 7, 259-269.

Hagey, T. J., Losos, J. B. and Harmon, L. J. (2010). Cruise foraging of invasive chameleon (Chamaeleo jacksonii xantholophus) in Hawai'i. Cambridge: Museum of Comparative Zoology.

Harmon, L. J., Harmon, L. L. and Jones, C. G. (2007). Competition and community structure in diurnal arboreal geckos (genus Phelsuma) in the Indian Ocean. Oikos 116, 1863-1878.

Huber, G., Gorb, S. N., Hosoda, N., Spolenak, R. and Arzt, E. (2007). Influence of surface roughness on gecko adhesion. Acta Biomater. 3, 607-610.

Irschick, D. J., Austin, C. C., Petren, K., Fisher, R. N., Losos, J. B. and Ellers, O. (1996). A comparative analysis of clinging ability among pad-bearing lizards. Biol. J. Linn. Soc. 59, 21-35.

Johnson, M. K. and Russell, A. P. (2009). Configuration of the setal fields of Rhoptropus (Gekkota: Gekkonidae): functional, evolutionary, ecological and phylogenetic implications of observed pattern. J Anat 214, 937-55.

Losos, J. B. (2009). Lizards in an evolutionary tree : the ecology of adaptive radiation in anoles. Berkeley: University of California Press.

Losos, J. B., Walton, B. M. and Bennett, A. F. (1993). Trade-Offs between Sprinting and Clinging Ability in Kenyan Chameleons. Functional Ecology 7, 281-286.

Melville, J., Harmon, L. J. and Losos, J. B. (2006). Intercontinental community convergence of ecology and morphology in desert lizards. Proceedings of the Royal Society B-Biological Sciences 273, 557-563.

Pesika, N. S., Gravish, N., Wilkinson, M., Zhao, B., Zeng, H., Tian, Y., Israelachvili, J. and Autumn, K. (2009). The Crowding Model as a Tool to Understand and Fabricate Gecko-Inspired Dry Adhesives. J. Adhesion 85, 512-525.

Pugno, N. M. and Lepore, E. (2008). Observation of optimal gecko's adhesion on nanorough surfaces. BioSystems 94, 218-222.

Revell, L. J., Johnson, M. A., Schulte, J. A., Kolbe, J. J. and Losos, J. B. (2007). A phylogenetic test for adaptive convergence in rock-dwelling lizards. Evolution 61, 2898-2912.

Russell, A. P. (2002). Integrative Functional Morphology of the Gekkotan Adhesive System (Reptilia: Gekkota). Integr. Comp. Biol. 42, 1154-1163.

Russell, A. P. and Johnson, M. K. (2007). Real-world challenges to, and capabilities of, the gekkotan adhesive system: contrasting the rough and the smooth. Can. J. Zoolog. 85, 1228-1238.

Sitti, M. and Fearing, R. S. (2003). Synthetic Gecko Foot-Hair Micro/Nano-Structures for Future Wall-Climbing Robots. In Proceedings of the IEEE International Conference on Robotics and Automation Vol. 1, pp. 1164-1170. Los Alamitos, CA, USA: IEEE.

Vanhooydonck, B., Andronescu, A., Herrel, A. and Irschick, D. J. (2005). Effects of substrate structure on speed and acceleration capacity in climbing geckos. Biological Journal of the Linnean Society 85, 385-393.

Wainwright, P. C. and Reilly, S. M. (1994). Ecological Morphology. Chicago IL: University of Chicago Press.

Zaaf, A. and Van Damme, R. (2001). Limb proportions in climbing and ground-dwelling geckos (Lepidosauria, Gekkonidae): a phylogenetically informed analysis. Zoomorphology 121, 45-53.